16,00 EUR K 8266

Felsbau

Rock and Soil Engineering

5/2004
SEPTEMBER

Journal for Engineering Geology, Geomechanics and Tunnelling

Teichanlage
Red Bull World II, Fuschl am See

Modellierung • Abdichtung • Pflasterung und Natursteingestaltung • Bepflanzung • Tierbesatz

INTERNATIONALE ERFAHRUNG IN DER ABDICHTUNGSTECHNIK

Inhalt Nr. 5/2004

FELSBAU
Rock and Soil Engineering

Fachzeitschrift für Ingenieurgeologie, Geomechanik und Tunnelbau

Österreichische Gesellschaft für Geomechanik

Verlag Glückauf GmbH

Editorial

This edition of FELSBAU is focused on the Design and Construction Issues of Bimrocks (Rock/Soil Mixtures). Some readers will be puzzled and amused by the unfamiliar word "bimrocks", which is a contraction of the term "block-in-matrix rocks", or mixtures of competent blocks embedded in weaker matrix. Bimrocks include melanges, fault rocks, lahars, weathered rocks, and other rock/soil mixtures. I coined the word "bimrocks" in 1992 to focus attention on the similar geotechnical properties and common construction difficulties encountered when designing for and excavating in rock/soil mixtures with diverse geological origins. So it is with great pleasure twelve years later, that I introduce this international collection of papers on bimrocks.

The successful characterization of bimrocks requires good engineering geology and structural geology. Wakabayashi and Medley share some guidelines on the geological characterization of bimrocks, with examples from their experience of the most intractable of bimrocks: melanges of the Franciscan Complex in California. Part of their paper focuses on the importance of describing the geology and geometry of blocks, which in tectonic bimrocks may range between sand and mountains. The sizes of blocks are not just of geological interest since incorrect assumptions about the size and distribution of blocks leads to unpleasant and sometimes dangerous excavation and tunneling conditions. In a most illuminating paper, Haneberg shows how incorrect geological characterizations can be when block sizes are estimated from outcrops in bimrock masses with an oriented fabric.

One of the fundamental geotechnical attributes of bimrocks is that the overall strength of a bimrock increases with increasing volumetric block proportion. However, estimation of volumetric block proportion is very challenging, so the contribution of Sönmez, Gokceoglu, Tuncay, Medley and Nefeslioglu is appreciated. These authors show that image analysis techniques are useful in measuring block properties of Ankara Agglomerate, a volcanic bimrock, and also suggest that there is some dependence between the overall UCS of the bimrock and the strengths of the different types of blocks.

Gunter Riedmüller, 1940 – 2003

The increase in bimrock strength with increasing volumetric block proportion is due to the "tortuosity" of pre-existing and induced failure surfaces as they are forced to pass around blocks. Medley shows that in model bimrocks there is such considerable variety in the geometry of these surfaces, that for design purposes it is appropriate to focus on analyzing the geotechnical behavior of failure zones rather than individual potential surfaces, the geometry of which can be estimated based on the scale of engineering interest.

It is impossible to characterize chaotic bimrocks as fully we would like. Nevertheless, despite the lack of full characterization, construction in chaotic geology can still be performed by using modern applications of the geotechnical observational method. As described by Moritz, Grossauer and Schubert for a tunnel in an Alpine tectonic melange, continuous monitoring and analyses of changes in orientations of the displacement vector allows short-term prediction of rock mass quality ahead of tunnel faces in low overburden conditions.

In a practical paper reporting the geotechnical design of a high dam in serpentinite bimrock, Glawe and Upreti show that serpentinite may not always deserve its bad reputation, although they also report on a serpentinite excavated for a tunnel in which the rock behaved as badly as we expect!

Sadly, there is one contribution in this collection that is missing: that of the late Professor Gunter Riedmüller, who died in November 2003. Gunter, besides being one of the leading engineering geologists of the world, was also one of the first geopractitioners to understand what I was trying to achieve with my work with bimrocks and used my simple ideas in his teaching and consulting practice. Because of our shared interests in bimrocks, Gunter quickly became a close friend and mentor, and it is thanks to him that I made several professional connections and friendships with Austrian geopractitioners.

But Gunter was more than a successful geopractitioner: his zest for Life encouraged many of us, as he wrote in his December 2002 poem "I Wish You Time to Live" distributed at his funeral in Graz, and translated for me by one of Gunter's students, Margit Kurka: *Do not forget to be playful and curious. Especially that what seems senseless and can't be measured in success keeps you young and alive... I wish you time to live, wherever you are and however you feel. My wish for you is that you perceive the opportunities, that are given to you to shape time. No matter how old you are, it is the most valuable gift to you besides health.*

Accordingly, it is with honor and love that I dedicate this collection of bimrock papers to the memory and legacy of the late Professor Gunter Riedmüller, a man with whom many of us were fortunate to share some time.

Ed Medley

Geological Characterization of Melanges for Practitioners

By John Wakabayashi and Edmund W. Medley

Many geotechnical engineers and engineering geologists (practitioners) believe that simply drawing contact lines or other features on a geologic map or cross section produces representative characterizations of the subsurface. But the results of most investigations are often grossly incorrect when working with melanges (from French: mélange, or mixture). Melanges are mappable but discontinuous, often chaotic rock units, composed of mixtures of often pervasively sheared, weak matrix enclosing a variety of stronger blocks of different lithologies and size (Figure 1). Melanges can form as submarine landslides (olistostromes), by tectonic processes as fault rocks, or by a combination of the two processes (1, 2, 3). The origins of melanges interest research geologists to the point of producing several thousand papers, but from an engineering viewpoint, the processes all produce mixtures of weak matrix and stronger blocks.

Despite more than 40 years of geological understanding of melanges and their origins, me-

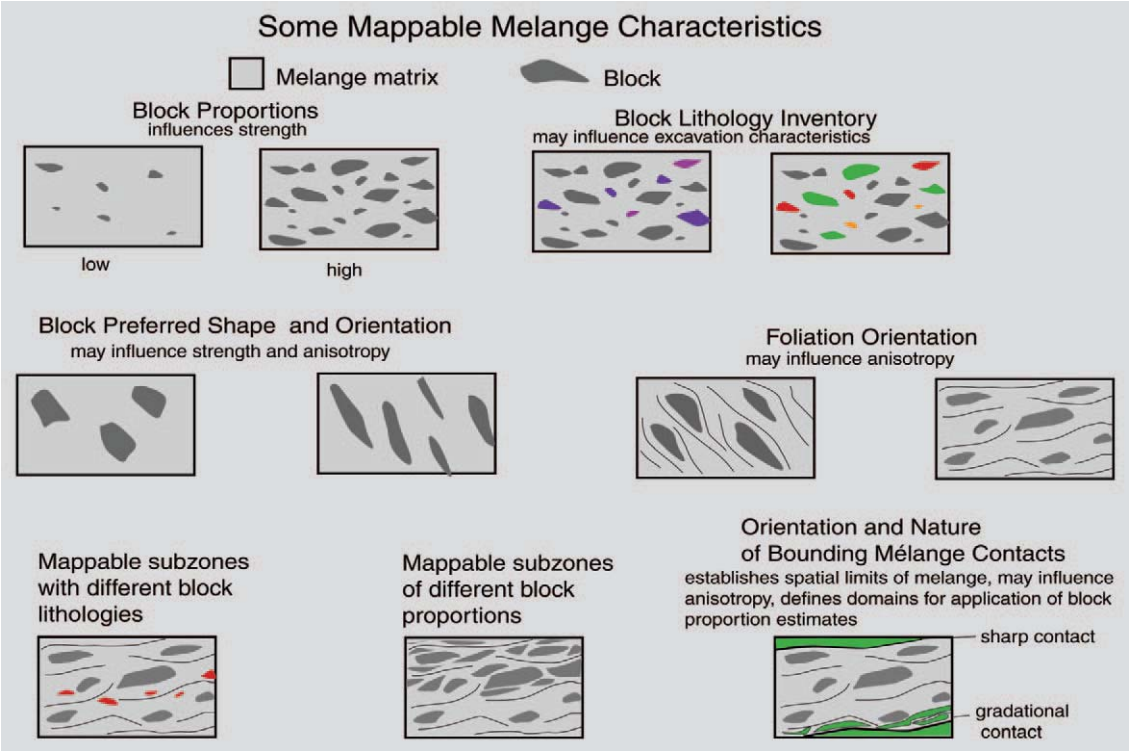

Fig. 1 Principal mappable engineering geology characteristics of a melange.

Bild 1 *Ingenieurgeologische Grundsatzmerkmale für die Kartierung von Melangen.*

Geologische Charakterisierung von Melangen für den Fachmann

Unter Melangen versteht man ungeordnete Einheiten von Fels, der aus einer Mischung aus Felsmasse mit niedriger Festigkeit und harten Gesteinsblöcken besteht. Obwohl Melangen weltweit anzutreffen sind und Gefügegeologen seit Jahrzehnten damit vertraut sind, wissen geotechnische und geologische Fachleute nicht Bescheid über die neuesten geologischen Konzepte bezüglich Melangen und deren ingenieurtechnischen Stellenwert; diese Unwissenheit resultiert in kostspieligen Planungsfehlern und unwillkommenen Überraschungen während der Baudurchführung. Basierend auf Erfahrungen in Franciscan Melange werden im Folgenden Identifizierungsmerkmale für Melangen und Zuordnungsmerkmale für externe und interne Details innerhalb der Melangeeinheiten vorgestellt und auch Richtlinien angeboten, die bei der Erstellung einer systematischen ingenieurtechnischen Charakterisierung von Melangen als Hilfestellung dienen.

Melanges are chaotic bedrock units consisting of mixtures of weak matrix and stronger blocks. Although melanges are globally common and have been familiar to structural geologists for decades, many geotechnical and geological practitioners are unaware of recent geological concepts of melanges and their engineering significance: such ignorance results in costly design errors and unwelcome surprises during construction. Based on experience with Franciscan complex melanges, criteria are provided for identifying melanges and mapping external and internal details within melange units, and guidelines offered for developing orderly engineering characterizations in melanges.

langes are unknown or misinterpreted by many practitioners. Costly and imprudent consequences derive from practitioners' errors in the mischaracterization of melange structures as "layer cake" strata, or incorrectly describing melanges as "soil containing boulders", or "miscellaneous soils", for example. To confuse matters, the word "melange" is also used by some practitioners to mean any mixture of rock and soil materials, which is inappropriate given the long-used geological meaning. Furthermore, some practitioners declare melanges as impossible to characterize and recommend geotechnical design be based on the properties of the weak matrix. Such simplification can lead to too-conservative and inappropriate designs and costly surprises and unsafe ground failures during construction.

Researchers have recently developed approaches to the engineering characterization of melanges and other bimrocks (block-in-matrix rocks) (4, 5, 6, 7, 8). Medley (9) defined bimrocks as geological mixtures of geotechnically significant blocks of rock within weaker, bonded rock matrices. Geotechnical significance means that there is sufficient mechanical contrast between the blocks and the matrix to force failure surfaces to negotiate around the blocks in tortuous fashion; and that there is a sufficient size and numbers of blocks to affect the overall mechanical properties of the geological mixture.

The authors of this paper, a Structural Geologist (Wakabayashi) and a Geological Engineer (Medley), consider it necessary to apply both first-order geologic field observations and quantitative engineering methods to the characterization of melange once it is identified, and to that end guidance for the identification, mapping, and characterization of melanges by practicing geologists and engineers is provided.

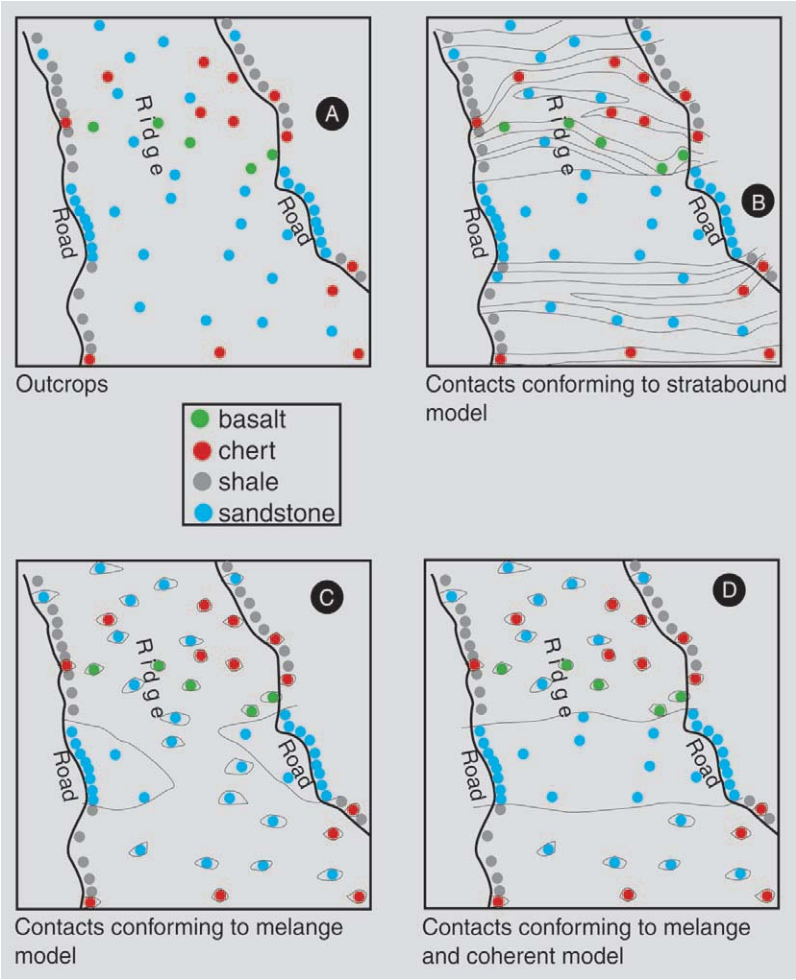

Fig. 2 Hypothetical geologic maps showing how prevailing geologic theories influence how contacts are drawn on maps. Map A: outcrops. Map B: geology interpreted as stratabound layers. Map C: entire area interpreted as melange. Map D: area composed of both melange and coherent thrust sheets.

Bild 2 *Theoretische geologische Karten, die zeigen, wie vorherrschende Theorien in der Geologie die Darstellung von Kontaktflächen beeinflussen. Abbildung A: Aufschlüsse. Abbildung B: Geologie interpretiert als stratigraphische Schichten. Abbildung C: Gesamtfläche interpretiert als Melange. Abbildung D: Fläche besteht aus Melangen und zusammenhängenden Überschiebungsdecken.*

Melanges – geologic concepts and misconcepts

A brief history of styles of mapping of melanges of the Franciscan Complex ("the Franciscan") of coastal California provides examples of how geologic knowledge influence how contacts are drawn on geologic maps and cross sections (Figures 2 and 3). The Franciscan hosts some of the world's most famous melanges (10,11), as well as engineering projects that have suffered problems because of their chaotic conditions.

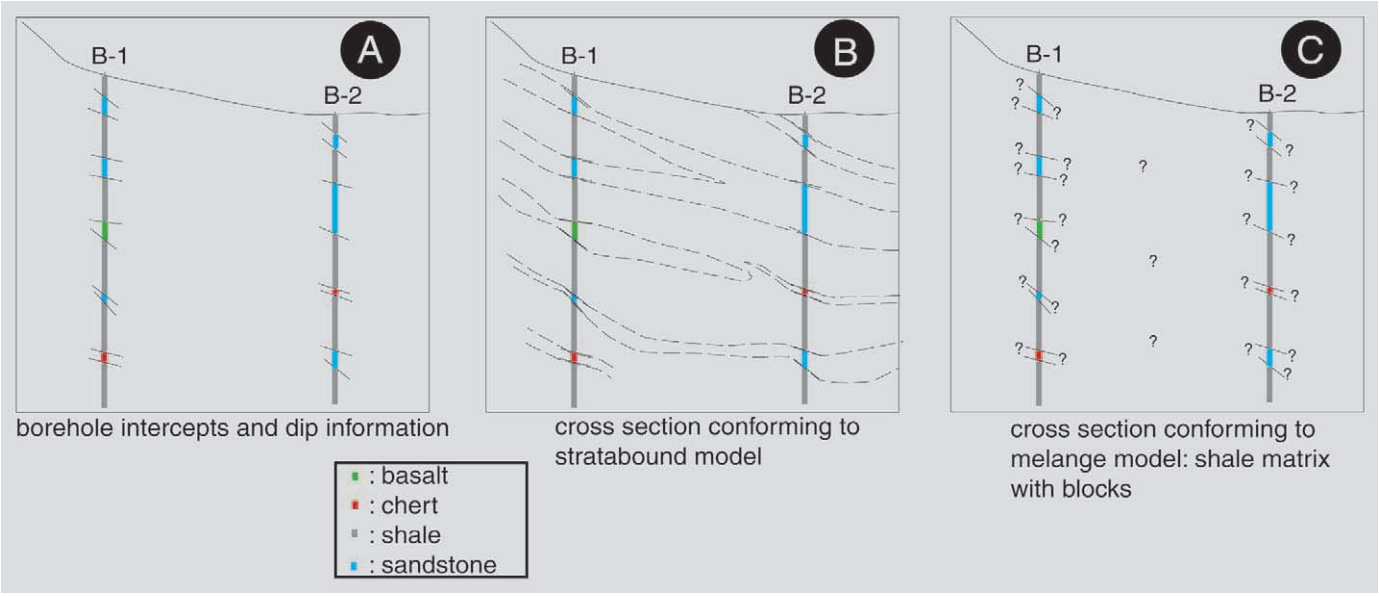

Fig. 3 Cross sectional diagrams showing the difference between assuming stratigraphic continuity and assuming melange structure when interpreting borehole data. A: borehole observations. B: Cross-section based on interpretation of stratabound geology (layers). C: Cross-section based on melange model.

Bild 3 *Querschnittsdiagramme zeigen den Unterschied zwischen angenommener Schichtenfolge und vermuteter Melangestruktur bei der Interpretation von Bohrkerndaten. A: Kernbohrungsbeobachtungen. B: Querschnitt basierend auf Auswertung von stratigraphischen Schichten. C: Querschnitt basierend auf einem Melangemodell.*

When mapping, geologists most commonly encounter the erosion-resistant blocks of a melange (Figure 4), rather than the weak matrix, which easily erodes and seldom forms observable outcrops except in bare natural slopes, or artificial cut slopes. Hence, prior to the 1960's most geologists mapped areas with scattered outcrops of sandstone, chert, basalt, or other rock types (Figure 2A) and then interpreted the melanges into the layer-cake continuous stratigraphic framework of the Franciscan "Formation" (12) (Figure 2B). If ignorant of melanges, many practitioners still map this way.

Greenly (13) first christened chaotic units in North Wales as "Autoclastic Mélange" but widespread recognition of melange structures did not follow until Hsü (10) formalized the melange concept. Melanges were then recognized as globally common, particularly in ancient orogenic belts associated with old subduction zones (2, 11). Following the acceptance of Hsü's (10) melange concepts, geologists mapping in the Franciscan and similar geologic confusion mapped outcrops as blocks in the usually unseen matrix (Figure 2C). Some geologists even classified the entire Franciscan as one large melange body and neglected the internal details, a simplification that can still be encountered in some academic research papers. By the mid-1970s, geologists such as Maxwell (14), began to discriminate the Franciscan into "coherent units", fault-bounded sheets of intact non-melange Franciscan geologic rock units; and discrete "melange units". This concept was expanded in the 1980s as the "terrane" concept explained the complex tectonic jigsaw of the North American Cordillera, with terranes being the individual puzzle pieces (15, 16). The Franciscan was then called the "Franciscan Assemblage". Although the terrane concept led to improved categorization of coherent units, identification of melanges regressed, as all Franciscan melange bodies were then collected into one "Central Terrane", based on an interpretation that all Franciscan melanges formed at the same time.

Wakabayashi (17, 18, 31) expanded on Maxwell's (14) concepts, by delimiting separate Franciscan melanges and coherent units, and then correlating melange units and coherent units to discrete structural levels within stacks of thrust nappes. Accordingly, an up-to-date structural geologist mapping Franciscan outcrops today might find and map both coherent and melange units, as shown schematically in Figure 2D. This modern approach reflects the appropriate current "Complex" suffix to "Franciscan Complex".

During a century of geologic mapping in the Franciscan Complex, the rocks have not changed, but the geologic maps have changed dramatically. Although geologists long ago recognized melanges and how to map them, many practitioners still treat melange bedrock as bedded geologic units. Others, also incorrectly, consider entire regions to be melange. Both groups thus fail to secure the geologic information that can be collected and used for engineering purposes.

Fig. 4 A view of landscape underlain by serpentinite matrix and shale matrix melange; Tiburon Peninsula, San Francisco area, California.

Bild 4 *Landschaftsansicht mit darunterliegender Serpentinit-Matrix und Schieferstein Matrixmelange; Tiburon Halbinsel, Bezirk San Francisco, Kalifornien.*

Mapping melanges – guidelines and cautions

In the Franciscan a gradation exists between coherent units and melanges, with an intermediate level of stratal disruption, commonly referred to as a "broken formation" (2), that renders identification of melange bimrocks for engineering purposes more difficult. The origins of melanges dictate the nature of the bounding contacts of a melange body. A purely sedimentary (or olistostromal) melange has sedimentary bounding contacts unless modified by later faulting, whereas the contacts of a tectonic melange are, by definition, faults. Furthermore, in melanges, tectonic signatures may include pronounced anisotropic rock mass fabrics that control matrix shears and block orientation (7, 8).

Despite the complexity of melanges, a knowledgeable and alert geologist can identify and map much useful information, as shown in Figure 1. Assuming that the melange has been correctly recognized, the overall boundary contacts of melange bodies will require standard "external" mapping of faults or depositional contacts, depending on the origin of the melange. "Internal" mapping of melanges requires detailed observations. When working with coherent geology (intact geologic units), a geologist commonly locates a few points along a contact and interpolates between them while "contact mapping". However, internal mapping of a melange is best accomplished by "saturation" mapping of every available outcrop. Detailed mapping will define the external contacts of the melange body, delineation of the boundaries of larger blocks, provide information to estimate the proportion of the blocks in the melange, and information on the variety of block lithologies. Several guidelines and common errors are summarized below.

Recognizing melanges and geomorphologic indicators

A melange must be recognized early in an investigation. One of the most common errors by practitioners in this regard is: not consulting a geologist nor reading a geological map. Even when available geology maps identify melanges, many geotechnical engineers (in particular) seem unable to conceive of the possibility that a "clay soil" may actually be pervasively sheared shale bedrock; that "bedrock" is discontinuous blocks, and that "boulders" are blocks that may be hundreds of meters in dimension. Such ignorance leads to mischaracterizations that could be avoided by consulting with a knowledgeable geologist.

Most units termed by structural geologists "melanges" have matrices with metamorphic grades less than greenschist facies and so will conform to the engineering definition of a bimrock. However, in some mappable melange bodies there may be areas that are bimrocks in

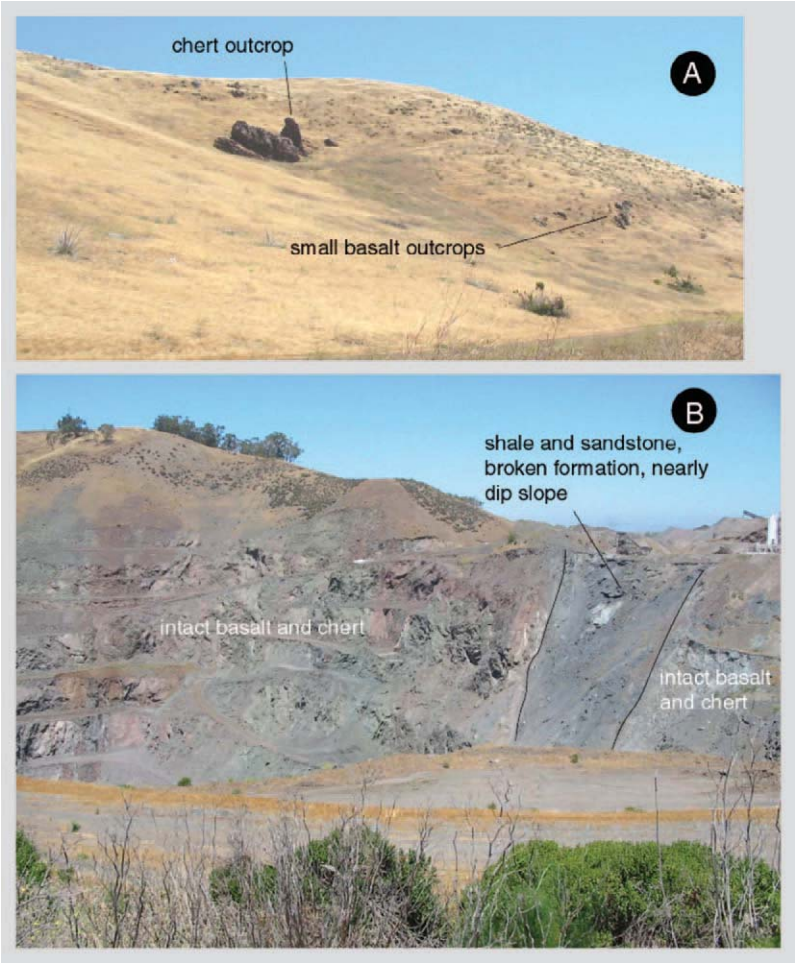

Fig. 5 Photos showing how geomorphology can be misleading in identifying melange. A: melange-like topography with a chert outcrop; B (taken a few hundred meters away from A) shows that the underlying bedrock is not melange.

Bild 5 *Fotoaufnahmen zeigen, wie irreführend Geomorphologie bei der Bestimmung von Melange sein kann. A: Melange-ähnliche Topographie mit Kieselerdeaufschluss. B: (aufgenommen aus einigen 100 m Entfernung von A) zeigt, dass das darunterliegende Felsgestein nicht Melange ist.*

one place but not in another. For example, in the northern Sierra Nevada of California, there are melange units of sub-greenschist metamorphic grade (19, 20) that are bimrocks because little recrystallization has occurred to strengthen the matrix relative to the blocks. However, further south, in the central Sierra Nevada, these same geologic units occur with upper greenschist and higher metamorphic grades (20) and the melange matrix is mechanically competent quartz-mica schist, and the melange is not a bimrock.

Melanges occur at all scales, from shear zones that are several km in outcrop dimension and structural thickness, to fault zones of meter or smaller scales. Franciscan Complex melanges are scale independent, meaning that melange have block and matrix structure at any scale of observation (9, 21, 22). Perhaps the only (and quite rare) exception to this scale independence are basalt matrix shear zones. The authors have observed such volcanic matrix limited to scales between from microscopic (millimeters) up to about a meter or so of structural thickness.

The most common field indicator of melanges is their geomorphologic expression. Because melange matrix is commonly weak, it is subject to slope movement and easily eroded. As a consequence it tends to form rolling topography with outcrops of larger blocks standing out in contrast, a geomorphology commonly referred to in California as "melting ice-cream topography" (see Figure 4). However, this characteristic geomorphic signature is not foolproof, for some coherent chert and basalt units will form somewhat similar topography with chert making up most of the blocky outcrops (Figure 5).

In some areas, scattered exposures of chert or basalt or limestone, in an area otherwise exhibiting only outcrops of sandstone and shale often indicates the presence of a melange, as does the presence of rocks such as sandstone, shale, chert, or basalt in an area that is otherwise serpentinite. Scattered metamorphic rocks that are of different metamorphic grade than surrounding rocks are also useful field indicators of a melange.

Serpentinite by itself is not necessarily an indicator of melange but it is commonly associated with melanges. Serpentinite in an area that is otherwise mostly sandstone and shale indicates the likelihood of the underlying rock unit being a melange. In serpentinite matrix melanges, the matrix is of sheared or disaggregated serpentinite and the most common blocks are usually massive serpentinites and less serpentinized ultramafic rocks, various mafic igneous rocks (gabbro, diabase, basalt), pelagic sedimentary rocks (chert, limestone), and metamorphic rocks (23, 1). But many serpentinite bodies are not melanges in a geologic sense, contrary to some misconceptions. Such bodies of rock usually occur as fault-bounded sheets or blocks and the serpentinite comprising them can range from massive and strong to sheared. Hence, a sheet composed entirely of serpentinite may exhibit block and matrix fabric, and thus be a bimrock, but not be a geologic melange.

Weathered melange exposures can be difficult to distinguish from colluvial soils, particularly if the colluvium itself has a melange source. Melanges interpreted as colluvium may lead to incorrect conclusions as to the subsurface geometry, since a colluvium deposit will have a base and a melange body may not. In a good exposure (such as the wall of a trench or test pit), some differences between melange-derived colluvium and weathered melange bedrock can be observed. Melange-derived colluvium will seldom have well-developed matrix foliation that is continuous over a square meter or so of exposure, whereas such foliation is commonly observable even in weathered bedrock. Melange-derived colluvium may have apparent foliation orientations that are fairly consistent and they will commonly be sub parallel to the slope, but the areas over which this foliation is visible will be patchy, for they will consist of individual pieces of matrix that have been incorporated into the soil. In melange-derived colluvium there may also be bits of former melange matrix that are rotated so that there are abrupt discontinuities in foliation orientation, in contrast to folding of the foliation or warping of foliation around blocks that characterize melange bedrock. The distinction between

weathered melange bedrock and melange-derived colluvium may be difficult to ascertain in borehole samples because a larger area of observation is generally needed to apply the criteria noted above.

Mapping matrix and foliations

The most common melange matrix types are shale/mudstone, sandstone, and serpentinite. Basalt or volcanic matrix (or mixed volcanic/shale matrix) is rare. Some melanges have a mixed serpentinite and shale matrix in which serpentinite can be interleaved as small as centimeters, although it is more common to find serpentinite as blocks in shale matrix melange (24).

Mapping melange foliation it is no different then mapping foliation in a metamorphic rock unit. Melange matrix foliation locally wraps around blocks and will have variable orientations, but over the extent of the mappable unit will commonly have a comparatively consistent foliation. When possible, the foliation orientations should be mapped to provide clues about the general orientation of the melange fabric which likely influences anisotropy in the strength of the melange, as described by Medley and Sanz (25). Shears may be so pervasive that the matrix is soil-like. Matrix sheared into scaly clay, in which the matrix is pervasively sheared and breaks into brittle chips of shale (Argille Scagliose of Northern Italy), may also be found and is diagnostic of melange.

Blocks – size distributions, lithologies, proportions, and orientations

Melange blocks vary greatly in character and size. To be considered a block there must be mechanical contrast between the block and the surrounding matrix, which can often be decided on the basis of striking both with a rock pick and observing the penetration or sound (4, 9). The block size distributions of observed Franciscan melanges are scale-independent or fractal (9, 22), and blocks will be found at all scales of engineering interest. In outcrops blocks are found as small as sand, whereas in regional-scale melange (several km in structural thickness), blocks can exceed a km in maximum dimension. The "size" of a "block" is thus dependent on the scale of observation and various criteria have been developed for determining critical scales (4, 9, 22). However, only rarely is the observed "size" of a block the same as the "diameter" of a block, for reasons explained by Medley (26, 27) and Haneberg (28). Once a "characteristic engineering dimension" or scaling dimension is selected that represents the scale of engineering interest of the bimrock (e.g. slope height, footing width, diameter of triaxial specimen), blocks are defined as being within about 5 to 70 % of that dimension, at least until the scale of interest changes (4). Since scales will change from reconnaissance-level site mapping to the scale of the proposed facility (e.g. cut slope, tunnel, foundation) it is best to decide early in the investigation what range of block sizes to examine and measure.

The lithologies of blocks vary from melange to melange and locally within any single melange unit. In shale matrix melanges, the most common block lithology is generally greywacke, with much smaller proportions of basalt, chert, limestone, plutonic and metamorphic rocks (9, 11). Identification of block lithologies and block discontinuity fabric is important for engineering purposes because certain block lithologies may pose greater excavation challenges than others, owing to their mechanical and discontinuity properties. For example an unexpected block of intact, fresh greenstone with an unconfined compressive strength of 200 MPa (30 000 psi) can seriously frustrate tunneling that has been designed to accommodate more tractable fractured greywackes. Also, fractured, weak blocks may offer little mechanical contrast with matrix and should thus prudently be assigned to matrix when considering overall geomechanical properties of the bimrock.

The volumetric proportion of blocks in a melange is an important engineering geology parameter because studies have shown that me-

lange strength is related to the volumetric proportion of blocks (5, 22, 29, 30). However, as described above, there are significant uncertainties to estimates of volumetric block proportions based on field observations (26, 27, 28).

Blocks in a melange will commonly have preferred shapes and orientation, much like imbricated pebbles in a gravel deposit. For blocks that are commonly disk shaped in three dimensions ("phacoids") the disk plane is generally parallel to sub parallel to the melange foliation. In addition, the long dimension of blocks in a melange may also have a preferred orientation. Similar to the matrix foliation, block shape orientation may also influence anisotropy in the overall strength of the melange so this is field geologic information that should be recorded as recommended also by Haneberg (28).

Internally, the block arrays of many melanges do not appear to exhibit any order, but some melanges have mappable sub zones within them. These sub zones can be distinguished by differences in block lithologies, block abundance, or even matrix type. For example a melange may consistently have a structurally lower zone that has common chert and basalt blocks, but have a structurally higher zone that lacks chert or basalt blocks. Different sub zones within a melange may actually correspond to spatially distinct (and thus mappable) subunits of different block proportions or block lithologies. This also applies to some melanges that have gradational contacts: mapping from the outside of the unit toward the middle one might observe a gradation from intact sandstone and shale to broken formation (block-in-matrix structure but no block types other then shale and sandstone) to a full melange with exotic blocks. This gradation corresponds to a difference in block proportions, and such a gradation is commonly mappable.

Interpretations from borehole observations

Interpretation of melanges from borehole data presents considerable additional challenges as indicated in Figure 3. Whereas surface float or geomorphic clues allows interpolation between outcrops, interpolation of block boundaries from boreholes is impossible unless the block is known to extend between the boreholes. Because of the potential for interpretation errors, backhoe pits or excavator trenches may yield more useful and economical subsurface information such as fabric orientations. Alternatively, as commonly performed in California, large diameter auger borings can be drilled to allow access by a geologist protected by a cage.

As noted previously, external contacts of melange can be interpolated between boreholes as for any geologic contact or fault. If internal sub zones are mappable, including gradations near

the external contacts, it may be possible to project these sub zone boundaries between boreholes. A cautionary note: contacts, particularly external contacts of a melange body, must be recognized. For example if a borehole at the dipping external boundary of a melange body penetrates the melange and terminates within a coherent unit, the coherent unit may inadvertently be classified as a block, leading to a too-high linear block proportion.

The lengths of the intercepts between the core and blocks (chords) can be totaled for several boreholes and divided by the total length of the boreholes to yield a cumulative linear block proportion, that subject to adjustments for uncertainty (26), yields an estimate of the volumetric block proportion of the melange explored. With considerably greater potential errors, the chords may also crudely indicate blocks size distributions subject to several cautions (27). Melange foliation and block preferred shape may also be recorded in a borehole with oriented core.

A common error when logging core in melange is to describe the alternating matrix and block intersections as "inter-layered" or interbedded" shale and sandstone. But such descriptions incorrectly imply stratal continuity and if used to describe melanges in geological reports can lead to misunderstandings when drawing cross sections, or to differing site conditions claims from earthwork and tunneling contractors.

It is common practice in Northern California to extend exploration boreholes in Franciscan melanges through soil and terminate the drilling 1 to 2 m into bedrock. A common error when exploring melanges to characterize them as "soil above bedrock", "miscellaneous soils" or "soil with boulders". The use of these inappropriate terms for Franciscan melange has been a factor in earthwork construction disputes. For example contractor have been known to excavate deeply in attempts to locate the "basal failure surface" in a pervasively sheared "clay soil", and to jackhammer unexpected "boulders" in excess of 5 m size. Such problems are avoided if practitioners do not draw straight lines between the "rock/soil contacts" they identify in exploration borings.

Conclusions

Melanges and similar bimrocks are common throughout the world and many engineering projects are constructed in these chaotic rock but the engineering geologic understanding applied to many of these projects has been obsolete for decades. The methods presented in this paper should help geologists and engineers learn how to identify and characterize melange, so that engineering assessment of melanges and other bimrocks can be performed. Admittedly, melanges are more difficult to characterize than "coherent" geologic units, but practitioners must

learn to characterize geological chaos in an orderly fashion, or else continue to perform costly and imprudent mischaracterizations.

References

1. Phipps, S.P.: *Ophiolitic olistostromes in the basal Great Valley sequence, Napa County, northern California Coast Ranges*. In: Raymond, L.A. (ed.): Melanges: Their nature, origin, and significance. Geological Society America, Special Paper 198, pp. 103-125, 1984.
2. Raymond, L.A.: *Classification of melanges*. In: Raymond L.A. (ed.): Melanges: Their nature, origin and significance. Geological Society of America, Boulder, Special Publication 228, pp.7-20, 1984.
3. Cowan, D.S.: *Structural styles in Mesozoic and Cenozoic melanges in the Western Cordillera of North America*. Geological Society of America Bulletin, Vol. 96 (1985), pp. 451-462.
4. Medley, E.W.: *Orderly characterization of chaotic Franciscan melanges*. Felsbau, Vol. 19 (2001), No. 4, pp. 20-33.
5. Lindquist, E.S. ; Goodman, R.E.: *The strength and deformation properties of a physical model melange*. In: Nelson, P.P.; Laubach, S.E. (eds): Proceedings of the 1st North American Rock Mechanics Conference (NARMS), Austin, Texas, pp. 843-850. Rotterdam: Balkema, 1994.
6. Goodman, R.E. ; C.S. Ahlgren: *Evaluating safety of concrete gravity dam on weak rock: Scott Dam*. J. of Geotechnical and Geoenvironmental Engineering, Vol. 126 (2000), pp. 429-442.
7. Riedmüller, G. ; Brosch, F.J. ; Klima, K. ; Medley, E.W.: *Engineering geological characterization of brittle faults and classification of fault rocks*. Feldsbau, Vol. 19 (2001), No. 4, pp. 13-19.
8. Button, E.A. ; Schubert, W. ; Riedmüller, G. ; Klima, K. ; Medley, E.W.: *Tunnelling in tectonic melanges – accommodating the impacts of geomechanical complexities and anisotropic rock mass fabrics*. Bulletin of Engineering Geology and the Environment, (in press).
9. Medley, E.W.: *The engineering characterization of melanges and similar block-in-matrix (bimrocks)*. Ph.D. dissertation, Dept. of Civil Engineering, University of California, Berkeley, California, USA,1994.
10. Hsü, K.J.: *The principles of melanges and their bearing on the Franciscan-Knoxville paradox*. Geological Society of America Bulletin, Vol. 79 (1968), pp. 1063-1074.
11. Cloos, M.: *Flow melanges and the structural evolution of accretionary wedges*. Geological Society America, Special Paper 198, pp. 71-80, 1984.
12. Taliaferro, N.L.: *Franciscan-Knoxville problem*. American Association of Petroleum Geologists Bulletin, Vol. 27 (1943), pp. 109-219.
13. Greenly, E.: *The geology of Anglesey*. Geological Survey of Great Britain. London, 1919.
14. Maxwell, J.C.: *Anatomy of an orogen*. Geological Society of America Bulletin, Vol. 85 (1974), pp. 1195-1204.
15. Blake, M.C. Jr. ; Howell, D.G. ; Jayko, A.S.: *Tectonostratigraphic terranes of the San Francisco Bay Region*. In: Blake; M.C. Jr. (ed.): Franciscan Geology of Northern California. Pacific Section Society of Economic Paleontologists and Mineralogists, Vol. 43, pp. 5-22, 1984.
16. Blake, M.C. Jr. ; Howell, D.G. ; Jones, D.L.: *Preliminary tectonostratigraphic terrane map of California*. United States Geological Survey Open File Report 82-593, 1982.
17. Wakabayashi, J.: *Nappes, tectonics of oblique plate convergence, and metamorphic evolution related to 140 million years of continuous subduction, Franciscan Complex, California*. Journal of Geology, Vol. 100 (1992), pp. 19-40.
18. Wakabayashi, J.: *Distribution of displacement on, and evolution of, a young transform fault system: the northern San Andreas fault system, California*. Tectonics, Vol. 18 (1999), pp. 1245-1274.
19. Day, H.W. ; Schiffman, P. ; Moores, E.M.: *Metamorphism and tectonics of the northern Sierra Nevada*. In: Ernst, W.G. (ed.): Metamorphism and crustal evolution of the western United States. Rubey Volume VII, pp. 737-763. Englewood Cliffs, New Jersey: Prentice-Hall, 1988.
20. Sharp, W.D.: *Pre-Cretaceous crustal evolution in the Sierra Nevada region, California*. In: Ernst, W.G. (ed.): Metamorphism and crustal evolution of the western United States. Rubey Volume VII, pp. 823-865. Englewood Cliffs, New Jersey: Prentice-Hall, 1988.
21. Medley, E.W.: *Using stereologic methods to estimate the volumetric block proportion in melanges and similar block-in-matrix rocks (bimrocks)*. Proceedings of the 7th Congress of the International Association of Engineering Geologists, Lisbon, pp.1031-1040. Rotterdam: Balkema, 1994.
22. Medley, E.W. ; Lindquist, E.S.: *The engineering significance of the scale-independence of some Franciscan melanges in California, USA*. In: Daemen, J.K. ; Schultz, R.A., (eds.): Proceedings of the 25th US Rock Mechanics Symposium, pp. 907-914. Rotterdam: Balkema, 1995.
23. Hopson, C.A. ; Mattinson, J.M. ; Pessagno, E.A. Jr.: *The Coast Range ophiolite, western California*. In Ernst, W. G., (ed.): The Geotectonic Development of California, pp. 419-510. Englewood Cliffs, New Jersey: Prentice-Hall, 1981.
24. Wakabayashi, J.: *Contrasting settings of serpentinite bodies, San Francisco Bay area, California: Derivation from the subducting plate vs. mantle hanging wall*. International Geology Review, 2004.
25. Medley, E.W. ; *Sanz. P.R.: Characterization of Bimrocks (Rock/Soil Mixtures) With Application to Slope Stability Problems*. In: Schubert, W. (ed.): Proc. Eurock 2004 and 53rd Geomechanics Colloquium, Salzburg, Austria. Essen: Verlag Glückauf GmbH, 2004.
26. Medley, E.W.: *Uncertainty in estimates of block volumetric proportion in melange bimrocks*. In: Marinos, P.G. ; Kpukis, G. ; Tsiambous, G. ; Stournaras, G. (eds.): Proc Int. Symp. On Engineering Geology and the Environment, pp. 267-272. Rotterdam: Balkema, 1997.
27. Medley, E.W.: *Estimating block size distributions of melanges and similar block-in-matrix rocks (bimrocks)*. Proc. 5th North American Rock Mechanics Symposium, Toronto, Canada, 2002.
28. Haneberg, W.C.: *Simulation of 3-d block populations to characterize outcrop sampling bias in block-in-matrix rocks (bimrocks)*. Felsbau, Vol. 22, No. 5, pp. 19-26 (this issue).
29. Lindquist, E.S.: *The strength and deformation properties of melange*. Ph.D. dissertation, Dept. of Civil Engineering, University of California, Berkeley, CA, USA, 1994.
30. Lindquist, E.S.: *The mechanical properties of a physical model melange*. Proceedings of the 7th Congress of the International Association of Engineering Geologists, Lisbon, pp.819-826. Rotterdam: Balkema, 1994.
31. Wakabayashi, J.: *Subduction and the rock record: Concepts developed in the Franciscan Complex, California*. In: Sloan, D. ; Moores, E.M. ; Stout, D. (eds.): Classic Cordilleran Concepts: A View From California. Geological Society of America, Special Paper 338, pp. 123-133, 1999.

Authors

John Wakabayashi, 1329 Sheridan Lane, Hayward, CA 94544, USA, E-Mail wako@tdl.com; Edmund W. Medley, Medley Geoconsultants, 1554 Winding Way, Belmont, CA 94002, USA, E-Mail emedley@bimrocks.com

Simulation of 3D Block Populations to Characterize Outcrop Sampling Bias in Bimrocks

By William C. Haneberg

Block-in-matrix rocks (bimrocks) are defined as "a mixture of rocks, composed of geotechnically significant blocks within a bonded matrix of finer texture" (1), a definition that encompasses a wide range of geologic materials including melanges, fault rocks, landslide debris, and glacial till.

Figure 1 shows a typical bimrock, in this case an outcrop of Mesozoic Franciscan Complex melange near Mendocino, California, USA. In this example the blocks visible in the outcrop are on the order of centimeters to decimeters in their longest dimension, but in other places they can range in size from meters to hundreds of meters in length. The geotechnical significance of bimrock blocks was illustrated by Lindquist (2) and Lindquist and Goodman (3), who showed that in physical models of melange, the angle of internal friction increased and the cohesive strength decreased as a function of block proportion in cases where block proportions exceeded 25 to 30 %.

Fig. 1 Typical bimrock outcrop of Franciscan Complex melange near Mendocino, California, USA. The white disk near the center of the photograph is a 2.3 cm diameter coin. (Photo courtesy of Ed Medley, 1994).

Bild 1 *Typischer „Bimrock"-Aufschluss in San Franciscan Melange in der Nähe von Mendocino, Kalifornien, USA. Die weiße Scheibe in Fotomitte stellt eine Münze mit 2,3 cm Durchmesser dar (Foto Ed Medley, 1994).*

The standard engineering practice is to use the strength of the weakest component (the bim-

Simulation von dreidimensionalen Gesteinsvorkommen zur Charakterisierung der Aufschlussstichprobenverzerrung in Block-In-Matrix Gesteinen (Bimrocks)

Die geotechnische und geohydrologische Charakterisierung von Block-in-Matrix Gesteinen (sogenannte Bimrocks) wie tektonische Melange, Störungsfurchen, Geschiebemergel und Erdrutschgeröll ist mit einigen Schwierigkeiten verbunden. Eine genaue und zuverlässige Charakterisierung ist jedoch extrem wichtig, da bekanntermaßen Blöcke oder die Größenverteilung der Gesteinsblöcke die Materialeigenschaften wie Durchlässigkeit, Scherfestigkeit und die Wahl des Bauverfahrens entscheidend beeinflussen. Geotechnische und hydrogeologische Methoden zur Baugrunduntersuchung wie Bohrungen und Aufschlusskartierung ergeben jedoch widersprüchliche Ergebnisse, da von ein- und zweidimensionalen Stichproben auf dreidimensionale Vorkommen geschlossen wird. Monte Carlo Computer Simulationen können zur Untersuchung der Verzerrungswerte verwendet werden, die bei der Ableitung der dreidimensionalen Gesteinsblockverteilung aus zweidimensionalen Darstellungen wie Aufschlusskarten oder Fotoaufnahmen entstehen. Die Simulation von zweidimensionalen Aufschlussdarstellungen von dreidimensionalen Gesteinen zeigt, dass Aufschlusskartierungen die Durchschnittsgesteinsgröße und das Gesamtblockvolumen um mehr als 10 % über- oder unterschätzen können, obwohl gleichförmige Gesteinsblöcke tendenziell unterschätzt werden. Die durch zweidimensionale Stichproben einfließende Fehlergrößenordnung bewegt sich im Bereich von ± 50 % für Durschnittsgesteinsblöcke und ± 80 % für das Gesamtblockvolumen. Ein gründlich geplantes statistisches Probenentnahmeprogramm von Gesteinsgröße und Ausrichtung in Verbindung mit numerischer Simulation birgt demnach die größte Chance auf verwendbare Information bezüglich der Gesteinsverteilungsstatistik, die wesentlichen Einfluss auf die Ingenieurplanung und Bauausführung haben kann.

Geotechnical and hydrogeological characterization of block-in-matrix rocks (bimrocks) such as melange, fault gouge, till, and landslide debris can be difficult, but accurate and reliable characterization is important because block or block size distributions are known to influence factors such as permeability, shear strength, and the choice of construction methods. Geotechnical and hydrogeological exploration methods such as drilling and outcrop mapping, however, produce biased results because they yield 1D or 2D samples of 3D populations. Monte Carlo computer simulations can be used to explore the amount of bias introduced when 3D block distribution information is inferred from 2D projections such as outcrop maps or photographs. Simulations of the 2D outcrop projections of 3D blocks show that outcrop mapping has the potential to overestimate or underestimate mean block sizes and total block volumes by tens of percent, although the tendency will be towards underestimation for blocks that are not highly elongated. The magnitudes of errors introduced by 2D outcrop sampling can be on the order of ± 50 % for mean block sizes and ± 80 % for total block volumes. Carefully designed statistical sampling of block sizes and orientations combined with numerical simulations, however, has the potential to yield valuable information about the statistics of block distributions that may have significant effects on the design and construction of engineered works.

rock matrix in this case), but information about bimrock block proportions can allow the use of more optimistic strength estimates (4). At the same time, however, the practitioner must consider the uncertainty associated with block proportion estimates in order not to overestimate the strength added by blocks (5) or risk serious underestimation of the volume of blocks that may be encountered during construction. An accurate prediction of the largest blocks to be encountered during tunneling or excavation may also be critical in the selection of appropriate methods and machinery, but the scale-independent fractal (or nearly fractal) distribution of bimrock blocks makes this a difficult proposition (1, 5, 6).

Blocks with permeability that is appreciably higher or lower than that of the surrounding matrix can also affect groundwater flow. Although he did not use the term "bimrock", Haneberg (7) used a series of analytical and numerical groundwater flow models to show how zones of anomalously high or low permeability could control the directions and magnitudes of seepage force vectors in potentially unstable slopes, in some cases creating localized zones of instability. The size, spacing, and permeability contrast of blocks should therefore be important considerations in the hydrogeologic characterization of bimrocks.

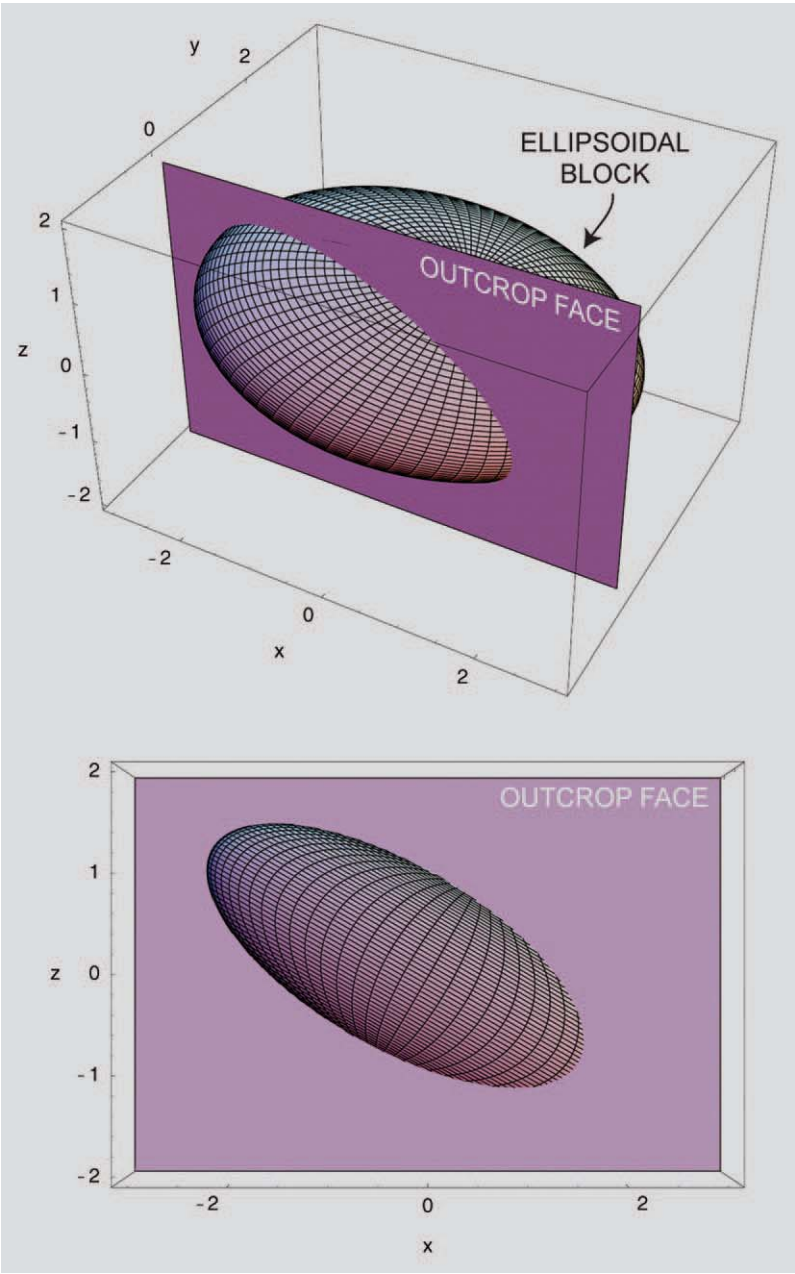

Fig. 2 A) Oblique view showing the intersection of an ellipsoid (representing a bimrock block) intersecting a plane (representing an outcrop face). B) View perpendicular to the outcrop plane, illustrating the 2D ellipse formed by the intersection of the ellipsoid and the plane.

Bild 2 *A) Schrägansicht eines Schnitts von Ellipsoid (Darstellung des Bimrock-Blocks) und Ebene (Darstellung der Aufschlussfläche). B) Lotrechte Ansicht der Aufschlussfläche zeigt die zweidimensionale Ellipse, die bei Verschneidung von Ellipsoid und Ebene entsteht.*

Most previous studies of bimrock sampling bias and block distribution characterization have been based on the application of stereological principles to measurements of blocks from borehole core and logs, outcrop maps of real bimrocks in the field, and scale-model bimrocks created in the laboratory (1, 6, 7, 8, 9). Medley (1) concluded that, although sampling can in some cases reliably replicate the mean or median block size, there is in general little equivalence between 1D chord lengths (e.g. from the intersection of blocks and borings or from outcrop scanlines) measured on maps and the true 3D block size distributions. As might be expected from consideration of the geometry of the problem, 1D sampling consistently underestimates the relative proportions of the largest blocks and overestimates the relative proportions of the smallest blocks.

In this paper, the 2D projection or expression of 3D blocks is referred to as the outcrop effect. One way to mathematically estimate the bias introduced by inferring bimrock block sizes from an outcrop face is to use an apparent radius, which is the radius of the circle formed by a sphere (representing a bimrock block) intersecting a plane (representing an outcrop face). The mean apparent radius of a group of spheres that have a true radius r and are randomly oriented relative to the outcrop plane can be found by solving the equation for a circle

$$x^2 + y^2 = r^2 \quad \text{.....[1]}$$

for y and then evaluating the expression

$$\bar{r}_{1D} = \frac{1}{r}\int_0^r y\,dx = \frac{1}{r}\int_0^r \sqrt{r^2 - x^2}\,dx = \frac{r\pi}{4} \quad \text{.....[2]}$$

The mean apparent radius for randomly located spheres cut by a planar outcrop face is therefore approximately 3/4 r. If the underlying block population can be approximated as a group of uniform spheres, then the calculation of the true block radius from a population of apparent block radii is trivial and the outcrop effect is consistent because apparent radii observed in outcrops will always be less than the true radii of the spheres.

Real bimrock blocks, however, are in general neither spherical nor uniformly sized and naïve inferences based on an assumption of uniformly sized spherical boulders can significantly over- or under-estimate effective radii and block size distributions of non-spherical blocks. Because of these complications, there exist no direct solu-

DER BESSERE WEG.

Plasser & Theurer entlastet die Straße. Das Verladesystem der MFS-Serie unterstützt die Materialbewältigung im Gleis- und Tunnelbau. Die Einheiten können in beliebiger Anzahl zusammengestellt werden: als Förderbandstraße, als Silo mit nahezu unbegrenzter Speicherkapazität oder als Kombination beider.

Plasser & Theurer
Export von Bahnbaumaschinen Gesellschaft m.b.H.
A-1010 Wien · Johannesgasse 3 · Tel. (+43) 1 515 72 - 0 · Telefax (+43) 1 513 18 01

Plasser & Theurer

tions to the inverse problem of reconstructing 3D block size distributions from 1D borehole or 2D outcrop measurements. If something is known about block shape and orientation, and perhaps the true block size distribution, then several indirect methods can be used to infer 3D distribution statistics from borehole or outcrop measurements (10, 11). These methods use numerical Monte Carlo simulations to generate populations of 3D blocks, from which apparent block size distributions are calculated and compared to the distributions of block sizes observed in outcrops or thin sections. There does not appear to exist, however, a simple but universal empirical conversion factor that will allow the practicing engineer or geologist to reliably infer 3D block size distributions from 1D or 2D samples of non-spherical blocks. Indeed: as shown below, a major conclusion of this paper is that the practitioner should be wary of using any such conversion factors without understanding the underlying assumptions.

Method

The results described in this paper were obtained using Monte Carlo simulations of ellipsoids (representing bimrock blocks or, as they are referred to in this paper, blocks) cut by planes (representing outcrop faces) as illustrated in Figure 2. For each simulation, 100 randomly oriented ellipsoids were generated. Then, the ellipse formed by the intersection of each ellipsoid with a planar outcrop face was determined, apparent equivalent radii were calculated in order to represent each block size with a single scalar, and summary statistics such as the mean apparent block size and the apparent block volume were calculated. In contrast to the apparent block size used in this paper, Medley (8) and Medley and Lindquist (12) used the maximum observed dimension to characterize the sizes of bimrock blocks. Haneberg (13) gives details of the derivations and Monte Carlo simulations that are summarized below, and an analogous exercise can be performed to evaluate the apparent block size distributions produced by the intersection of linear boreholes with ellipsoidal blocks (W.C. Haneberg, 2004, unpublished data).

The general expression for an ellipsoid with arbitrary orientation and semi-major axes a, b, and c is (14):

$$\left(X-U\right)\cdot R^{T}\cdot V\cdot R\cdot\left(X-U\right)=1 \quad \text{.....[3]}$$

in which X = {x, y, z} is a vector containing the three Cartesian coordinate directions, U = {Δx, Δy, Δz} is a displacement vector describing the center of the ellipsoid relative to the coordinate system origin.

The shape matrix V is a diagonal matrix containing the lengths of the three semi-major axes of the ellipsoid

$$V=\begin{bmatrix} a^{-2} & 0 & 0 \\ 0 & b^{-2} & 0 \\ 0 & 0 & c^{-2} \end{bmatrix} \quad \text{.....[4]}$$

Equation [3] can be written for the special case of a sphere by letting a = b = c in equation [4].

The rotation matrix R contains information about the angular orientation of the ellipsoid relative to the coordinate system and, as illustrated below, is the product of three component rotation matrices that can be defined using several different conventions. This paper will use roll, pitch, and yaw angles that have physical meanings and will be familiar to readers who have sailed a boat or flown an airplane. Roll (ψ) is the amount of rotation of the ellipsoid about the x axis, pitch (ϕ) is that about the z axis, and yaw (θ) is that about the y axis. R can be written as the dot product of roll, pitch, and yaw matrices

$$R=R_{roll}\cdot R_{pitch}\cdot R_{yaw} \quad \text{.....[5]}$$

in which

$$R_{roll}=\begin{bmatrix} 1 & 0 & 0 \\ 0 & \cos\psi & \sin\psi \\ 0 & -\sin\psi & \cos\psi \end{bmatrix} \quad \text{.....[6]}$$

$$R_{pitch}=\begin{bmatrix} \cos\phi & \sin\phi & 0 \\ -\sin\phi & \cos\phi & 0 \\ 0 & 0 & 1 \end{bmatrix} \quad \text{.....[7]}$$

$$R_{yaw}=\begin{bmatrix} \cos\theta & 0 & \sin\theta \\ 0 & 1 & 0 \\ -\sin\theta & 0 & \cos\theta \end{bmatrix} \quad \text{.....[8]}$$

The outcrop effect can be simulated by setting either x, y, or z = 0 in equation [3], which changes the equation from one describing an ellipsoid to one describing an ellipse lying in the plane of the other two coordinate axes. In the examples that follow, the outcrop effect was accomplished by setting z = 0 to obtain the equation for an ellipse in the x-y plane representing an outcrop face. Then, the offset Δz was varied randomly to simulate the effect of blocks located different distances from the outcrop plane. The equation for an inclined ellipse that is produced by setting, for example, z = 0 has the form

$$C_1 x^2 + C_2 xy + C_3 y^2 = 1 \quad \text{.....[9]}$$

in which C_1, C_2, and C_3 are real coefficients. At this point, equation [9] can be plotted for each ellipse to produce a graphical representation of the apparent block size distribution arising as a consequence of the outcrop effect. Calculation of the size of each ellipse requires additional work to determine its semi-axes, from which its area and apparent block size can be calculated. The two semi-axes of the ellipse are given by

$$\begin{Bmatrix} \hat{a} \\ \hat{b} \end{Bmatrix} = \frac{1}{\sqrt{\lambda}} \quad \text{.....[10]}$$

in which λ is a vector containing the two eigenvalues of the matrix

$$\begin{bmatrix} C_1 & C_2/2 \\ C_2/2 & C_3 \end{bmatrix} \quad [11]$$

It is convenient to represent the volume of the blocks using a scalar that has the same units for both the original ellipsoids and the ellipses formed on the outcrop plane. This can be accomplished using an equivalent radius, which is the radius of a circle having the same area as the ellipse or the radius of a sphere having the same volume as the ellipsoid. The equivalent radius of an ellipse in the outcrop plane, which is also by definition an apparent radius, is

$$r_{2D} = \sqrt{\hat{a}\,\hat{b}} \quad [12]$$

whereas the equivalent radius of the original ellipsoid is given by

$$r_{3D} = \sqrt[3]{a\,b\,c} \quad [13]$$

The equivalent radius of an ellipse formed by the intersection of an ellipsoid with a plane is an apparent equivalent radius because its value will depend on the orientation and position of the ellipsoid relative to the outcrop plane. The equivalent radius of the ellipsoid, however, is not apparent because it is calculated using the actual values of a, b, and c. Once equivalent radii have been calculated for all of the ellipsoids and ellipses in a simulation, the mean block size, block sorting, and other standard size distribution measures can be calculated and compared to evaluate the degree of bias introduced by the outcrop effect.

Table 1 Geometric variables for the four Monte Carlo simulations.
Tabelle 1 *Geometrische Variablen für die vier Monte Carlo Simulationen.*

Case	Axial ratio a : b : c	Equivalent radius size distribution	Outcrop offset	Roll ψ	Pitch ϕ	Yaw θ
I	3 : 2 : 1	constant	$0 \le \Delta z \le 1$	0°	0°	0°
II	3 : 2 : 1	constant	$0 \le \Delta z \le 1$	± 10°	± 10°	± 10°
III	3 : 2 : 1	constant	$0 \le \Delta z \le 1$	± 45°	± 45°	± 45°
IV	3 : 2 : 1	Pareto	$0 \le \Delta z \le 1$	± 45°	± 45°	± 45°

To illustrate the calculation of equivalent radii, consider an ellipsoid with semi-axes a = 5, b = 3, and c = 1 that is rotated 20° about the z-axis and intersects the x-y plane at z = 0. The ellipse formed by the intersection of the ellipsoid and the outcrop plane is

$$1 = 0.0483\,x^2 - 0.0457\,xy + 0.103\,y^2 \quad [14]$$

which has the coefficient matrix eigenvalues λ ={0.111, 0.040} and, from equation [10], semi-axes $\hat{a}$ = 5 and $\hat{b}$ = 3. Note that in this case $\hat{a}$ =a and $\hat{b}$ = b because there was no rotation around the x or y axes. In general, this will not be true. The apparent equivalent radius in the plane of the outcrop is, using equation [12], $r_{2D} = (5 \cdot 3)^{0.5} = 3.87$, which is larger than the ellipsoid equivalent radius of $r_{3D} = (5 \cdot 3 \cdot 1)^{0.33} = 2.47$ obtained from

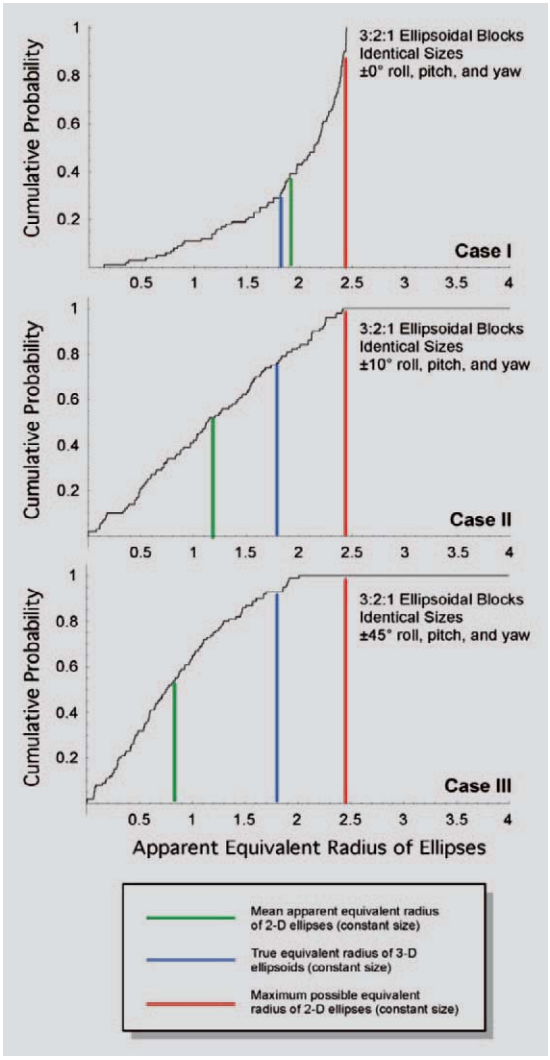

Fig. 3 Apparent cumulative size distribution curves for 2D ellipses produced by the outcrop effect for case I, II, and III Monte Carlo simulations of 3D ellipsoids with uniform size located at random distances from the outcrop face. Red line: maximum possible apparent equivalent radius of an ellipse formed by the intersection of a 3 : 2 : 1 ellipsoid with the outcrop plane. Blue line: True equivalent radius of a 3 : 2 : 1 ellipsoid. Green line: Mean apparent equivalent radius of ellipses in each simulation. Variables as described in Table 1.

Bild 3 *Summengrößenverteilungskurven für zweidimensionale Ellipsen, entstanden durch den Aufschlusseffekt für die Fälle I, II und III der Monte Carlo Simulationen von dreidimensionalen Ellipsoiden gleicher Größe mit underschiedlicher Entfernung von der Aufschlussfläche. Rote Linie: größtmöglicher äquivalenter Radius, der bei der Verschneidung eines 3 : 2 : 1 Ellipsoids mit der Aufschlussfläche entsteht. Grüne Linie: Mittlerer äquivalenter Radius für Ellipsen in jeder der Simulationen. Variablen siehe Tabelle 1.*

equation [13]. In this case, therefore, the outcrop effect would lead one to underestimate the largest dimension of the ellipsoid but overestimate the equivalent block radius of the ellipsoid.

Results

The results of four test cases illustrate the degree of bias that can be introduced by the outcrop effect (Table 1). Block orientation was allowed to vary but block size was held constant in the first three cases. In the fourth case, block sizes were specified using a fractal-like Pareto distribution of equivalent radii to simulate the apparent "well-graded" block size distribution that might arise from the fragmentation and shearing leading to the formation of a melange, fault rock, or perhaps landslide debris. Ellipsoids with semi-axis ratios of 3 : 2 : 1 were used in all of the simulations described in this paper, with the long and intermediate semi-axes of the ellipsoids originally parallel to the x-y outcrop plane. This corresponds to a bimrock with bullet- or torpedo-shaped ellipsoidal blocks. The outcrop offset for each ellipsoid was chosen at random from a uniform distribution with $0 \le \Delta z \le 1$. Haneberg (13) describes the results of a similar set of simulations using ellipsoids with 5 : 3 : 1 axial ratios.

The ellipsoids generated in Case I were offset from the outcrop face but not rotated ($\psi = \phi = \theta = 0$). As shown in Figure 3, the apparent cumulative block size distribution curve inferred from the ellipses in the outcrop plane overestimates the mean equivalent radius by approximately 5 % and overestimates the total block volume by 45 %, which is consistent with the concave-upward cumulative distribution curve that asymptotically approaches the maximum possible equivalent block size of $(3 \cdot 2)^{0.5} = 2.45$ length units (red lines in Figure 3). The blue lines in Figure 3 show the equivalent radius of the identically sized 3D ellipsoids, which is $(3 \cdot 2 \cdot 1)^{0.33} = 1.82$.

It is important to note that in the cumulative plots for cases I, II, and III there is no corresponding cumulative distribution for the 3D ellipsoids because the ellipsoids are all the same size; the apparent size distribution curve for the blocks is solely a result of the outcrop effect. The over-prediction of mean block size and total block volume is in part an artifact of the initial ellipsoid orientation relative to the outcrop plane. Had the intermediate and short axes been placed parallel to the outcrop, the ellipses in the outcrop plane likely would have underestimated the mean block size and volume.

If the roll, pitch, and yaw angles are all allowed to vary uniformly over a range of ± 10° as in case II, however, the cumulative distribution curve approaches a straight line up to the theoretical limit of 2.45 (see Figure 3). The outcrop effect leads to an under-estimation of the mean equivalent radius by 35 % and under-estimation of the total block volume by 44 % in this simulation. As above, different results would have been obtained had the initial orientation of the ellipsoids or their axial ratios been different.

Rotation of the ellipsoids with roll, pitch, and yaw angles drawn from uniform distributions ranging over ± 45° (case III) leads to a similar under-estimation of 54 % for the mean equivalent radius and 76 % for the total block volume. The three apparent block size distribution curves in Figure 3 show that the mean block size and total block volume errors increase as block orientation becomes more irregular even if the underlying 3D block size does not change.

Results from cases I, II, and III show the complexity that can arise due solely to the orientation and position of a population of identically sized ellipsoidal blocks relative to an outcrop face. The block size distribution of bimrocks such as melange and fault rocks, though, can be simulated using Pareto distributions that are closely related to fractal size distributions (15). Medley and Lindquist (12), in particular, discussed the engineering implications of fractal bimrock block size distributions.

The probability density function (PDF) of a Pareto distribution as implemented in the software used to perform the calculations in this paper is, using an approach described by Haneberg (13):

$$\mathrm{PDF}(r_{3D}) = \alpha\, k^{\alpha}\, r_{3D}^{-(1+\alpha)} \qquad r_{3D} \ge k \quad \ldots\ldots\ldots\ldots [15]$$

in which r_{3D} is the equivalent radius of an ellipsoid being simulated, $k > 0$ is the minimum possible radius, and α is a shape parameter that is equivalent to the fractal dimension of the distribution. This formulation is slightly different than the Pareto distribution given in some references, which assume a minimum value of zero and shift the abscissa by an increment k. The shape of the PDF curve and the geometric significance of α, however, are the same in both versions.

Published estimates of fractal dimensions for artificially and naturally produced rock fragments range from about 1.9 to 3.5, with a mean value in the range of 2.5 to 2.6 (15). Medley and Lindquist 12) estimated a fractal dimension of 2.3 for Franciscan Complex melanges in northern California. In this study, a value of $\alpha = 2.5$ was chosen as a typical fractal dimension for the case IV simulation. In order to generate a Pareto distribution with an average block size similar to those in cases I, II, and III, the mean equivalent radius of the Pareto-distributed blocks was set equal to the equivalent radii of the blocks used in the first three simulations $\bar{r}_{3D} = (3 \cdot 2 \cdot 1)^{0.33} = 1.82$. The analytical expression for the mean of the Pareto distribution is

$$\bar{r}_{3D} = \frac{k\,\alpha}{\alpha - 1} \quad \text{.....[16]}$$

Assuming a value of $\alpha = 2.5$, setting equation [16] equal to 1.82, and solving for k yields the value of k = 1.12, which was used in the case IV simulation.

The Case IV simulation results show the amount of complexity that is added to outcrop patterns when real block sizes are of random dimensions as well as the blocks having random orientation and position relative to the outcrop face (Figure 4). This situation is more typical of the disorder common in many bimrocks than are cases I, II, and III. In this simulation, the mean apparent equivalent radius was underestimated by 54 % and the total block volume was underestimated by 89 %. Comparison of the ellipsoid and ellipse cumulative distribution curves also shows that 21 % of the Pareto-distributed ellipsoids are likely to have equivalent radii greater than the largest value calculated from the 100 ellipses seen in the simulated outcrop. The probability that the largest ellipsoid in the underlying Pareto distribution has an equivalent radius more than twice as great as the largest block inferred from the ellipses in the outcrop plane is approximately 8 %. This result has significant economic and constructability implications for earthwork, excavation, or tunneling projects in which the size of the largest block expected to be encountered during excavation is inferred solely from uncorrected outcrop or borehole data.

Conclusions

The inference of 3D bimrock block size distributions from 2D outcrop maps and, although not described here, 1D borehole logs without supplementary 3D rock mass fabric data, has the potential to produce significant errors in estimated mean block sizes, maximum block sizes, and total block volumes. Results of the simple Monte Carlo simulations described in this paper suggest that inferred mean block sizes may be in error by as much as 50 % and block volumes by as much as 90 %. Perhaps most importantly for design and construction planning, outcrop or borehole sampling will almost inevitably underestimate the largest block likely to be encountered during a project. The sizes and volumes of spherical blocks will in all cases be under-estimated by outcrop sampling. The sizes and volumes of mildly elongated ellipsoidal blocks will tend to follow the

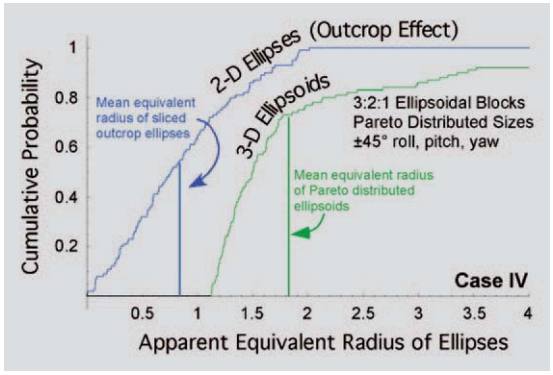

Fig. 4 Apparent cumulative size distribution curves for 2D ellipses produced by the outcrop effect for case IV Monte Carlo simulation of 3D ellipsoids with Pareto-distributed equivalent radii located at random distances from the outcrop face. Variables as described in Table 1.

Bild 4 *Summengrößenverteilungskurven für zweidimensionale Ellipsen, entstanden durch den Aufschlusseffekt für Fall IV der Monte Carlo Simulationen von dreidimensionalen Ellipsoiden mit nach Pareto-verteilten äquivalenten Radien mit unterschiedlicher Entfernung von der Aufschlussfläche (Variablen siehe Tabelle 1).*

same pattern of under-estimation, although exceptions are possible if the two longest axes of the ellipsoids are nearly parallel to the outcrop face. Perhaps most importantly, simple empirical measures relating factors such as apparent 1D or 2D block dimensions with actual 3D dimensions are likely to be of very limited, if any, utility to the practicing engineer or engineering geologist. These factors will depend very heavily on the block geometry and orientation, and will therefore differ from project to project.

The orientation of blocks relative to the outcrop face and block shape determine whether 2D sampling underestimates or overestimates 3D parameters. Therefore, an understanding of the 3D fabric of bimrocks should be considered an essential supplement to 2D outcrop or 1D borehole characterization projects. Knowledge of the local structural geology and regional tectonic setting of a project area, for example, can be used to estimate block orientation variability by applying spherical statistics to equal-area projections of rock fabric data. Sampling of alluvium derived from bimrocks may provide important constraints on block dimensions in cases where 3D exposures do not exist. In situations where the bimrock matrix is friable or otherwise unlithified, excavation and careful measurement of complete blocks should be considered an essential aspect of site characterization. Once this kind of information is obtained, practicing engineers and geologists can use indirect comparison methods such as those described by Sahagian and Proussevitch (10) to back-calculate true block size distributions.

References

1. Medley, E.W.: *Estimating block size distributions of melanges and similar block-in-matrix rocks (bimrocks)*. In: Hammah, R. ; Bawden, W. ; Curran, J. ; Telesnicki, M. (eds.): Proceedings of the 5th North American Rock Mechanics Symposium (NARMS), pp. 599-606, 2002.
2. Lindquist, E.S.: *The mechanical properties of a physical model melange*. In: Olivera, R. ; Rodrigues, L.F. ; Coelho, A.G. ; Cunha, A.P. (eds.): Proceedings, 7th International Congress, International Association of Engineering Geology: Lisbon, Portugal, pp. 819-826, 1994.
3. Lindquist, E.S. ; Goodman, R.E.: *Strength and deformation properties of a physical model melange*. In: Nelson, P ; Laubach, S.E. (eds.): Proceedings of the 1st North American Rock Mechanics Symposium, Austin, Texas, USA, pp. 843-850, 1994.
4. Goodman, R.E. ; Ahlgren, C.S.: *Evaluating safety of concrete gravity dam on weak rock: Scott Dam*. J. Geotechnical and Geoenvironmental Eng., Vol. 126 (2000), pp. 429-442.
5. Medley, E.: *Uncertainty in estimates of block volumetric proportions in melange bimrocks*. In: Marinos, P.G. ; Koukis, G.C. ; Tsiambaos, G.C. ; Stournaras, G.C. (eds.): Proc. International Congress, International Association of Engineering Geologists, Engineering Geology and the Environment, Athens, Greece, 1997.
6. Medley, E. ; Goodman, R.E.: *Estimating the block volumetric proportions of melanges and similar block-in-matrix rocks (bimrocks)*. In: Nelson, P.P. ; Laubach, S.E. (eds.): Proceedings of the 1st North American Rock Mechanics Symposium, Austin, Texas, USA, pp. 851-858, 1994.
7. Haneberg, W.C.: *Groundwater flow and the stability of heterogeneous infinite slopes underlain by impervious substrata*. In: Haneberg, W.C. ; Anderson, S.A., (eds.): Clay and Shale Slope Instability. Geological Society of America Reviews in Engineering Geology 10, pp. 63-78, 1995.
8. Medley, E.W.: *Engineering characterization of melanges and similar block-in-matrix rocks (bimrocks)*. Ph.D. dissertation, Department of Civil Engineering, University of California at Berkeley, 1994.
9. Medley, E.W.: *Using stereological methods to estimate the volumetric proportions of blocks in melanges and similar block-in-matrix rocks (bimrocks)*. In: Olivera, R.; Rodrigues, L.F. ; Coelho, A.G. ; Cunha, A.P. (eds.): Proceedings 7th International Congress, International Association of Engineering Geology: Lisbon, Portugal, pp. 1031-1040, 1994.
10. Sahagian, D.L. ; Proussevitch, A.A.: *3D particle size distributions from 2D observations; stereology for natural applications*. Journal of Volcanology and Geothermal Research, Vol. 84 (1998), pp. 173-196.
11. Higgins, M.D.: *Measurement of crystal size distributions*. American Mineralogist, Vol. 85 (2000), pp. 1105-1116.
12. Medley, E. ; Lindquist, E.S.: *The engineering significance of the scale-independence of some Franciscan melanges in California, USA*. In: Daemen, J.J.K. ; Schultz, R.A. (eds.): Rock Mechanics, Proceedings of the 35th U.S. Symposium, Reno, Nevada, pp. 907-914, 1995.
13. Haneberg, W.C.: *Computational Geosciences with Mathematica*. Berlin, Heidelberg, New York: Springer-Verlag, 2004.
14. Herbison-Evans, D.: *Animated Cartoons by Computer Using Ellipsoids*. University of Sydney, Basser Department of Computer Science, Technical Report 94, (online version) http://linus.it.uts.edu.au/~don/pubs/cartoon.html (2002).
15. Turcotte, D.L.: *Fractals and Chaos in Geology and Geophysics.* 2nd ed. Cambridge: University Press, 1997.

Acknowledgements

My interest in bimrock sampling and simulation was motivated by many conversations with Ed Medley, whose contributions and references are greatly appreciated. Wolfram Research, Inc. donated a copy of the Mathematica software used in this research. Thanks also to Isabelle Pawlik, PE, of Jacobs Associates, San Francisco for the German translations.

Author

William C. Haneberg, Haneberg Geoscience, 10208 39th Avenue SW, Seattle WA 98146 USA, E-Mail bill@haneberg. com

Relationships between Volumetric Block Proportions and Overall UCS of a Volcanic Bimrock

By Harun Sönmez, Candan Gokceoglu, Ergün Tuncay, Edmund W. Medley and Hakan A. Nefeslioglu

Block-in-matrix rocks (bimrocks) are mixtures of stronger blocks or rock enclosed by weaker matrix rocks (1). The overall strength of bimrocks tends to be greater than the strength of the matrix alone because the presence of blocks influences the mechanical properties above a threshold volumetric proportion of blocks (2). Therefore, the determination of the volumetric block proportion of bimrocks is of crucial importance for the estimation of their overall mechanical properties.

Three measurement methods are commonly used to determine the volumetric block proportion of bimrocks:

- One-dimensional (scanline and borehole);
- Two-dimensional (image analyses on photographs and window mapping); and
- Three-dimensional (sieve analyses).

Although the sieve analysis method is the most exact method for laboratory-scale studies, separation of blocks from the weaker matrix is often impossible, depending on the number and size of blocks, and the degree of contact strength between blocks and matrix. Accordingly, extensive studies have been performed on means of determining volumetric block proportions using one-dimensional (boreholes) and two-dimensional (image analyses and physical model) methods. These studies have revealed that the accurate determination of 3D volumetric block proportion using 1D and 2D methods is widely influenced by the amount of sampling and actual block proportion, as well as the shapes, block size distribution and orientation of the blocks (1, 3, 4).

In this study, node-counting and image classifications on grayscale and Red-Green-Blue (RGB)

Beziehung zwischen Gesteinsblockvolumen und Druckfestigkeit von vulkanischem Block-in-Matrix Gestein (Bimrock)

Der Beitrag befasst sich mit dem Zusammenhang zwischen Gesteinsblockvolumen und Druckfestigkeit von Ankara Agglomerat. Dieser Fels besteht aus überwiegend vulkanischem Gestein gemischt mit Tuffmatrix; rosafarbene und schwarze Andesitbblöcke mit harter bis sehr harter Konsistenz werden von einer Tuffmatrix mit relativ geringer Festigkeit umgeben. Das Blockvolumen wurde mithilfe eines Bildanalyseverfahrens näherungsweise ermittelt. Die rosafarbenen und schwarzen Andesitblöcke des sogenannten Bimrock (Block-in-Matrix Gestein) wiesen erhebliche Farbunterschiede zur Tuffmatrix auf, was die Bildanalyse von schwarz-weiß und RGB Farbfotoaufnahmen von Aufschlüssen wesentlich erleichterte. Die mithilfe des Bildanalyseverfahrens ermittelten Gesteinsblockabmessungen wurde mit den Schätzungen verglichen, die durch Anwendung der nulldimensionalen „Knotenzählmethode" ermittelt wurden. Aufgrund der annähernden Gleichförmigkeit der Vulkangesteinsblöcke kann angenommen werden, dass die zweidimensionalen Abmessungen des Gesteinsblocks, ermittelt durch die Messung anhand von Fotoaufnahmen, dem Blockvolumen entsprechen. Das gemessene Gesteinsblockvolumen wurde zur annäherungsweisen Bestimmung der einachsigen Druckfestigkeit von Ankara Agglomerat als Funktion des Volumengehalts eines Gesteinsblock verwendet. Hierzu wurden auf Regression basierende Gleichungen entwickelt. Das Verhältnis zwischen dem Blockvolumen und der Druckfestigkeit von Ankara Agglomerat hat einen nicht linearen Verlauf, was darauf schließen lässt, dass die Gesamtfestigkeit des Bimrock von der Festigkeit der einzelnen Gesteinblocktypen abhängt. Diese Abhängigkeit mag bedingt sein durch die underschiedlichen Festigkeitseigenschaften zwischen Gesteinsblöcken und Felsmatrix und erfordert weiterreichende Untersuchungen.

This paper describes a study into the relationship between volumetric block proportions and unconfined compressive strength (UCS) of Ankara Agglomerate, a volcaniclastic block and tuff matrix mixture containing relatively weak tuff matrix surrounding stronger pink andesite blocks and very strong black andesite blocks. Volumetric block proportions were estimated using image analysis methods. The pink and black andesite blocks in the bimrock exhibited significant color contrasts with the tuff matrix, which facilitated image analysis of grayscale and RGB colored photographs of outcrops. Estimates of block proportions from image analysis were checked against estimates generated using the zero-dimensional "node-counting method". 2D block proportions estimated from measurements of photographs were considered to be equivalent to the volumetric block proportions because the volcanic blocks were approximately equi-dimensional. The measured volumetric block proportions were incorporated into a further stage of the study by developing regression-based equations to estimate the overall uniaxial compressive strength of Ankara Agglomerate as a function of volumetric block proportions. The non-linear relationship between volumetric block proportions and overall UCS of Ankara Agglomerate, suggests a dependence between overall UCS of the bimrock and the strengths of the different types of blocks. This dependence may be due to variations in block/matrix strength contrasts and requires further study.

Table 1 Statistical evaluations of uniaxial compressive strength (UCS) and unit weight (γ) for the constituents of Ankara Agglomerate (5, 13).

Tabelle 1 *Statistische Auswertungen von einachsiger Druckfestigkeit (UCS) und Wichte (γ) für Bestandteile des Ankara Agglomerats (5, 13).*

Statistical parameter	γ [kN/m³]	UCS [MPa]
Black Andesite Blocks		
Number of samples	35	33
Average	24.30	91.09
Standard deviation	0.231	11.62
Minimum	23.84	72.15
Maximum	24.70	119.89
Pink Andesite Blocks		
Number of samples	16	16
Average	22.66	49.85
Standard deviation	0.936	11.44
Minimum	21.03	33.99
Maximum	23.35	78.03
Tuff Matrix		
Number of samples	23	21
Average	16.88	10.55
Standard deviation	0.883	1.89
Minimum	15.17	6.41
Maximum	18.23	14.42

Fig. 1 Outcrop of volcanic block and tuff mixture (PA: pink andesite blocks, BA: black andesite blocks; T: tuff).

Bild 1 *Aufschluss einer Vulkangesteinsblock- und Tuffmischung (PA: rosafarbene Andesitblöcke, BA: schwarze Andesitblöcke; T: Tuff).*

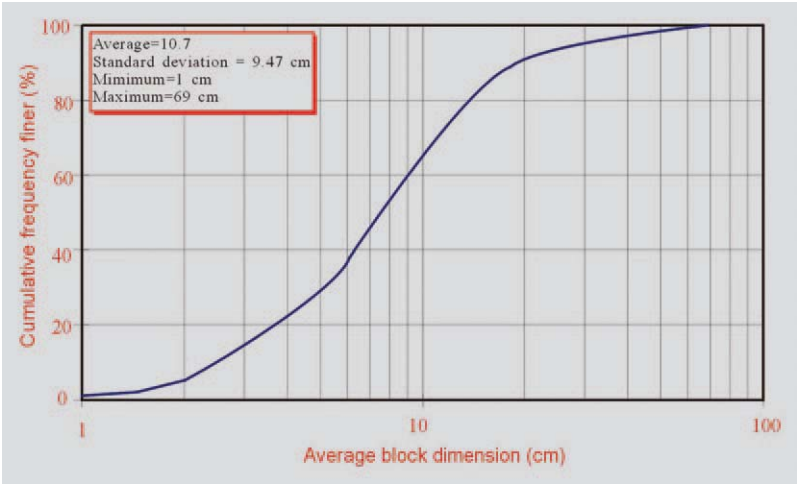

Fig. 2 Block-size distribution of andesite blocks in volcanic block and tuff mixture.

Bild 2 *Blockgrößenverteilung von Andesitblöcken in Vulkangesteinsblock- und Tuffmischung.*

colored photographs were performed to determine the volumetric block proportion of Ankara Agglomerate, a volcanic block and tuff mixture, which according to the criteria of Medley (1, 3), is a bimrock at laboratory and outcrop scales. The longest and shortest observable dimensions of the blocks were measured from photographs taken from different locations and orientations, in order to evaluate the shape of the blocks as well as identify the relationships between 2D block proportion obtained from photographs, and an estimate of the 3D volumetric block proportions.

The general procedure outlined in this paper was used to generate estimates of volumetric block proportions, which were then incorporated into a conceptual approach for the determination of the overall UCS of Ankara Agglomerate (5, 13), the preliminary results of which are reported in this paper.

Properties of the volcanic block and tuff mixture

Ankara Agglomerate is a volcaniclastic block and tuff mixture composed of pink (lighter) and black (darker) andesite blocks ranging in size from a few centimeters to about one meter (Figure 1). The blocks are cemented by weak tuff matrix. To determine the engineering properties of the constituents of the volcanic block and tuff mixture, a series of laboratory tests were performed on specimens of the pink and black andesite blocks and tuff matrix, collected from a site in Ankara, Turkey (5). The uniaxial compressive strength (UCS) and unit weight tests on the blocks and tuff were performed in accordance with the suggested method of ISRM (6). The results of the tests are summarized in Table 1. The average values of UCS for pink and black andesite blocks are 49.9 and 91.1 MPa, respectively, and that of the tuff matrix is 10.6 MPa. The minimum and maximum ratio of UCS of blocks to the UCS of tuff matrix is 2.4 and 18.7, respectively. Furthermore, a total of 270 NX-size core samples of Ankara Agglomerate were tested in accordance with the ISRM procedure (6) to obtain the overall UCS values of Ankara Agglomerate. The maximum and minimum UCS values of Ankara Agglomerate were 5.7 and 55 MPa, respectively, and the average UCS value was 24.9 MPa.

Medley (1) has suggested a threshold value of at least 2 for the ratio of UCS of block to UCS of matrix for a geological rock mixture to be considered as a bimrock. The UCS data of the constituents of the volcanic block and tuff mixture (see Table 1) clearly indicates that there was significant mechanical contrast between blocks and matrix, and that the volcanic block and tuff mixture investigated could be evaluated as a bimrock.

In addition, Medley (1) has also suggested that in a bimrock at the scale of engineering interest, the size and volume of blocks be sufficient to affect the overall properties of the mixture. Medley

(1) also suggested that at any scale of interest being considered ("characteristic engineering dimension"), blocks would range between 5 and 70 % of that scale. The 2D measurements of blocks in the Ankara Agglomerate revealed that the block sizes ranged between 1 and 69 cm (mean value, 10.7 cm), as indicated in the block-size distribution graph shown as Figure 2. Blocks ranged to about 1 m in size in observed outcrops. Hence, at the characteristic engineering dimensions of the laboratory test specimens (cm scale), the Ankara Agglomerate is a bimrock, because block sizes occupied the full 5 to 70 % range in laboratory scale. However, at the scale of an outcrop (for example, 10 m height) Ankara Agglomerate has "small blocks" limited to between 0.5 and 1 m in size.

The results of this study, based on laboratory scale specimens and photographs of outcrops are applicable to larger volumes of the Ankara Agglomerate if it can be demonstrated that the Ankara Agglomerate has some scale-independence in block size distributions (1, 7).

Determination of volumetric block proportions by image analysis

Previous research (2) revealed that the overall strength of a bimrock mass having between about 25 and 70 % volumetric block proportion is directly related to the volumetric block proportion, with no dependence on the strength of the blocks. Below 25 % the strength can be taken as that of the matrix (2). Accordingly, for the purposes of study into the geomechanical behavior of Ankara Agglomerate (5, 13), the overall strength of the volcanic block and tuff mixture was assumed to be primarily dependent on the volumetric proportion of andesite blocks. It was thus vital that the volumetric block proportions be determined.

In some bimrock materials at laboratory scale, careful sieve analysis can be used to separate hard blocks from weak matrix to obtain representative block size distributions and volumetric block proportions (8). However in this study, separation of the andesite blocks from weak tuff matrix was impossible because of the weak welding ("cementation") between the volcanic blocks and matrix. Instead of physically separating block and matrix constituents, image analysis methods were used to estimate the volumetric block proportions. Advantage was taken of previous research where 1D scan-line surveys, and node-counting (zero dimensions) and 2D image analyses have also been used to estimate volumetric block proportions (1, 3, 4, 9). Based on correlations between 1D, 2D and 3D evaluations these earlier studies indicate that the quantity of sampling, the actual volumetric block proportion, and the shape and orientation of blocks control uncertainties in estimation of volumetric block proportion (1, 9).

To define the block dimensions and shapes of the volcanic block and tuff mixture, the longest and shortest dimensions of individual block were measured from scanlines oriented at different directions across photographs taken of different outcrops of the Ankara Agglomerate. As shown in Figure 3, 75 % of the measured blocks have 2D major:minor dimension ratios less than 1.2, which indicated that the blocks are approximately equi-dimensional in 2D and 3D. The rationale for this assumption was that the fragmented, volcaniclastic genesis of the bimrock resulted in probable random block orientations within the rock mass, and that the many measurements in 2D sufficiently captured 3D block dimensions. In that case, the uncertainties in the estimation of 3D block proportions, based on 2D measurements, would be less than those for bimrocks with ellipsoidal blocks such as melanges studied by Medley (1, 9) or the idealized mixtures analyzed by Haneberg (12).

To estimate the volumetric block proportions of the volcanic block and tuff mixture at field scale, image classifications and node-counting methods were performed on grayscale and RGB colored photographs of the bimrock. For this purpose, scaled photographs were taken perpendicular to nearly planar exposures of Ankara Agglomerate (see Figure 1). The overall objec-

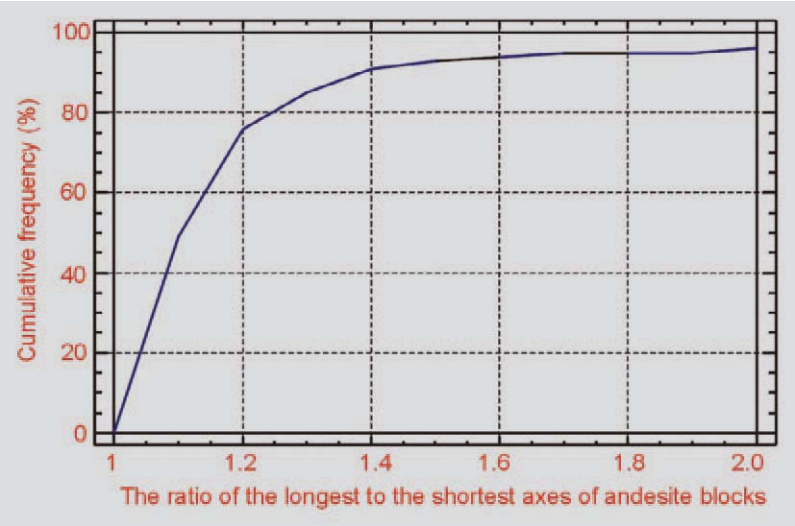

Fig. 3 Cumulative frequency distribution of the ratio of the lengths of longest axes to lengths of shortest axes of andesite blocks.

Bild 3 *Summenhäufigkeitsverteilung des Längenverhältnisses von längster zu kürzester Hauptachse von Andesitblöcken.*

tive of image classification procedures is to automatically categorize pixels into classes or themes (10) using "unsupervised classifications" or "supervised classifications". In the unsupervised approach, the image data are first classified by aggregating them into the natural spectral (tonal) grouping or clusters present in the image (10), whereas supervised classification involves a training step followed by a classification step. In this study, the supervised image classification method of training, classification and output stages were performed for the determination of the pink block, black block and tuff matrix constituents of the Ankara Agglomerate, using both grayscale and colored photographs of outcrops exposures.

The colored photographs of agglomerate exposures (outcrops and drill core) were scanned in RGB and grayscale with high resolution. Some known constituents on parts of the colored images were first defined in the training stage of image classification (Figure 4a). In the training stage of the grayscale photographs, the pixel value ranges of each constituent were determined within the overall grayscale tonal spectrum of 0 to 255 grayscale shades. The black andesite has a range of grayscale pixel values of 0 to 61 in. Except for some small deviations in the unweathered core samples, the range of grayscale pixel values for the tuff and pink andesite is generally between 62 to 115 and 116 to 255, respectively, according to the image analyses performed by Gokceoglu and others (11). In the second stage, whole images were classified on the

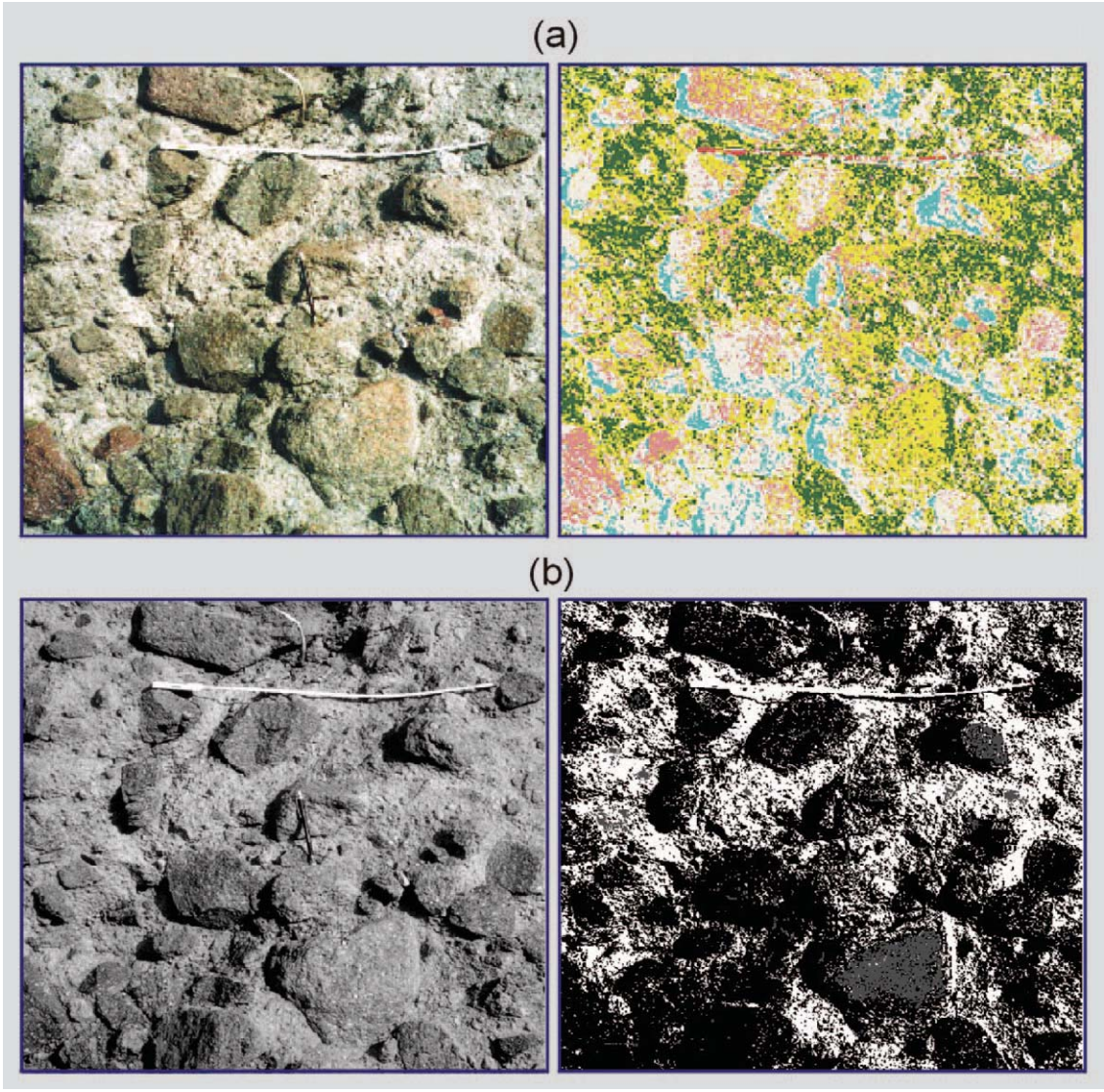

Fig. 4 Original and classified views of Ankara Agglomerate exposures (a) RGB colored image and (b) grayscale image (white scale bar is 1 m long).

Bild 4 *Original und klassifizierte Ansichten von Ankara Agglomerat Aufschlüssen: a) RGB Farbfotoaufnahmen und b) Schwarz-weiß Aufnahmen (weiße Messskala entspricht 1 m).*

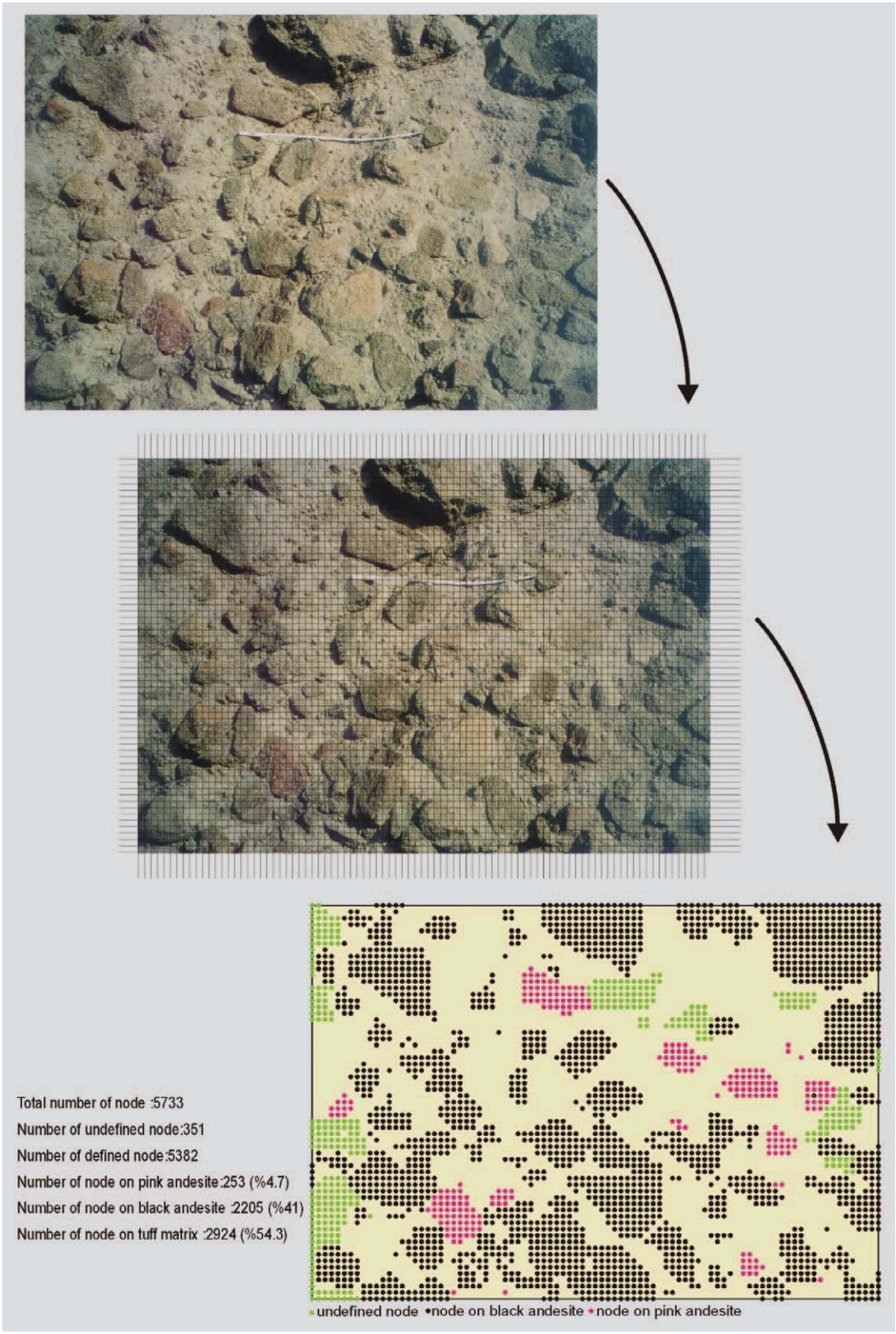

Fig. 5 Stages of the node-counting classification.

Bild 5 *Phasen der Knotenzählzuordnung.*

basis of the results of the training stage. Each pixel in the image data set was categorized into the constituents (Figure 4b) using a minimum-distance-to-means classifier, since the minimum-distance-to-means strategy is mathematically simple and computationally efficient (10).

In the node-point-counting method, a mesh having squares of 1 cm^2 was overlaid on the photographs (Figure 5). At each intersection (node) of the mesh, the underlying material was visually classified as being tuff, black andesite or pink andesite. (This method is similar to point-counting performed by mineralogists and petrologists using rock thin sections viewed through microscopes in order to determine mineralogical proportions necessary to petrographically classify

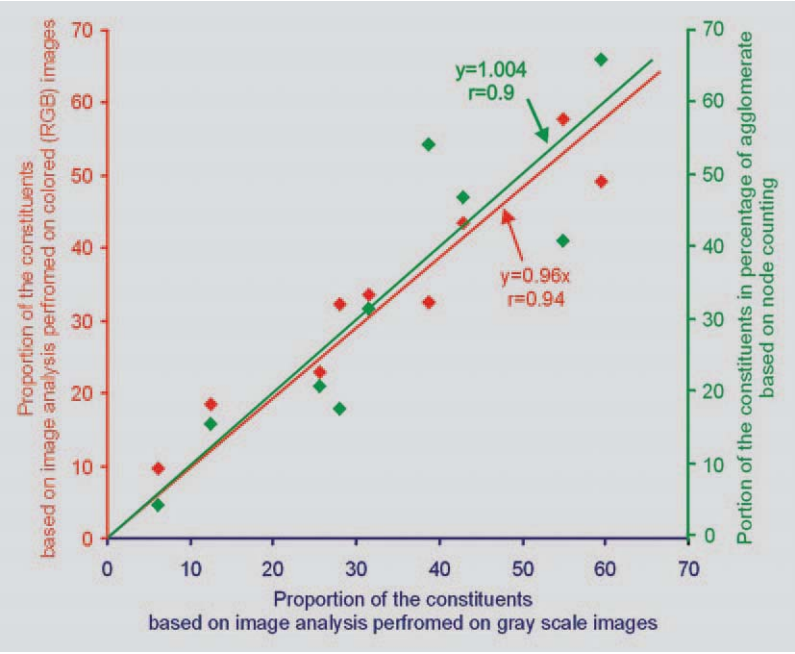

Fig. 6 Cross-check between proportions of the constituents of agglomerate estimated from the image analysis method performed on grayscale images, compared to estimates based on image analyses performed RGB colored images (red plot), and the node-counting method (green plot).

Bild 6 *Überprüfung der Größenverhältnisse von Agglomeratbestandteilen, geschätzt anhand Bildanalyse von Schwarz-weiß Aufnahmen, im Vergleich zu Schätzungen mithilfe der Bildanalyse von RGB Farbbildern (rote Linie), und Knotenzählmethode (grüne Linie).*

the rock sampled by the thin section.) The percentages of each constituent of the agglomerate exposures were determined by dividing the number of node intersections for each constituent by the total number of intersections of the mesh (see Figure 5).

A cross-check between the proportions of the constituents obtained from image classification employed on grayscale and colored photographs showed that similar estimations of the proportion of the constituents was obtained (Figure 6). As can be seen from Figure 6, there is no significant difference between the two methods, hence the more practical image classification method was used to obtain further estimates of volumetric block proportions of the volcanic block and tuff mixture.

Preliminary evaluation of the UCS of Ankara Agglomerate

The volumetric block proportion data described in this paper are being used to develop relationships between volumetric block proportions and overall UCS for Ankara Agglomerate (13). The proportion of the constituents of Ankara Agglomerate core samples were determined by using grayscale image analysis performed on both halves of split core samples.

In a further stage of the study, the relation between block proportions and the UCS values of the Ankara Agglomerate core samples was evaluated. It was also of interest to determine if there was any dependence between overall UCS and strengths of the two block types. In other words, since black andesite is stronger than pink andesite, it was assumed that the mechanical influence of stronger black andesite blocks on the overall UCS could be higher than the influence of the weaker pink blocks.

The sum of the proportions of black and pink andesite blocks was equal to the total volumetric block proportion in the specimens. However, a composite block proportion was used to study the differences in overall UCS due to differences in the proportions of the two different block types. A weighted "equivalent block proportion", or EBP, accommodates two or more types of blocks differing in individual mechanical properties:

$$EBP = \sum_{i}^{n} VP_i \frac{UCS_i}{UCS_{max\_block}} \quad \text{.....[1]}$$

where VP is the volumetric block proportion of i^{th} block, UCS is the uniaxial compressive strength, n is the number of different types of blocks, and UCS_{max_block} is the uniaxial compressive strength of the stronger block type.

The uniaxial compressive strengths of the Ankara Agglomerate specimens were then normalized by dividing them by the average uniaxial compressive strength of the matrix: this parame-

ter is denoted as UCS_N. The distributions of the data between EBP and UCS_N are illustrated in Figure 7.

Two exponential type equations were obtained by regression analyses of the data of shown in Figure 7:

$$UCS_N = 1.3361\exp(1.12 \times EBP) \quad \text{.....[2]}$$

$$UCS_N = \exp(1.6874 \times EBP) \quad \text{.....[3]}$$

As shown in Figure 7, the regression line forced to intersect to value of "1" on the y axis (data pair of EBP=0, UCS_N=1) yields a trend that is more slightly more representative of the data than the unforced trend. The relationship of Figure 7 is non-linear, particulary above about 70 % equivalent block proportion, suggesting that the dependence of overall bimrock strength on block proportion is more complex than previously understood. The plot also indicates that at high equivalent block porportions the overall bimrock becomes uniformally stronger, with less data scatter. This behavior supports the recommendation of Medley (1), based on the work of Lindquist and Goodman (2), that at high volumetric block proportions (greater than about 70 to 75 %), block/matrix rock mixtures should be considered as a blocky rock masses with wide infilled joints, for which fabric conventional rock engineering methods should be applied.

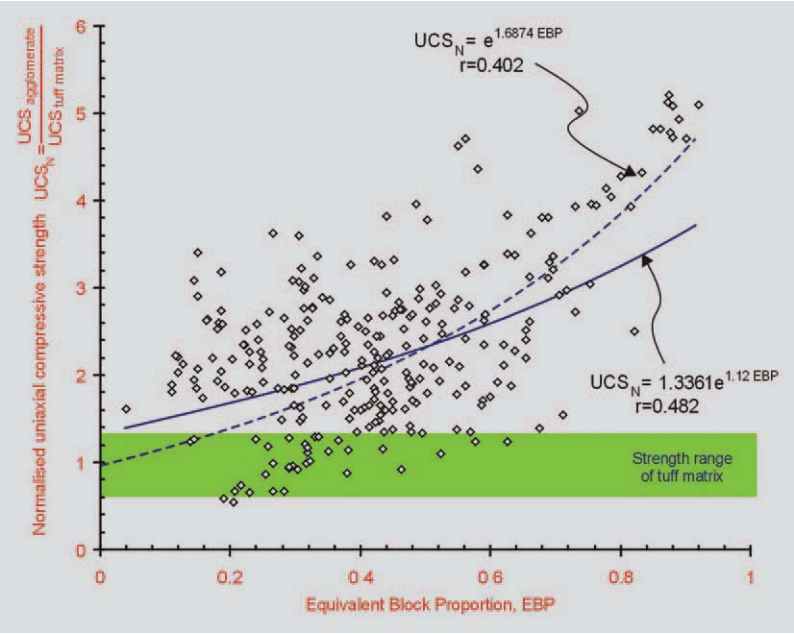

Fig. 7 Relationships between equivalent block portion (EBP) and UCS of Ankara agglomerate. Trend forced through intercept (0, 1) is slightly more representative of data.

Bild 7 *Beziehungen zwischen äquivalentem Blockanteil (EPB) und Druckfestigkeit von Ankara Agglomerat. Verlauf durch Schnittpunkt (0,1) repräsentiert Daten etwas besser.*

The preliminary work also revealed an apparent but unexpected relationship between the strength of the blocks and the overall UCS for the two different types of blocks. Until now it has been assumed that overall bimrock strength is

not influenced by block strength, as long as there is sufficient block/matrix strength contrast to force failure surfaces around blocks (1, 2). However, this study shows that the interaction between blocks and matrix is more complex than previously assumed, and that block/matrix strength contrasts for two or more mechanically diverse blocks may also influence the overall mechanical behavior of the bimrock. Further work is underway to examine the problem.

Conclusions

Based on the work performed for this study, the following conclusions are presented:

- If there is sufficient color contrast between constituent blocks and matrix, image analysis methods are practical for the determination of the block proportions of outcrops, laboratory specimens and similar exposures of bimrocks.
- If the shapes of blocks of a bimrock are approximately equi-dimensional in 3D, the block proportions obtained from 2D measurements can be considered equivalent to the 3D volumetric block proportions.
- When using image classification on grayscale images, the surfaces must be slightly weathered or unweathered. If the surfaces are weathered, image classifications using coloured photographs should be employed.
- The relationship between equivalent block proportion (EBP) and UCS values of Ankara agglomerate indicates that the effect of EBP on UCS is small for lower EBP values , but exponentially increases with higher values of EBP.
- There is an apparent dependence between UCS and individual block strengths, which requires further study.

References

1. Medley, E.W.: *The engineering characterization of melanges and similar block-in-matrix-rocks (bimrocks)*. PhD thesis, Dept. of Civil Engineering, Univ. of California, Berkeley, 1994.
2. Lindquist, E.S ; Goodman R.E.: *The strength and deformation properties of the physical model melange*. In: Nelson, P. ; Laubach, S.E. (eds.): Proceedings of the First North American Rock Mechanics Conference (NARMS), Austin, Texas. Rotterdam: Balkema,1994.
3. Medley, E.: *Orderly characterization of chaotic Franciscan Melanges*. Felsbau, Vol. 19 (2001), No. 4, pp. 20–33.
4. Gokceoglu, C.: *A fuzzy triangular chart to predict the uniaxial compressive strength of the Ankara Agglomerates from their petrographic composition*. J. Eng. Geol., Vol. 66 (2002), pp. 39–51.
5. Sonmez, H. ; Tuncay, E. ; Gokceoglu, C.: *Models to predict the uniaxial compressive strength and the modulus of elasticity for Ankara Agglomerate*. Int. J. Rock Mech. Min. Sci., Vol. 41 (2004), No. 5, pp. 717-729.
6. ISRM: *ISRM suggested method: rock characterization, testing and monitoring*. London: Pergamon Press, 1981.
7. Medley, E. ; Lindquist, E.S.: *The engineering significance of the scale-indepence of some Franciscan Melanges in California, USA*. In: Daemen, J.K. ; Schultz, E.A.(eds.): 35th US Rock Mech. Sym, pp. 907-914. Rotterdam: Balkema, 1994.
8. Lindquist, E.S.: *The strength and deformation properties of melange*. PhD thesis, Dept.of Civil Engineering, Univ. of California, Berkeley, 1994.
9. Medley, E.: *Uncertainty in estimates of block volumetric proportions in melange bimrocks*. In: Marinos, P.G. ; Koukis, G.C. ; Tsiambaos, G.C. ; Stournaras, G.C., (eds.): *Proc. International Congress, International Association of Engineering Geologists, Engineering Geology and the Environment*, Athens, Greece, 1997.
10. Lillesand, T.M. ; Kiefer, R.W.: *Remote sensing and image interpretation*. 2nd ed. New York: Wiley, 1987.
11. Gokceoglu, C. ; Kasapoglu, K.E. ; Sonmez, H.: *Prediction of uniaxial compressive strength of Ankara Agglomerates from their petrographical composition*. In: Moore, D. ; Hungr, O. (eds.): *Proceedings of the Eighth International Congress of IAEG and the Environment*, Vancouver, Canada, pp. 455-459. Rotterdam: Balkema, 1998.
12. Haneberg, W.C.: *Simulation of 3-D block populations to characterize outcrop sampling bias in block-in-matrix rocks (bimrocks)*. Felsbau, Vol. 22 (2004), No. 5, pp. 19-26.
13. Sonmez, H. ; Gokceoglu, C. ; Medley, E. ; Tuncay, E.; Nefeslioglu, H.A.: *A conceptual approach for determining the uniaxial compressive strength of bimrocks.* In preparation, 2004.

Acknowledgement

This research was supported by TUBITAK (The Scientific and Technical Research Council of Turkey: Project No: 102Y033). Thanks also to Isabelle Pawlik, PE, of Jacobs Associates, San Francisco, USA, for the German translations.

Authors

Dr. Harun Sönmez, Dr. Candan Gokceoglu and Ergün Tuncay, Department of Geological Engineering, Applied Geology Division, Hacettepe University, 06532 Beytepe-Ankara, Turkey, E-Mail haruns@hacettepe.edu.tr, cgokce@hacettepe.edu.tr, etuncay@hacettepe.edu.tr; Dr. Edmund W. Medley, Medley Geoconsultants, 1554 Winding Way, Belmont, California, 94002, USA, E-Mail emedley@bimrocks.com; and Hakan A. Nefeslioglu, General Directorate of Mineral Research and Exploration, 06520, Ankara, Turkey, E-Mail hanefeslioglu@mta.gov.tr

Observations on Tortuous Failure Surfaces in Bimrocks

By Edmund W. Medley

Although heterogeneous geological mixtures of competent blocks of rock encased in weaker matrix have long frustrated designers, contractors and owners, only recently have geotechnical design guidelines been available for characterizing geological chaos (1, 2). As a step in the process of understanding the common geomechanical behavior of the vast variety of soil/rock mixtures, the author introduced the term "bimrock" (block-in-matrix rock) to include melanges, sheared serpentinites, breccias, decomposed granites, weathered rocks with corestones, and tectonically fragmented rocks such as fault rocks (3). Bimrocks are defined as geological mixtures composed of geotechnically significant rock blocks within a bonded rock matrix of finer texture (3). The term "geotechnical significance" means that there is a sufficient volume of blocks with mechanical contrast between blocks and matrix to induce failure surfaces to pass around the blocks. The overall strength of bimrocks increases with increases in volumetric block proportions, the geomechanical advantage being due to the extra effort expended by tortuous failure surfaces forced around competent blocks (4, 5). The factor of safety for slope stability also depends on volumetric block proportion, as well as block orientations (6).

From a study of failed physical model melanges, this paper summarizes the characteristics of tortuous failure surfaces and their dependence on volumetric block proportions and block orientations and presents a preliminary guideline for estimating the thickness of potential failure zones in bimrocks.

Background on melanges and tortuosity

The most intractable bimrocks are fault rocks and melanges (from French: mélange, or mixture), exemplified by those of the Franciscan Complex of California, popularly known as "the Franciscan". Figure 1 shows an example outcrop of a Franciscan melange. Melanges occur globally in mountainous terrains, and are notorious for their role in slope instability and for providing unexpected and expensive difficulties during excavation and tunneling; and construction claims are common for unexpected "mixed face" tunneling conditions and differing site conditions claims.

Although melanges are common, only relatively recently have guidelines been presented for their geotechnical characterization (1, 7). Clues to melanges are the presence of rocks of different lithologies juxtaposed in improbable fashion (7), or the "scaly clay" fabric of intensely sheared shale with blocks, such as the "argille scagliose" of Northern Italy. Blocks in Franciscan melanges are commonly greywacke, are roughly ellipsoid with minor : major axes of 1:2

Beobachtungen an geschwungenen Versagensflächen in Bimrocks

Bimrocks (so genannte Block-in-Matrix Gesteine) bestehen aus einem Gemisch von kompetenten Gesteinsblöcken umgeben von Matrixgestein mit geringer Festigkeit, die sehr oft geschert sind und sich wie Lockergestein verhalten. Beispiele hierfür sind Melangen und Störungsgesteine. Eine vorläufige Studie bezüglich der Geometrie von über 70 Versagensflächen in physikalischen Modellmelangen deutet darauf hin, dass Zug-Druck-Linien von Versagensflächen, Blockvolumen und Blockausrichtung nur unwesentlich voneinander abhängig sind. Es ist deshalb sinnvoller, mögliche Versagensflächenbereiche zu untersuchen als potenzielle Versagensmodelle zu entwickeln. Diese Bereiche/Zonen bewegen sich in einer Größenordung von 5 bis 15 % der ingenieurtechnischen Kenngröße (wie Böschungshöhe und Dammfußbreite). Es besteht kaum eine Beziehung zwischen den beobachteten extrem uneinheitlichen Versagensflächen in Bimrock und Profilarten für die Auswahl des Trennfugenrauigkeitskoeffizienten. Eine Abhängigkeit besteht jedoch zwischen Blockvolumen und dem Größenverhältnis von Versagensflächen in Kontakt mit Gesteinblöcken.

Bimrocks (block-in-matrix rocks) are mixtures of competent blocks of rock surrounded by weak matrix rocks, which are often sheared and soil-like, and are exemplified by melanges and fault rocks. A preliminary study of the geometries of over 70 failure surfaces in physical model melanges indicates that there is little dependence between failure surface trajectories, volumetric block proportions and block orientations. Rather than attempt to model potential failure surfaces, it is more reasonable to analyze potential failure zones; the thickness of which ranges between 5 and 15 % of the characteristic engineering dimension that scales the problem at hand (such as slope height and dam footing width). There is little relationship between the observed highly irregular bimrock failure surfaces and type profiles for the selection of joint roughness coefficients. There is dependence between volumetric block proportion and the proportion of failure surfaces that contact blocks.

Fig. 1 Franciscan melange at Trinidad Beach, Humboldt County, Northern California. Yellow arrows indicate one of several shears.

Bild 1 *Franciscan Melange am Trinidad Strand, Humboldt County, Nordkalifornien. Gelbe Pfeile kennzeichnen eine von mehreren Scherungen.*

and greater, and often have slickensided and polished surfaces. Block shapes influence the tortuosity of failure surfaces most when coupled with the orientation of the blocks: elliptical blocks have the greatest deleterious effect on slope stability when the direction of the major axes is co-incident with the direction of shearing (6). Well-fractured blocks may have little strength contrast with matrix and should then be considered matrix. Melange rock masses can contain block-poor and block-rich regions (6).

Blocks in Franciscan melanges are found at all scales of engineering interest and the range of block sizes extends more than seven orders in magnitude, between sand and mountains (8). The author (1, 3) suggests appropriate scaling dimensions be selected over the range of scales of engineering interest, (termed the "characteristic engineering dimension") such as the diameter of a laboratory triaxial specimen, the height of a landslide, the diameter of a tunnel, or the width of a dam foundation. At the selected scale of interest, blocks are limited to between about 5 and 70 % of the characteristic engineering dimension. The materials below the 5 % limit are matrix and those above 70 % are blocky rock masses.

The overall mechanical properties of bimrocks are mainly affected by the mechanical properties of the matrix, the volumetric block proportion, the block shapes, the block size distributions and the orientation of the blocks relative to failure surfaces. When the block proportions are between about 25 and 70 %, the increase in the overall mechanical properties of bimrocks are directly related to the volumetric block proportion of blocks in the rock mass (5). Tortuosity is defined as "winding or twisted" (9) and is a property defined in medicine, groundwater hydrology and fluvial geomorphology, but is not commonly used in rock engineering.

The increase in the overall friction strength due to tortuosity can be as much as 15° to 20° above the matrix friction strength. Increases in volumetric block proportion also lead to a decrease in the bimrock cohesion. Irfan and Tang (10) identified similar relationships between volumetric block proportion and shear strength for Hong Kong colluvium containing boulders to 7 m in size.

Matrix rocks in Franciscan melanges are most often fractured and broken to completely sheared soil siltstone and shale. Shears pass around blocks (Figures 1 and 2), and may be numerically denser around large blocks. Melanges are often extensively sheared to soil: about 800 shears per meter were counted in a Franciscan melange (11). Common rock engineering terminology used to indicate the quality of the rock surfaces of rock mass "discontinuities", such as "waviness", "sinuosity" and even "roughness", do not adequately reflect the often extreme irregularity and dimensional variations exhibited by failure surfaces in chaotic melanges and fault rocks.

The block/matrix contact of melanges is generally the weakest component of the bimrock, particularly if the contact is also part of a pre-existing shear and there is potential for future failure of a melange rock mass to occur along pre-existing failure surfaces. Accordingly, there is geotechnical motivation to understand the geometry and characteristics of failure surfaces in bimrocks and the contribution of block/failure contact strengths to their geomechanical properties for slope instability studies (6) or dam foundation analyses (2, 12).

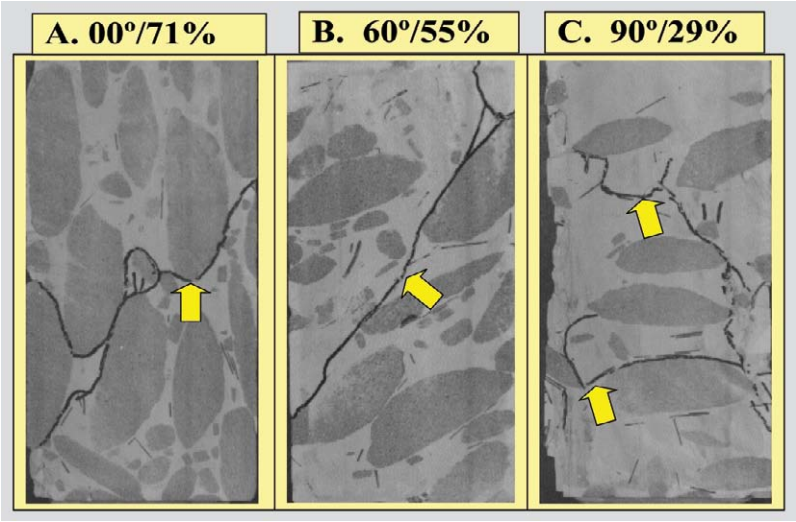

Fig. 2 Cross-sections through 150 mm diameter triaxial specimens of model melange of differing overall block orientations relative to vertical axial loading (degrees) and volumetric block proportions (%). Arrows indicate black lines of tortuous failure surfaces. Specimens as tested by Lindquist (4): A: H0150, B: M60200, C: L9050. After (3).

Bild 2 *Querschnitt durch dreiachsige Probekörper mit 150 mm Durchmesser aus typischer Melange mit unterschiedlicher Gesteinsblockausrichtung relativ zur Vertikalachslast (°) und dem Blockvolumen (%). Pfeile kennzeichnen die schwarzen Linien der geschwungenen Versagensflächen. Probekörper wie von Lindquist gestestet (4): A: H0150, B: M60200, C: L9050. Nach (3).*

Measurement of tortuosity characteristics in model bimrock

As a part of his research, Lindquist fabricated and triaxially tested over one hundred 150 mm, 300 mm high cylindrical specimens of model melange composed of mixtures of hard blocks and weaker matrix (4, 5). Specimens had one of three general volumetric block proportions (about 30, 50 or 70 %); one of four possible overall block orientations included relative to the vertical axial loading direction (0°, 30°, 60° and 90°); and one of five possible confining stress conditions ranging between 50 psf (2.5 kPa) and 250 psf (12.5 kPa). The specimens were tested triaxially to failure and some specimens were cut to reveal the internal patterns of failure. As shown in Figure 2, failure surfaces generally passed around blocks.

The block size distribution of the blocks in the bimrock mixtures conformed to a Franciscan-type, fractal (well-graded) size distribution (4, 8), with blocks ranging in size between about 115 and 12 mm. Since the specimen diameter indicates the laboratory scale of interest, the block sizes thus ranged between 75 and 8 % of the appropriate characteristic engineering dimension.

Adopting a procedure developed by the writer (3, Section 2.8.2) Lindquist documented the external patterns of failure surfaces of about 60 of his specimens (4). The specimens were wrapped in transparent kitchen “cling film” (known as Saran

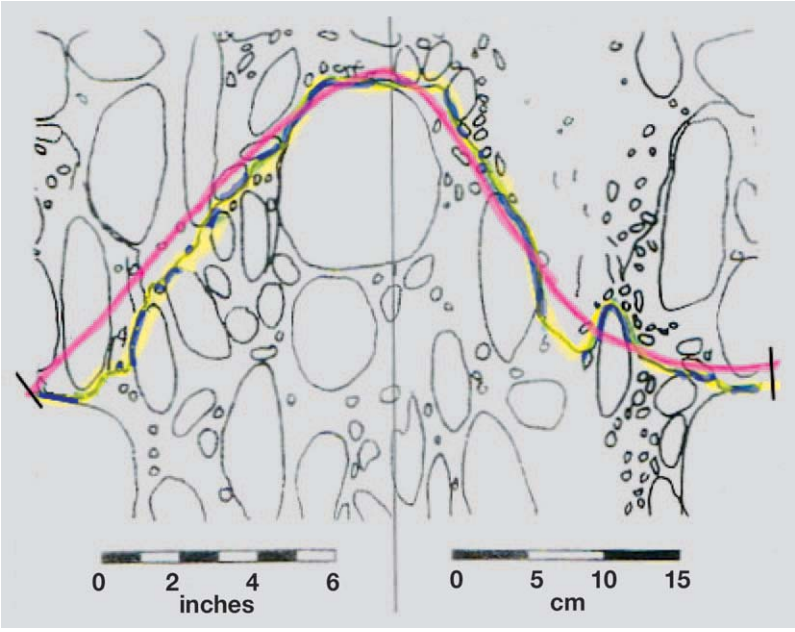

Fig. 3 Scanned tracing of circumferential surface of triaxial specimen C in Figure 2. Measurements were made of: a) the length of the tortuous failure surface (yellow highlighted line); b) the length of estimated smooth mean surface (red line); and c) total length of the block contacts along the failure surface. Specimen H0150. After (4).

Bild 3 *Umfangsabwicklung des dreiachsigen Probekörpers C in Bild 2. Messungen von: a) Länge der geschwungenen Versagensfläche (gelbe Linie); b) Länge der geschätzten ausgeglichenen Durschnittsfläche (rote Linie); und c) Blockkontaktgesamtlänge entlang der Versagensfläche. Probekörper H0150. Nach (3).*

Wrap in the USA), and the outlines of blocks and failure surfaces traced with a felt pen. Folded flat onto white cardboard, the tracings were photocopied, as shown in the example of Figure 3. The tracings are 2D projections of cylinders, and as such there is some distortion of blocks by "stretching" in the horizontal direction, the amount being a function of block orientations (3, Section 2.8.2).

Copies of Lindquist's tracings were used in this study to investigate characteristics of the failure surfaces. The failure surfaces were expressed on the cylinder surface as irregular lines that tortuously negotiated around blocks as shown by the yellow highlighted line in Figure 3. The lines were measured using a flexible chain made of fine links that allowed it to be draped around tight bends. Once a length of the chain was placed along all of a failure surface, it was removed, straightened and measured. The length was declared to be L', the tortuous length.

A smooth line was also drawn through a path estimated to be that which the failure could have produced in the absence of the blocks, as shown by the red line in Figure 3. The template for the estimated smooth line was the simple linear pattern of failures in matrix-only specimens tested by Lindquist (4). Furthermore, it was also assumed that the actual failure surfaces deviated as little as possible from the tortuous surfaces, as a matter of energy conservation. This line was also measured manually by the chain, and declared to be L_o. For this study, it was assumed that the degree of horizontal "stretching" was the same for both the actual failure line and estimated smooth failure line. About 70 tortuous failure lines and smooth lines were measured.

The individual lengths of block/failure surface contact (tangents; blue line segments in Figure 3) were also measured, and these were totaled to produce a total block/failure contact length, identified as t.

Compilations of manual tracings of the failure lines, such as those shown in Figure 4, were sketched for specimens grouped by common volumetric proportion and block orientations (but individual confining stresses). The traces were made using a light table, with Lindquist's drawings (such as Figure 3) taped to the light table underneath the tracings. Each actual tortuous failure line was drawn relative to its companion smooth line, by continuously turning the tracing paper such that the common straight line for each group was co-incident with the underlying estimated smooth failure surface line. In this fashion, the entire tortuous failure surface line was captured as an irregular trajectory of departures from the smooth line. Some specimen sketches had more than one failure

surface and these were also traced. Figure 4 shows clearly that the trajectories have very little in common, other than being invariably irregular. For comparison with rock mass joints, Figure 4 also shows six type profiles, enlarged to match the scales of the tracings, which are commonly used to select joint roughness coefficients (JRC) 10 through 20 (13). The profiles, which are standard in rock engineering, illustrate that the "roughest" surfaces normally expected when characterizing rock joints, are relatively subdued compared to the tortuous failure profiles.

Including the profiles of Figure 4, over 70 profiles were scanned. The areas (A) under the irregular trajectories were measured digitally using SigmaScan Pro, which is commercially available image analysis software (14). The length of the smooth line L_o, was also re-measured digitally.

Results and discussion

Several parameters were generated from the measurements, as illustrated in Figure 5. Although there are more than 15 parameters for the characterization of 3D surface roughness used in materials science (16), the measures used in this study were few and intuitive. A summary of the results is presented in Figure 6 and in Table 1.

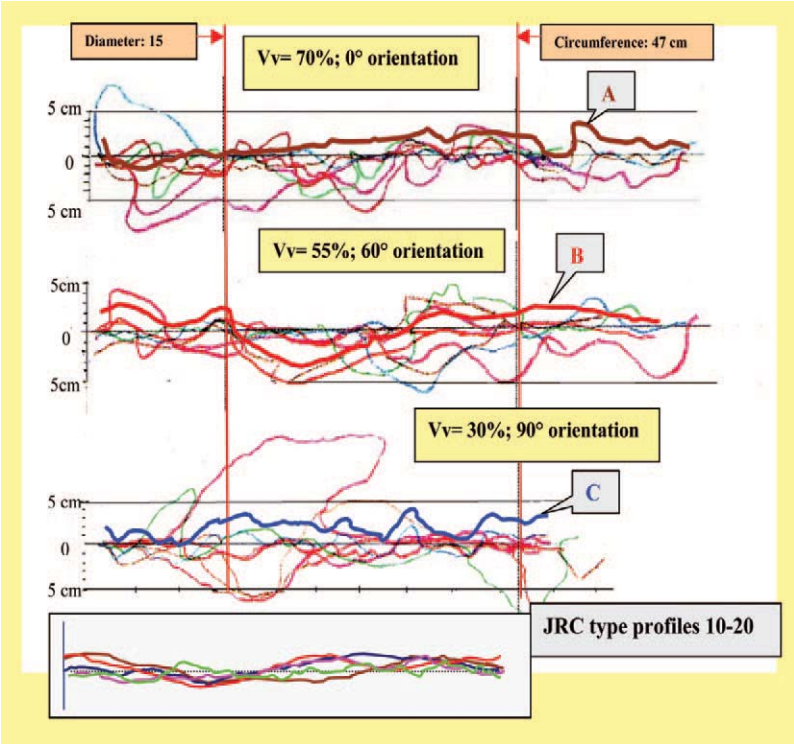

Fig. 4 Scans of traced lines of failure surfaces and compared to type profiles for JRC 10 to 20 (13). Horizontal scale same as vertical scale. Highlighted tracings of failure surfaces are for specimens shown in Figure 2 (A, B, C).

Bild 4 *Linienabwicklungen der Versagensflächen im Vergleich zu JRC Typendarstellung 10 bis 20 (13). Horizontalmaßstab entspricht Vertikalmaßstab. Hervorgehobene Abwicklungen der Versagensflächen entstammen den Probekörpern aus Bild 2 (A, B, C).*

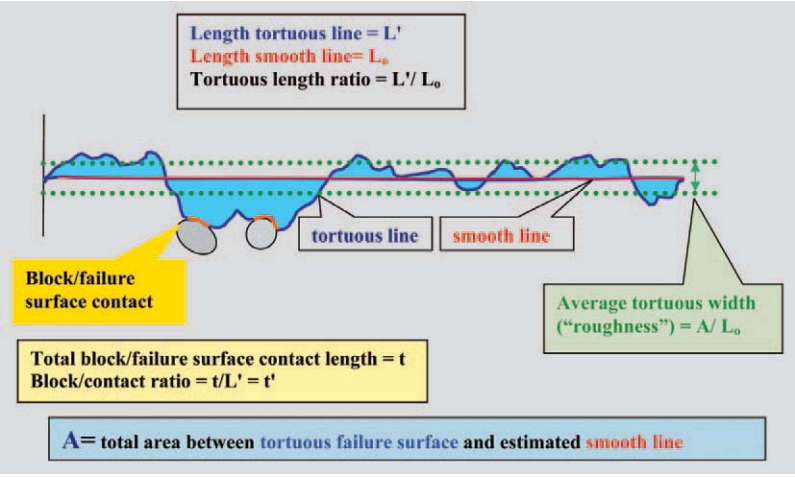

Fig. 5 Parameters measured and calculated from traced lines of tortuous failure surfaces.

Bild 5 *Kenngrößen gemessen und berechnet anhand von Abwicklungslinien der geschwungenen Versagensflächen.*

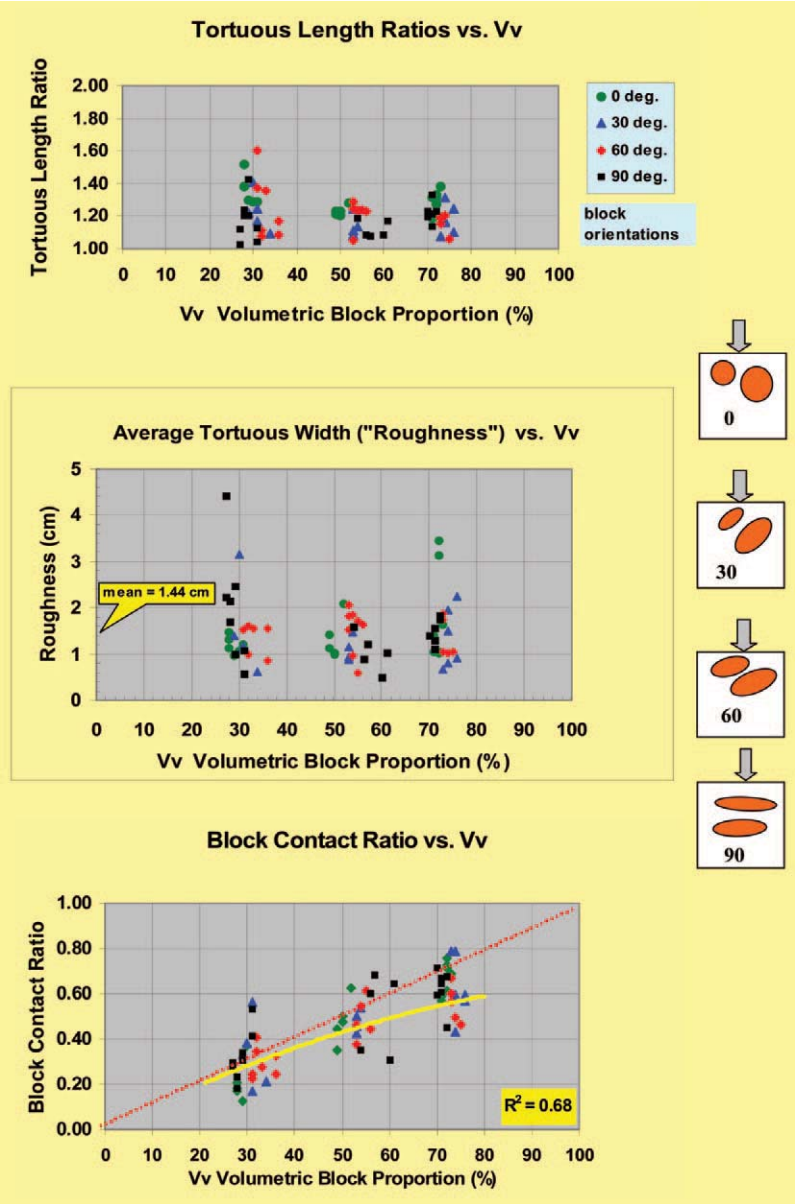

Fig. 6 Plots of volumetric block proportions and: top) tortuous length ratios; middle) block/failure surface contact ratios and, bottom) average tortuous width.

Bild 6 *Darstellungen von Blockvolumen gegenüber: oben) geschwungenen Längenverhältnissen; Mitte) Kontaktverhältnissen zwischen Gesteinsblock und Versagensflächen und, unten) mittlere Schwingungsbreite.*

One measure of tortuosity is the ratio of the length of the tortuous line connecting two points to the length of the shortest line between the same two points. This is referred to as the "tortuous length ratio" (L'/Lo) in this paper. As shown in Figure 6 (top plot), there is relatively little sensitivity between the tortuous length ratio, volumetric proportion and block orientation. For lower block proportions (about 30 %) there is more variability in the tortuous length ratio.

Overall, there is little systematic variation between the geometry of failure surfaces with block proportions and block orientations, as suggested by the results summarized in the top plot of Figure 6, together with the unruly appearance of the failure profiles shown in Figure 5. However, further work is needed to understand the reason for variations, and particularly why there is relatively little variation at about 50 % volumetric block proportion.

Based on this preliminary study, there appears to be little to be gained from attempts to predict "type failure surfaces" for use in design. Rather, it is better to accept that completely random possible profile geometries are likely and focus instead on defining failure zones, which contain a multitude of actual and potential individual shear surfaces, much like shear zones and fault zones (15).

A simple measure of a potential "failure zone" is to identify an overall mean width for many possible tortuous failure surfaces. Such an average width is used to tolerance surfaces in mechanical engineering, where surface roughness is defined as the average deviation of a surface above a mean line (17). Surface roughness (or in this case, "average tortuous width") was calculated by dividing the total of the areas between the irregular surface and the mean line (A), by the length of the mean line (or L_o, in this study), as shown in Figure 5. The length L_o used was that measured digitally rather than the manual length measured for the tortuous length ratio study described above.

Figure 6 (middle plot) shows that there is little dependence between the average tortuous width, volumetric block proportions and block orientations, although there is more variation for the lowest block proportions. A plot of areas is not shown since it would look very similar to the plot of tortuous widths, because the average mean (smooth) line length is relatively constant (Table 1: mean length about 60 cm, standard deviation about 10 cm). The mean tortuous width value for all 73 failure surfaces measured from Lindquist's triaxial specimens is 1.44 cm, with a standard deviation of 0.68 cm, shown in Table 1. Accordingly, since the triaxial specimen diameter is 15 cm, the mean tortuous width is thus approximately 10 % of the diameter plus or minus about 5 % (for one standard deviation).

This finding is of use to the practitioner, through the property of scale-independence

Table 1 Summary of Statistics.
Tabelle 1 *Zusammenfassung der statistischen Ergebnisse.*

Parameter	Unit	Symbol	Count	Mean	Standard deviation	Minimum	Maximum
Length Smooth Line*	cm	L_o	72	58.2	10.4	31.6	77.8
Length Tortuous Line	cm	L'	72	70.9	13.7	38.9	110.2
Tortuous Extension Ratio		L'/ L_o	72	**1.22**	**0.046**	1.03	1.6
Total Length block Contacts	cm	t	72	32.9	12.5	9.7	66.8
Block Contact Ratio		t/ L'	72	**0.46**	**0.18**	0.12	0.79
Tortuous Area	cm^2	A	73	84.2	37.7	24.9	225.4
Length Smooth Line**	cm	L_o	73	59.4	9.5	41.7	81
Tortuous Width	cm	A/L_o	73	**1.44**	**0.68**	0.5	4.45

* L_o measured manually, ** L_o measured digitally

common to many bimrocks over the range of scales of engineering interest. A basis for Lindquist's work (4) was that the models were scale models of real melanges, because of the scale independence of Franciscan melanges (8). In other words, Franciscan melanges and many other bimrocks, appear similar when observed within the range of scales of centimeters to hundreds of meters (7, 15). Scale-independence also applies to the geometry of pre-existing shears and induced failure surfaces. Hence, a preliminary implication of the study is that at any scale of engineering interest, once the characteristic engineering dimension has been selected (1), a first-order estimate of the thickness of a potential failure zone would be 5 to 15 % of that width.

A validation of this guideline was the selection of a 3 m thick potential failure zone below Scott Dam, California (2, 3). The dam is about 40 m high and 45 m wide at the base. Selecting the dam width as the characteristic engineering dimension for a study of possible basal shear of the dam through foundation rock. Using the preliminary rule described above, a potential failure zone would be between 2.3 m and 6.8 m thick, and the estimated 3 m thick failure zone selected was thus appropriate.

In the geotechnical analysis of a potential failure zone, consideration should be given to the strengths of the block/matrix and block/shear zone contacts. As written above, block/shear surface contacts are considered to be the weak-

est elements of bimrocks when shears pre-exist. Although overall bimrock frictional strength is increased for volumetric block proportions between about 25 and 75 %, there are indications that cohesive strength decreases as block proportion increases because block/matrix contacts increase (2, 4, 5). For pre-sheared matrix, is should thus be presumed that cohesion will decrease even more, although currently there are no methods available to predict the decrease.

Figure 6 (bottom) and Table 1 summarize the results for block/failure surface contact ratios (t/L'). There is some initial linear dependence between the proportion failure surfaces that are tangent to blocks, and the volumetric block proportions, but the linear dependence weakens beyond about 50 % volumetric block proportion. However, it would be conservative to assume that the linear dependence continues (as indicated by the red line on the plot). For design purposes, it may be possible to then assume that the overall cohesion of the potential failure zone be the cohesion of matrix, reduced by a factor that has a relationship to the estimated block volumetric proportion (as yet unknown). The reduction may be similar to the empirical factors used in soils mechanics for pile/soil adhesion or retaining wall/backfill. Work is underway to identify such factors (Pablo Sanz Rehermann, personal communication).

Conclusions

The study summarized in this paper indicates that there is little value in defining potential failure surfaces for bimrocks. Instead, it is both prudent and appropriate to define failure zones with thickness between 5 and 15 % of the appropriate characteristic engineering dimension. The paper also demonstrates that conventional rock engineering approaches of design, which incorporate joint roughness coefficients selected on the basis of type profiles, will be inappropriate, since the "roughness" of the failure surfaces in bimrocks far exceeds the roughness of the JRC type categories. Furthermore, the "joints" are not joints, but are relatively thick zones of rock/soil mixtures that require analysis involving soils engineering approaches.

Earlier findings from stability analyses that showed that the factor of safety is related to volumetric block proportion (6) is encouraging because commonly used analytical tools may then become useful to the practitioner investigating the slope stability of geologically complex mixtures such as melanges, fault rocks and other bimrocks. However, an important caveat must be repeated: any geotechnical prediction made of bimrock properties that are based on estimates of block volumetric proportions or block sizes are subject to considerable uncertainties, as described fully in other papers (18, 19, 20).

For slope stability studies, it also appears that the findings of this paper could possibly be integrated with conventional geotechnical analytical methods, since trial failure surfaces could be defined with thicknesses between 5 and 15 % of the characteristic engineering dimension, which for slope stability studies, is appropriately the slope height (6).

Despite the encouraging results of this preliminary study, more work must be performed, and research into case histories and practitioner experiences be extended.

References

1. Medley, E.W.: *Orderly Characterization of Chaotic Franciscan Melanges*. Felsbau Vol. 19 (2001), No. 4, pp. 20-33.
2. Goodman, R.E. ; C.S. Ahlgren: *Evaluating safety of concrete gravity dam on weak rock: Scott Dam*. J. of Geotechnical and Geoenvironmental Engineering Vol. 126 (2000), pp. 429-442.
3. Medley, E.W.: *Engineering Characterization of Melanges and Similar Block-in-Matrix Rocks (Bimrocks)*. PhD dissertation, Dept. Civil Engineering, Univ. California at Berkeley; Ann Arbor: UMI, Inc. 1994.
4. Lindquist, E.S.: *The strength and deformation properties of melange*. PhD dissertation, Dept. of Civil Engineering, University of California, Berkeley, CA, USA, 1994.
5. Lindquist, E.S. ; Goodman, R.E.: *The strength and deformation properties of a physical model melange*. In Nelson, P.P. ; Laubach, S.E. (eds.): Proc. 1st North American Rock Mechanics Conference (NARMS), Austin, Texas. Rotterdam: Balkema. 1994.
6. Medley, E.W. ; W. Sanz, P.R.: *Characterization of bimrocks (rock/soil mixtures) with application to slope stability problems*. In Schubert, W. (ed.): Proc. EUROCK 2004 & 53rd

Geomechanics Colloquium. Essen: Verlag Glückauf GmbH, 2004.
7. Wakabayashi, J. ; Medley, E.W.: *Geological characterization of melanges for practitioners*. Felsbau Vol. (2004), No. 5, pp. 10-18 (this issue).
8. Medley, E.W. ; Lindquist, E.S.: *The engineering significance of the scale-independence of some Franciscan melanges in California, USA*. In Daemen, J.K.; Schultz, R.A. (eds.): Proceedings of the 35th US Rock Mechanics Symposium, pp. 907-914. Rotterdam: Balkema, 1995.
9. Merriam-Webster: *Merriam-Webster Online Dictionary*. www.m-w.com, 2004.
10. Irfan, T.Y. ; Tang, K.Y.: *Effect of the coarse fraction on the shear strength of colluvium in Hong Kong*. TN 4/92. Hong Kong Geotechnical Engineering Office, 1993.
11. Savina, M.E.: *Studies in bedrock lithology and the nature of downslope movement*. PhD dissertation, University of California, Berkeley, 1982.
12. Glawe, U. ; Upreti, B.N.: *Better understanding the strengths of serpentinite bimrock and homogeneous serpentinite*. Felsbau Vol. 22 (2004), No. 5, pp. 53-60 (this issue).
13. Barton, N. ; Choubey, V.: *The shear strength of rock joints in theory and practice*. Rock Mechanics Vol. 10 (1977), pp. 1-54.
14. Jandel Scientific: *SigmaScan Pro, v. 4.0*. Jandel Corp., San Rafael, California, 2000.
15. Riedmüller, G. ; Brosch, F.J. ; Klima, K.; Medley. E.: *Engineering geological characterization of brittle fault rocks and classification of fault rocks*. Felsbau Vol. 19 (2001), No. 4, pp. 13-19.
16. Centre for Ultra Precision Technologies: *Development of a basis for 3D Surface roughness Standards: 14 (+3) parameters for surface roughness*. University of Huddersfield, United Kingdom. htpp://zeus/plmsc.psu.edu/~manias/MatSC597/roughness/definitions.html. 2004.
17. Engineering and Technology Department: *Surface tolerancing; Engineering Design Course*. University of Staffordshire, United Kingdom, http://www.staffs.ac.uk/schools/engineering_and_technology/des/aids/graphics/surftole.html, 2004.
18. Medley, E.W.: *Uncertainty in estimates of block volumetric proportion in melange bimrocks*. In Marinos, P.G. ; Kpukis, G. ; Tsiambous, G. ; Stournaras, G. (eds.): Proc Int. Symp. On Engineering Geology and the Environment, pp. 267-272. Rotterdam: Balkema, 1997.
19. Medley, E.W.: *Estimating block size distributions of melanges and similar block-in-matrix rocks (bimrocks)*. Proc. 5th North Amer. Rock Mechanics Symposium, University of Toronto, Toronto, 2002.
20. Haneberg, W.C.: *Simulation of 3D block populations to characterize outcrop sampling bias in bimrocks*. Felsbau Vol. 22 (2004), No. 5, pp. 19-26 (this issue).

Acknowledgments
Thanks to John Burton, PE, GE and Dr. Bill Haneberg for their reviews and help. Mein Dank geht an Isabelle Pawlik (Jacobs Associates, San Francisco, USA) und Margit Kurka (Michael West Associates, Denver, USA) für die "last-minute" Übersetzungen ins Deutsche.

Author
Edmund W. Medley, Principal Engineer, Medley Geoconsultants, Belmont, California, USA, E-Mail emedley@bimrocks.com

Short Term Prediction of System Behaviour of Shallow Tunnels in Heterogeneous Ground

By Bernd Moritz, Karl Grossauer and Wulf Schubert

Several complications have to be expected when tunnelling in heterogeneous ground, such as in bimrocks (block-in-matrix rocks) or fault zones:

- The necessity of using different excavation methods, such as drill-and-blast and an excavator, sometimes during the same round.
- The frequently changing stresses and deformations of the rock mass and the support.
- The potential for several different failure mechanisms, such as excessive overbreak, collapse of the face and crown, brittle failure of hard blocks, and long term creep of matrix, to name only a few.
- The heterogeneous distribution of ground water with the potential for heavy water inflows especially in fault zones.

Kurzzeitprognose des Systemverhaltens von seicht liegenden Tunneln in heterogenem Gebirge

Der Artikel behandelt die Auswertung und Interpretation von Verschiebungsdaten sowie die Prognose der Verschiebungen für seicht liegende Tunnel in heterogenem Gebirge. In den letzten Jahren wurden die Auswertemethoden erheblich verbessert und ausgeweitet. Für tief liegende Tunnel wurden im Speziellen die Trendänderungen der Verschiebungsvektororientierung erfolgreich zur Kurzzeitprognose der Gebirgsqualität in den der Ortsbrust voraus liegenden Gebirgsbereichen herangezogen. Unklar war allerdings, ob solche Auswerte- und Prognosemethoden auch für Bereiche mit geringem Spannungsniveau angewendet werden können. Die Auswertung von Verschiebungsmessdaten von seicht liegenden, in einer tektonischen Melange in den Ostalpen Österreichs aufgefahrenen Tunneln hat gezeigt, dass die oben beschriebenen verbesserten Auswertemethoden ebenfalls zur Kurzzeitprognose bei seicht liegenden Tunneln herangezogen werden können, vorausgesetzt die aufbereiteten Messdaten liegen in entsprechend guter Qualität und Genauigkeit vor.

The paper deals with the evaluation, interpretation and prediction of monitored displacements for a shallow tunnel in heterogeneous ground. Over the last few years evaluation methods in tunnelling have been considerably improved and extended. In particular the changes in the displacement vector orientation have been successfully used in deep tunnels for the short term prediction of the rock mass quality ahead of the face. Up to recently it has not been clear if such methods can be used also in low stress environments as well. However, using data from shallow tunnels excavated in a tectonic melange in the Eastern Alps of Austria, it is apparent that the described improved methods of measurement data evaluation can also be used in shallow tunnels for short term prediction, providing the measurement data are of good quality.

Establishing a reliable ground model in heterogeneous ground during the design phase is close to impossible. Even with an exceptional effort in mapping, drilling, and geophysical investigation there still remain considerable uncertainties with respect to location, size and quality specific and individual weak and competent components. This lack of certainty about ground conditions requires continuing ground investigations and updating of the ground model during construction, to be able to adjust excavation and support methods to the ground conditions, and allow a safe construction process. Possible methods for the refinement of the ground model during construction are: probing ahead, geophysical methods, and evaluation of displacement monitoring data, or a combination thereof. But both probing ahead with drillings and geophysical investigations demand a temporary stop to the excavation, and thus are rather costly. In addition, probe drillings give only pinpoint information, while the interpretation of results of geophysical investigations is difficult and the state of the art needs further development.

For the purposes of short term prediction of the rock mass condition ahead of the face and around the tunnel, the evaluation of 3D displacement monitoring data has been shown to be very efficient. In-situ observations, (1, 2, 3), as well as theoretical studies (4, 5, 6, 7) have shown the potential for an advanced analysis of displacement monitoring data to reliably predict the rock mass conditions. The trends of both vector orientation and the spatial orientation of the displacement vectors allow a good short term prediction of the rock mass structure and quality ahead and outside the excavation area.

Initially it was thought that these methods yielded reliable results only at relatively high overburden and poor ground but recent experience has shown that these new methods can also be successfully used in heterogeneous ground and low overburden conditions. Tools have been developed to predict the system behaviour of the combined rock mass support system (8). The observed system behaviour can easily be compared to the predicted one, and the development of critical conditions detected in timely fashion.

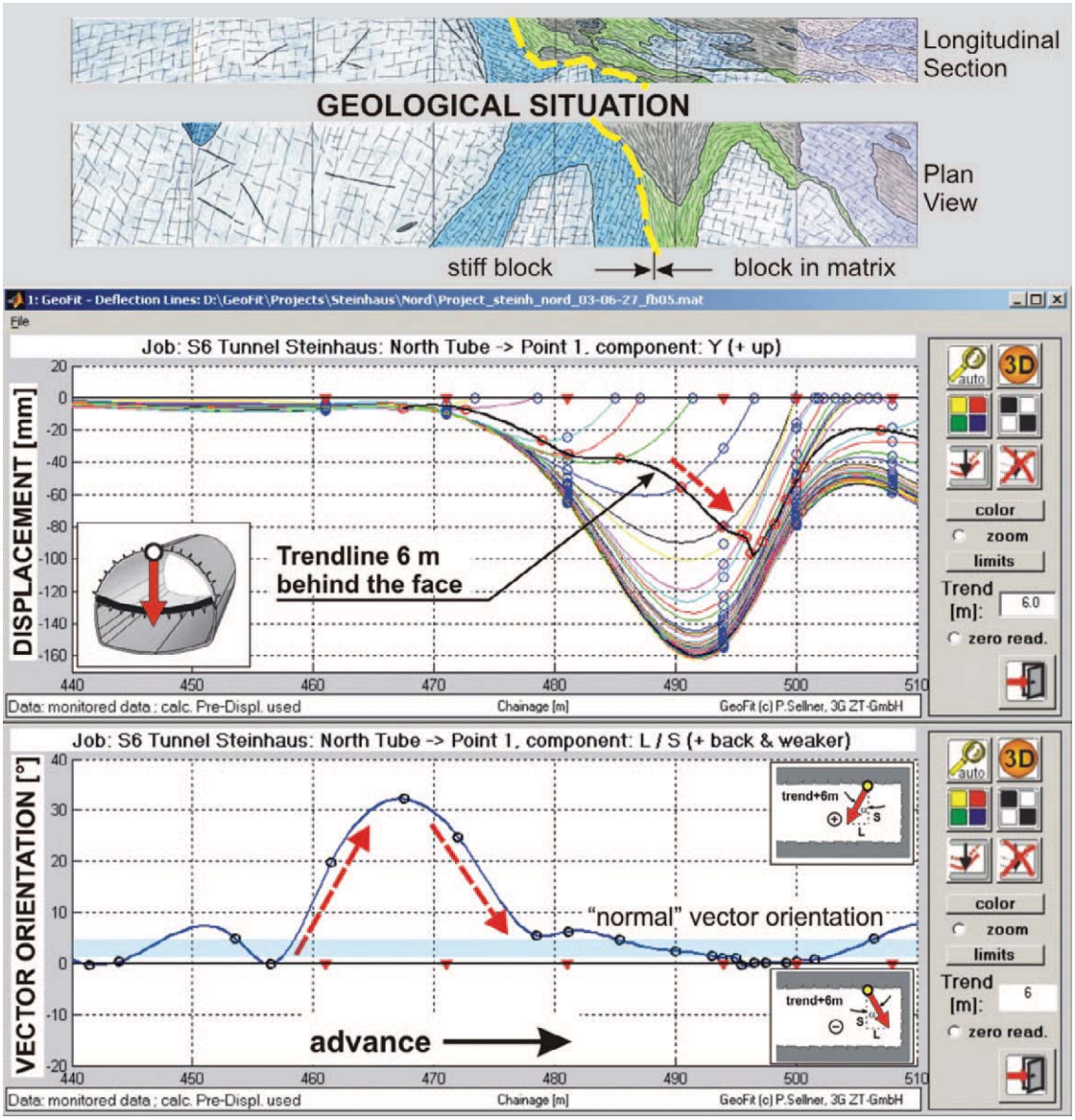

Fig. 1 Top: Geological situation (12) with lime marble (light blue coloured), lime schist (dark blue coloured) and cataclastic phyllites (grey and green coloured). Middle: Development of crown settlements. Bottom: Trend of displacement vector orientation (L/S) of the crown between tunnel metre 440 and 510. All diagrams shown were produced with GeoFit (13).

Bild 1 *Oben: Geologische Verhältnisse (12) mit Kalkmarmor (hellblau gefärbt), Kalkschiefer (dunkelblau gefärbt) und Phyllitkataklasite (grau und grün gefärbt). Mitte: Räumliche Entwicklung der Firstsetzungen. Unten: Trend der Verschiebungsvektororientierung (L/S) der Firste zwischen Station 440 und 510 m. Alle gezeigten Diagramme wurden mit GeoFit (13) erzeugt.*

This paper describes the observed system behaviours of shallow tunnels excavated in a tectonic melange in the Eastern Alps of Austria. Also illustrated is how advanced methods of displacement monitoring data evaluation can assist in in-situ short term predictions on site and in decision making about the selection of excavation and support methods.

Case studies

Geological conditions

The case histories described in this paper are from a tunnel located within a unit of the "Semmering-Unterostalpine" geologic sequence. The geological situation is characterized by a tectonic block-in-matrix rock (bimrock) mixture com-

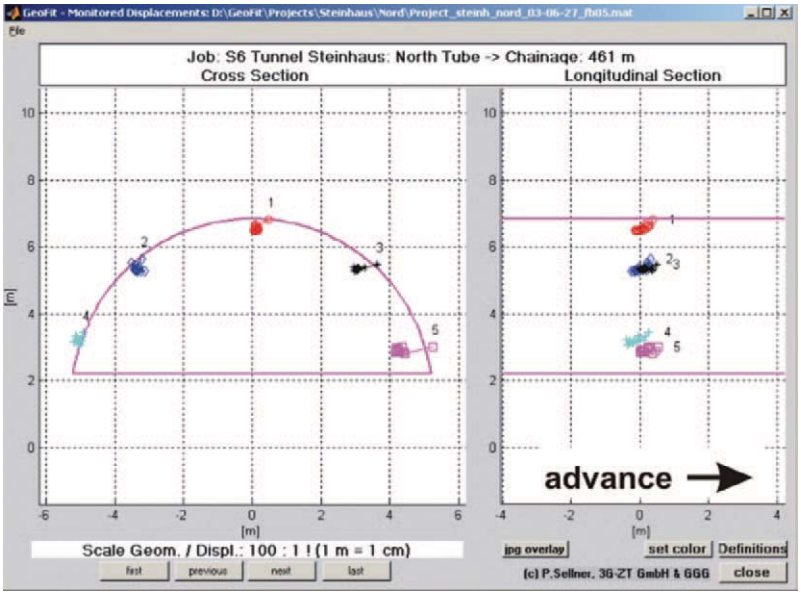

Fig. 2 Monitoring section MS461: Displacement vector orientation in a cross section and a longitudinal section (13).

Bild 2 *Messquerschnitt MS461: Verschiebungsvektororientierung im Querschnitt und Längsschnitt (13).*

posed of predominantly quartzitic, carbonatic, chloritic phyllites and gouge matrix material with embedded blocks of marble and quartzite. This chaotic tectonic mixture was generated from the surrounding host rocks during thrusting associated with the alpine orogeny and was further disaggregated during subsequent strike slip faulting. This bimrock is geologically defined as a polygenetic melange after Raymond (9, 10).

The melange is dominated by a north to north east shallowly to moderately dipping foliation formed during thrusting. However, local folding around the blocks results in continuous variations in the local dip and dip direction. The blocks are typically lenticular in shape and orientated with their long axes sub-parallel to parallel to the foliation. The original structures formed during thrust tectonics are overprinted by brittle strike slip faulting along steeply dipping east-northeast trending strike slip faults associated with the Mur-Murztal fault zone. This combination of tectonic events has created an extremely heterogeneous rock mass exhibiting varying degrees of rock mass strength and spatially complex distribution.

Case study 1: Underpass in a residential area; tunnelling from stiff to soft rock mass

The first case illustrates the behaviour of the rock mass-support system (in the following referred to as system behaviour) in the vicinity of a fault zone intersecting a larger block. For this case study, a section between tunnel metre 440 and 510 is evaluated (Figure 1). Up to tunnel metre 475 the tunnel was excavated in a lime marble block (Figure 1, Top: indicated by light blue colour) of considerable size and high strength and stiffness (11, 12). The fault zone consists of a matrix of chloritic and cataclastic phyllites (indicated by green and grey colour), with some smaller embedded blocks (Figure 1, Top: "block-in-matrix").

Unfortunately the distance between the measuring sections was rather large, as the block was originally expected to be continuous for some distance. A closer spacing of the measuring sections would have allowed more reliable observation the trend described below. A careful analysis of the data after encountering the fault zone with the excavation showed that even with the few data available, and the low amount of displacements observed, the fault zone could have been predicted.

Data were evaluated using the GeoFit software (13) to provide a reliable and accurate procedure for prediction of displacements. The program GeoFit is based on analytical functions which simulate the time-dependent behaviour of the rock mass and support as well as the face advance effect. Several of the Figures shown below were generated by the program GeoFit (13).

As can be seen from Figure 1 (Middle) the vertical displacements of the crown in the section of the stiff block were in the millimetre range. But after the face reached the weak rock, a considerable increase in the displacements was observed, reaching a maximum of about 150 mm at tunnel metre 490. The evaluation of the ratio between longitudinal and vertical displacements (L/S) (Figure 1, Bottom) shows a strong deviation from the "normal" value starting at around tunnel metre 460. The longitudinal displacement increases sig-

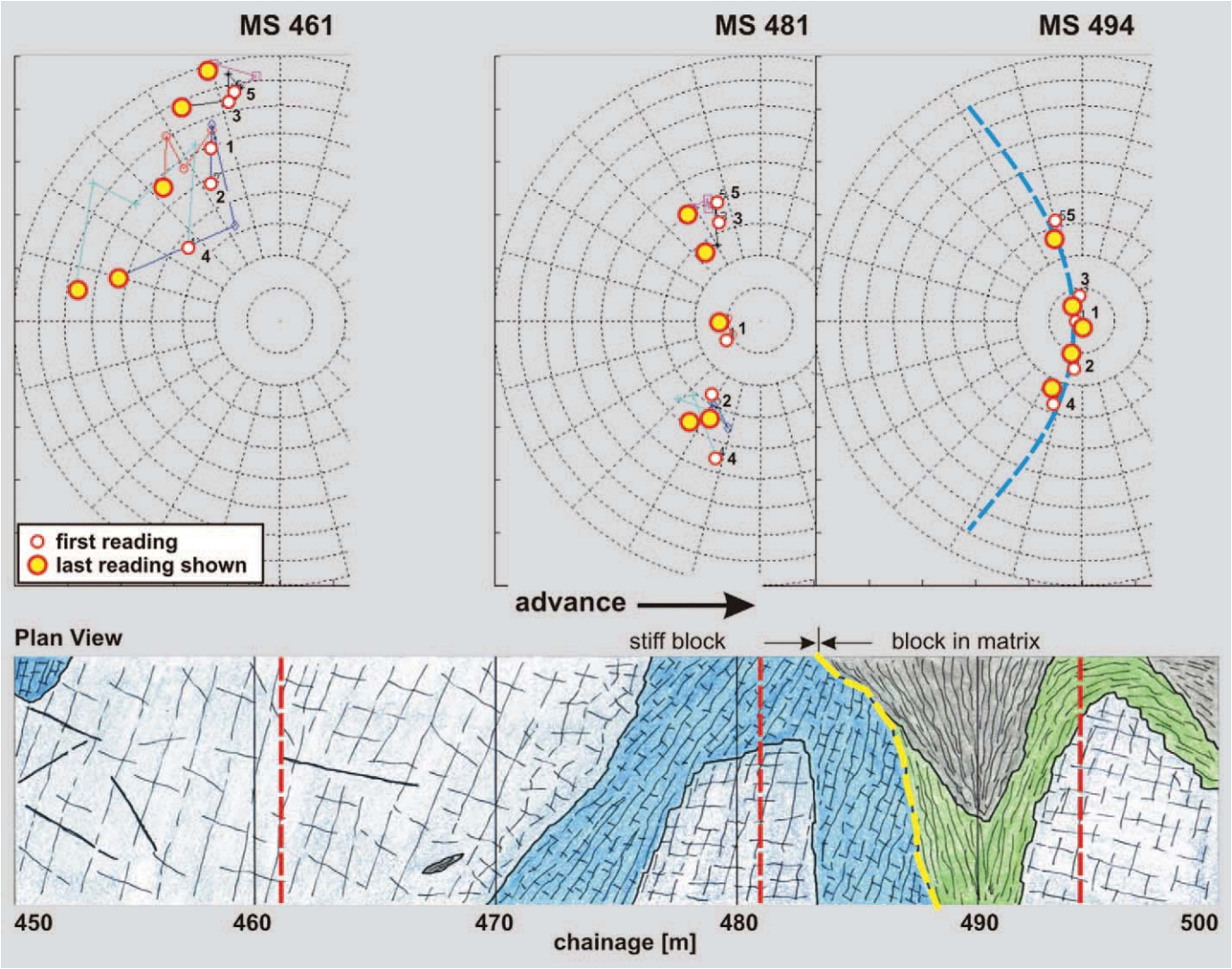

Fig. 3 Top: Stereographic projection (lower hemisphere): Spatial orientation of displacement vectors in monitoring sections MS461, MS481 and MS494 (13). Bottom: Geological situation (12) with lime marble (light blue coloured), lime schist (dark blue coloured) and cataclastic phyllites (grey and green coloured).

Bild 3 *Oben: Langenkugelanalyse (untere Hemisphäre): Räumliche Orientierung der Verschiebungsvektoren in den Messquerschnitten MS461, MS481 und MS494 (13). Unten: Geologische Verhältnisse (12) mit Kalkmarmor (hellblau gefärbt), Kalkschiefer (dunkelblau gefärbt) und Phyllitkataklasite (grau und grün gefärbt).*

nificantly, while the settlements remain more or less constant. The displacement vector in this case strongly points away from the direction of excavation. Based on previous experience and research results (6, 14), this trend clearly indicates that a weaker rock mass is ahead of the face. After entering the shear zone at approximately tunnel metre 485, the displacement vector orientation returns to "normal" again.

The orientation of the transition can be determined by analysing the displacement vector orientations shown in the cross section and longitudinal section of Figure 2, or by evaluating the spatial vector orientation, plotted in the stereonet shown in Figure 3 (Top). From both plots it can be seen that the displacements are strongly

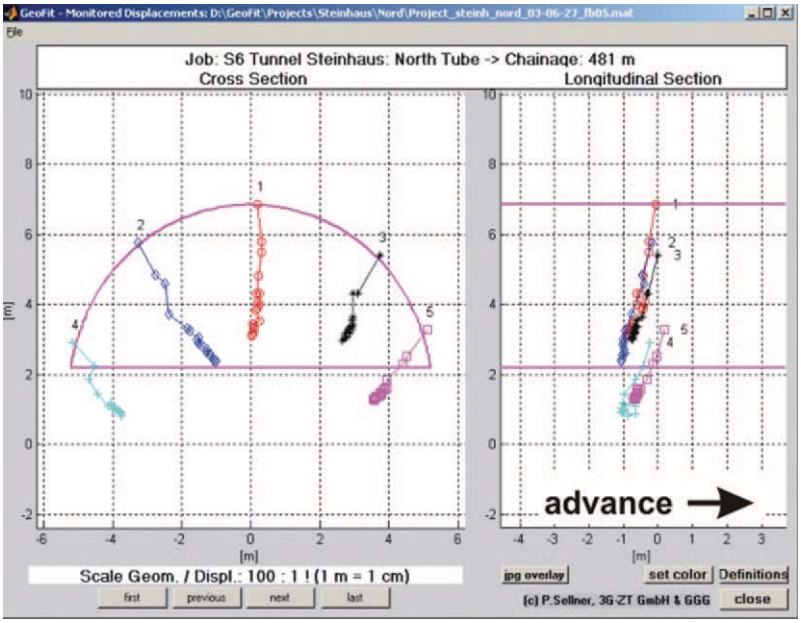

Fig. 4 Monitoring section MS481: Displacement vector orientation in a cross section and a longitudinal section (13).

Bild 4 *Messquerschnitt MS481: Verschiebungsvektororientierung im Querschnitt und Längsschnitt (13).*

asymmetrical, with the higher magnitudes at the right side, which indicates that the weak material will be encountered first on this side.

The stereographic projection (lower hemisphere) of Figure 3 (Top) shows the spatial orientation for all points in the top heading. With some practice the orientation of significant geological features outside the tunnel can be estimated. At tunnel metre 461 – this is about 20 m ahead of the transition – all vectors point to the left and backwards, indicating the increased stress at the right sidewall in the stiffer zone caused by the weak material ahead.

At measuring section MS481 the vector orientations are nearly in the "normal" position again, while the vectors in measuring section MS494 plot very steeply, showing a generally uniform settlement of the whole top heading.

Clearly, such abrupt changes in the deformation magnitude over a few metres will impose

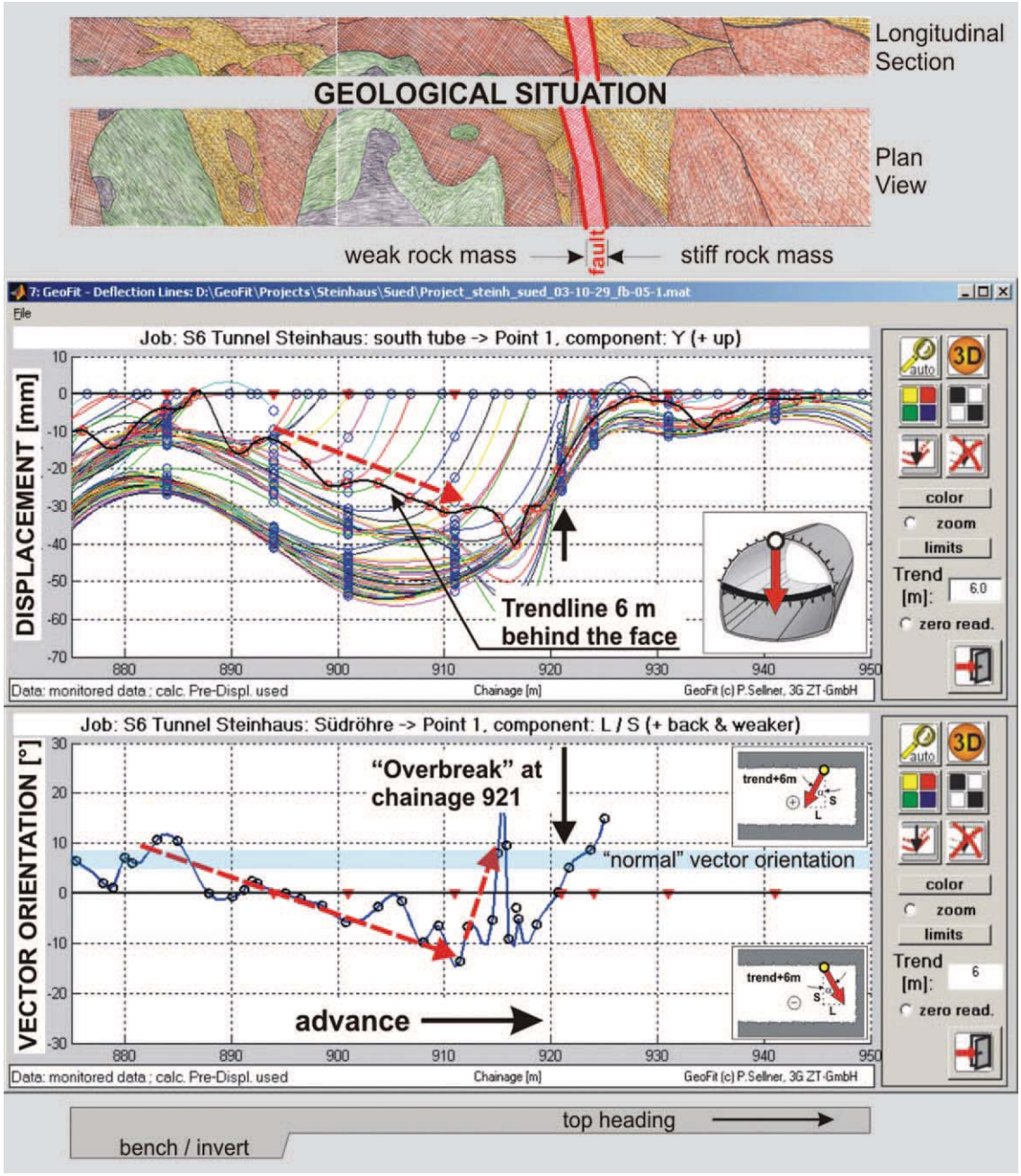

Fig. 5 Top: Geological situation (12) with quarzitic-cataclastic rock (yellow and orange coloured), fault (red coloured), cataclastic phyllites (green and grey coloured) and stiffer rock mass (orange coloured). Middle: Development of crown settlements. Bottom: Trend of displacement vector orientation (L/S) of the crown between tunnel metre 875 and 950 (13).

Bild 5 *Oben: Geologische Verhältnisse (12) mit quarzitisch-kataklastischem Gebirge (gelb und orange gefärbt), Störung (rot gefärbt), kataklastische Phyllite (grün und grau gefärbt) und steiferem Gebirge (orange gefärbt). Mitte: Räumliche Entwicklung der Firstsetzungen. Unten: Trend der Verschiebungsvektororientierung (L/S) der Firste im Abschnitt zwischen Station 875 und 950 m (13).*

high strains and stresses on the tunnel lining. Thus, the advantage of an early detection of changes in the rock mass stiffness is that the excavation and support methods (e.g. for this case increase of support measures) can be adjusted in time, with the aim of reducing the differences in strain in the rock mass-support system.

Figure 4 shows the displacement path in a cross section and longitudinal section for monitoring section MS 481, which is situated in the vicinity of the transition (see Figure 3, Bottom). The displacements in the cross sections are much more uniform than those observed at MS 461. The ratio of longitudinal to vertical displacement (L/S) is almost "normal", indicating a continuation of weak material for some distance ahead.

Case study 2: Tunnelling from soft to stiffer rock mass

Case study 2 illustrates a situation where the tunnel advance is from softer rock toward a stiffer rock mass. The section discussed is between tunnel metres 875 and 950 of the parallel tube discussed in case study 1 and as shown in Figure 1. The overburden in the analysed section is about 25 m thick. The geological condition (Figure 5, Top) is characterized by a quarzitic-cataclastic rock (indicated in Figure 5 by yellow and orange colours) with intercalated cataclastic phyllites (green and grey coloured). At tunnel metre 921 a fault (red colour) was encountered, crossing the tunnel axis nearly perpendicularly, followed by a comparatively stiffer block (orange coloured). Associated with the increasing proportion of fault gouge, the displacements also in-

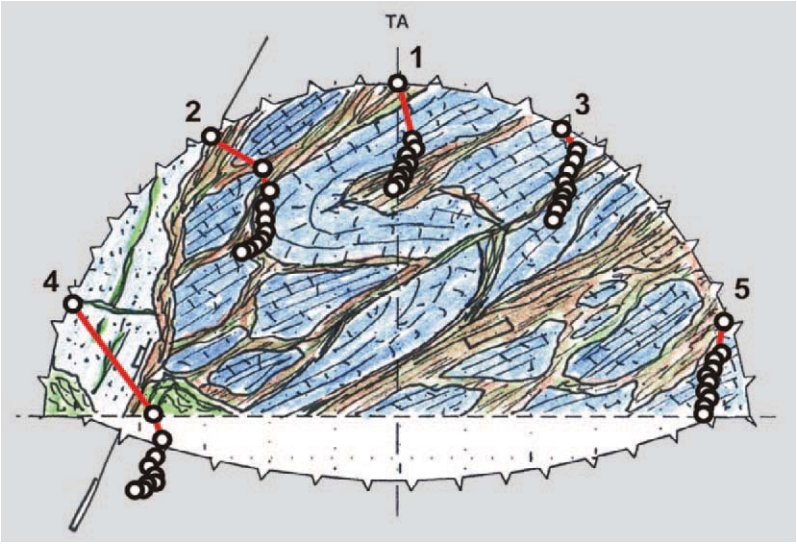

Fig. 6 Face map at tunnel metre 1097.5 (12): Blocks of dolomite marble (light and dark blue coloured) embedded in a soft, weathered matrix consisting of cataclastic phyllites (green and brown coloured) and displacement vector plot at monitoring section MS1101 (13).

Bild 6 *Brustbild bei Station 1097,5 m (12): Dolomitmarmorschollen (hell und dunkelblau gefärbt) in einer weichen, verwitterten Matrix aus kataklastischen Phylliten (grün und braun gefärbt) in der Zusammenschau mit der Verschiebungsvektororientierung im Messquerschnitt MS 1101 (13).*

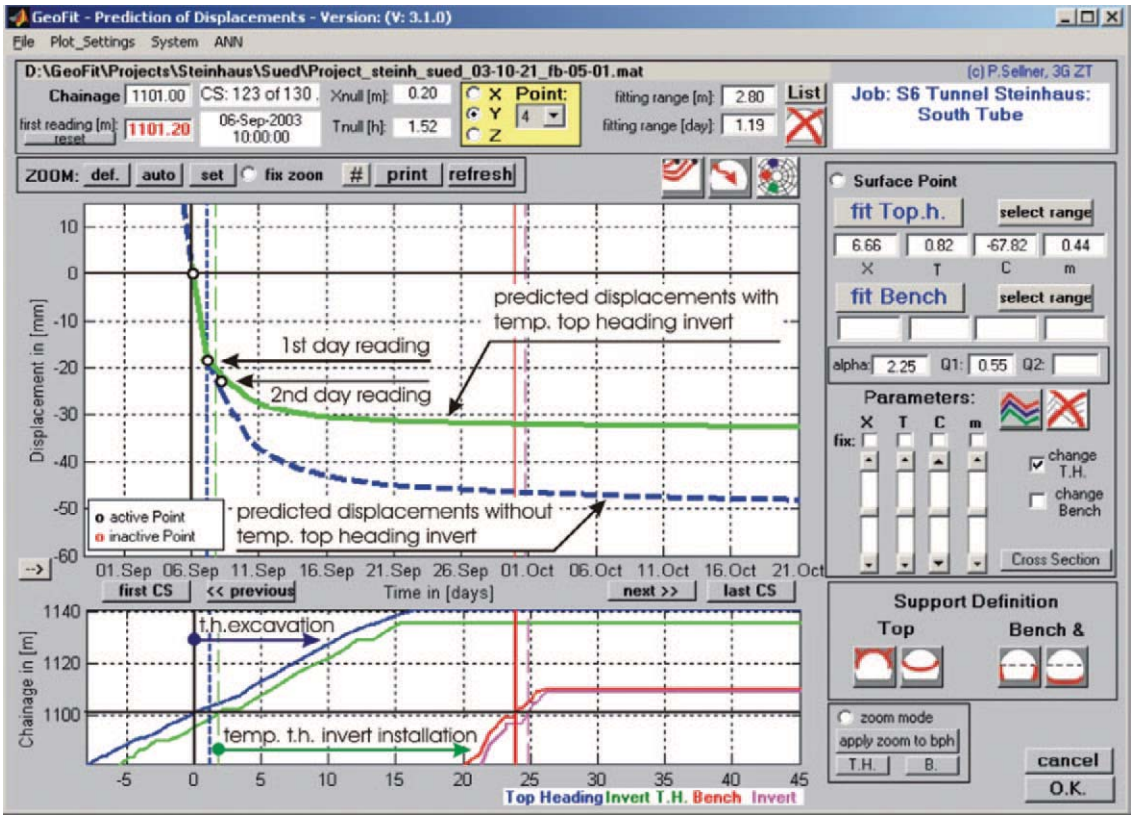

Fig. 7 Time-displacement characteristic of point No. 4 located in the left sidewall in monitoring section MS1101: Prediction of displacements with (green solid line) and without (blue dashed line) temporary invert from a few readings of the measured displacements (black circles) during top heading excavation (13).

Bild 7 *Zeit-Verschiebungscharakteristik des linken Kalottenfußpunkts Nr. 4 im Messquerschnitt MS1101: Prognose der Verschiebungen mit (grün durchgezogene Linie) und ohne (blaue strichlierte Linie) temporärem Kalottensohlgewölbe nach zwei Folgemesssungen (schwarze Kreise) während des Kalottenvortriebs (13).*

crease between tunnel metre 890 and 910 (Figure 5, Middle).

Between tunnel metre 875 and 915 (Figure 5, Bottom) the trend of the orientation of the displacement vector shows a deviation from a positive "normal" vector orientation (backwards) to a negative (forward). Basically such tendencies indicate a "stiffer" rock mass ahead of the face (14, 6) and therefore lower displacements could be expected compared to those observed in the already excavated sections. This tendency abruptly changes close to the fault at about tunnel metre 912, indicating another change in mechanism, the nature of which could not be explained at the time of excavation. At tunnel metre 921, just at the location of the fault, an overbreak occurred, with a volume of about 40 m³.

Later investigations from overbreaks at different tunnel sites showed a similar behaviour. The mechanism is not yet investigated in full detail, but the current interpretation is that the change in tendency of the displacement vector orientation is associated with the beginning of a failure process at the face. Due to the stress concentration in the stiffer section close to the transition, the stress level in the weak material is comparatively low, increasing the risk of an overbreak. This diagnostic indicator has since been successfully used at other sites to warn of imminent overbreaks. The appropriate measures to reduce the risk in such situations are to increase the face support (e.g. by a certain number of face bolts, or a thicker sealing) and by carefully excavating in several sections with subsequent support of the excavated areas.

Case study 3: Tunnelling in bimrock conditions

Case study 3 illustrates an example of the prediction of displacements in a section of the tunnel

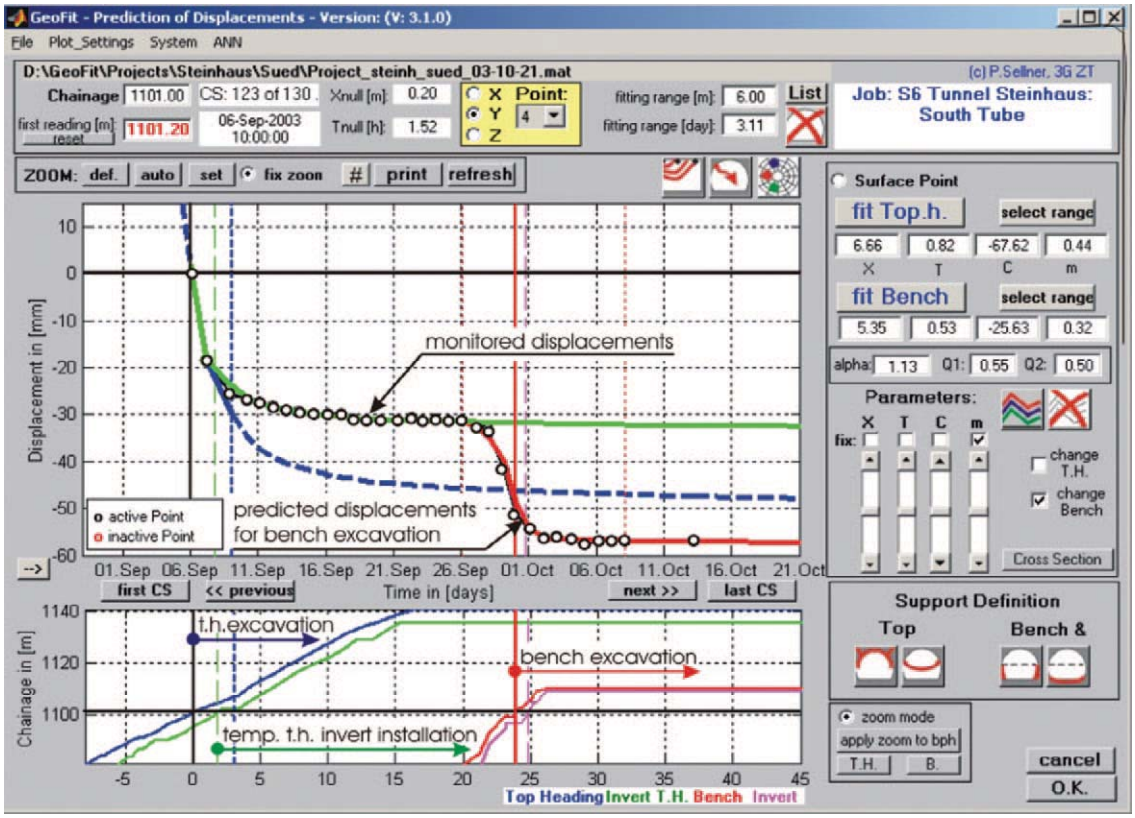

Fig. 8 Time-displacement characteristic of point No. 4 located in the left sidewall in monitoring section MS1101: Predicted displacements with (green solid line) and without (blue dashed line) temporary invert during top heading and bench/invert excavation (red line) (13) in comparison with the measured displacements (black circles).

Bild 8 *Zeit-Verschiebungscharakteristik des linken Kalottenfußpunkts Nr. 4 im Messquerschnitt MS1101: Prognostizierte Verschiebungen mit (grün durchgezogene Linie) und ohne (blaue strichlierte Linie) temporärem Kalottensohlgewölbe während des Kalotten- und Strosse/Sohlevortriebs (rote Linie) (13) im Vergleich zu den gemessenen Verschiebungen (schwarze Kreise).*

excavated in bimrocks. The monitoring section discussed is at tunnel metre 1101 of the same tunnel as described for case study 2. The overburden in this section above the crown is about 15 m. The geological condition (Figure 6) is characterized by smaller blocks (dolomite marble indicated by light blue and dark blue colour) embedded in a soft, weathered matrix consisting of cataclastic phyllites (green and brown coloured).

Besides a prediction of the geological conditions ahead of the face, a reliable prediction of the system behaviour is required. With the knowledge of the "normal" behaviour of the system the measured displacements can be compared to the predicted values in order to detect deviations in the behaviour in a timely fashion.

Figure 7 shows the development of the settlements over two days, for measuring point 4 located in the left sidewall in monitoring section MS 1101 (see Figure 6, black circles). The dashed blue line in Figure 7 shows the predicted displacements of the top heading and the solid green line shows the predicted system behaviour with an additional top heading invert installed close to the face.

The plot of Figure 7 shows the whole predicted displacement path including the pre-displacements developing ahead of the face, and after the excavation until the zero-reading is taken. For this example, final settlements of about 33 mm during top heading excavation are predicted. It can be seen that the temporary invert very effectively reduces displacements, leading to a quick stabilization of the top heading.

Figure 6 shows the displacement paths for several days at a cross-section for monitoring station MS 1101 and at the location of the face map illustrated. The asymmetrical deformation pattern of the system rock mass-support can be clearly seen. The displacements on the left sidewall are greater

than those on the right side. This is attributed on the one hand to the influence of the slope, dipping to the right; and on the other hand, to the lesser block/matrix ratio at the left side.

Figure 8 shows the predicted and observed displacements. It can be seen that the observed displacements were almost exactly the same as those predicted during top heading and bench/invert excavation. The bench excavation causes additional settlements of around 25 mm (red line, predicted displacements). Any significant deviation of the monitored displacements from the predicted behaviour would have been interpreted as an abnormal behaviour, requiring detailed analysis such as described elsewhere as an example of overstressing and failure of the temporary top heading invert (15, 16).

Conclusions

Tunnelling in heterogeneous rock mass is one of the most difficult tasks in subsurface engineering. The difficulty of establishing a reliable ground model during the design necessitates continuous updating of observed ground conditions during construction. A lot of time and money can be saved by using advanced displacement monitoring data evaluation methods for short term prediction of the rock mass structure and quality instead of the conventional approach of probing ahead. Recent experience has shown that the use of advanced displacement monitoring and data evaluation can be used to predict the rock mass quality and thus assist in the timely adaptation of excavation and support methods in shallow tunnels in heterogeneous rocks. Furthermore, a new tool, developed to predict the development of displacements, has proved to be very valuable for checking the "normality" of the system behaviour, allowing the timely detection of unfavourable developments.

References

1. Schubert, W.: *Erfahrungen bei der Durchörterung einer Großstörung im Inntaltunnel*. Felsbau 11 (1993), Nr. 6, pp. 443-447.
2. Schubert, W.: *Dealing with squeezing conditions in Alpine tunnels*. Rock Mechanics and Rock Engineering, Vol. 29 (1996), No. 3, pp. 145-153.
3. Schubert, W. ; Riedmüller, G.: *Geotechnische Nachlese eines Verbruchs – Erkenntnisse und Impulse*. In: Semprich, S. (ed.): Mitteilungsheft 13 des Instituts f. Bodenmechanik und Grundbau, pp. 59-68, Graz University of Technology, Austria, 1995.
4. Schubert, W. ; Budil, A.: *The Importance of Longitudinal Deformation in Tunnel Excavation*. Proceedings of the 8th International Congress on Rock Mechanics ISRM, Vol. 3, pp. 1411-1414, 1995.
5. Budil A.: *Längsverschiebungen beim Tunnelvortrieb*. Doctoral thesis, Graz University of Technology, Austria, 1996.
6. Steindorfer, A.F.: *Short Term Prediction of Rock Mass Behaviour in Tunnelling by Advanced Analysis of Displacement Monitoring Data*. Doctoral thesis, Graz University of Technology, Austria. In: Riedmüller, G. ; Schubert, W. ; Semprich, S. (eds.): Schriftenreihe der Gruppe Geotechnik Graz, Heft 1. Graz, 1998.
7. Schubert, W. ; Grossauer, K. ; Kim C.Y.: *Interpretation of Displacement Monitoring Results for Tunnels in Heterogeneous Rock Mass*. Proceedings of the 6th International Geotechnical Conference, pp. 99-106, Bratislava, 2003.
8. Sellner, P.J.: *Prediction of Displacements in Tunnelling*. PhD thesis, Graz University of Technology, Austria. In: Riedmüller, G. ; Schubert, W. ; Semprich, S. (eds.): Schriftenreihe der Gruppe Geotechnik Graz, Heft 9, Graz, 2000.
9. Raymond, L.A.: *Classification of melanges. In Melanges: Their Nature, Origin, and Significance*. In: Raymond, L.A. (ed.): Geological Society of America: special pub. 198, pp. 7-20, 1984.
10. Medley, E.W.: *Orderly Characterization of Chaotic Franciscan Melanges*. Felsbau 19 (2001), No. 4, pp. 20-33.
11. Riedmüller, G. ; Schubert, W. ; Goricki, A. ; Pölsler, P.: *Investigation strategies for the design of the Semmering base tunnel*. Felsbau 18 (2000), No. 4, pp. 28-36.
12. ÖSAG: *S6 – Semmering Schnellstraße, Tunnel Steinhaus, Baugeologische Dokumentation*. Geoteam Semmering, Dr. N. Heim/Dr. S. Jacobs, 2000-2003.
13. www.geofit.3-g.at.
14. Schubert, W. ; Steindorfer, A.: *Advanced Monitoring Data Evaluation for Tunnels in Poor Rock*. Proceedings EUROCK ´96, Vol. 2, pp. 1041-1046, Rotterdam: Balkema, 1996.
15. Sellner, P. ; Grossauer, K. ; Schubert, W.: *Advanced Analysis and Prediction of Displacements and System Behaviour in Tunnelling*. In Dinis da Gama, C. ; Ribeiro e Sousa, L. (eds.): Proceedings EUROCK 2002. pp. 539-546, 2002.
16. Sellner, P. ; Grossauer, K.: *Prediction of displacements for tunnels*. Felsbau 20 (2002), No. 2, pp. 22 – 28.

Authors

Dipl.-Ing. Dr.techn. Bernd Moritz, Geoconsult ZT GmbH, Sterneckstrasse 52, A-5020 Salzburg, Austria, E-Mail bernd.moritz@geoconsult.at; Dipl.-Ing. Karl Grossauer, o. Univ.-Professor Dipl.-Ing. Dr.techn. Wulf Schubert, Institute for Rock Mechanics and Tunnelling, Graz University of Technology, Rechauerstrasse 12, A-8010 Graz, Austria, E-Mail grossauer@tugraz.at; schubert@tugraz.at

Better Understanding the Strengths of Serpentinite Bimrock and Homogeneous Serpentinite

By Ulrich Glawe and Bishal N. Upreti

This paper describes two projects in which serpentinite caused significant problems: during design of the Kusan-3 HEPP dam in Indonesia; and during construction of the Berke powerhouse access tunnel in Turkey.

Case history 1: Kusan-3 HEPP dam, Indonesia

The principal features of the Kusan-3 HEPP, which is located in the Meratus Mountain Range in South Kalimantan, Indonesia, are the 100 m high RCC-dam and the 130 MW surface powerhouse at the toe of the dam. The general arrangement of the project is shown in Figure 1. The foundation rock mass consists of serpentinite, pyroxenite, peridotite, and diorite dykes (Figure 2).

The investigations described below were performed in the tender design stage of the project. However, although the design is economical and technically viable, the construction of the dam has been delayed. The dam was eventually designed with a trapezoidal shape, with a vertical upstream face and a downstream slope of 0.7 H : 1 V. It was necessary to introduce a curve in the axis of the dam to optimize foundation conditions. As described below, the geology has influenced the dam design: The axis (see Figure 1) has been selected to ensure that the dam height and footprint area on the serpentinite is minimized. For the selected axis, the maximum height of the section founded on serpentinite is only 72 m. The structure was designed as a two-dimensional body, perpendicular to the dam axis, since the arching action induced by the curvature will not be significant.

Field investigation indicated that about 28 % of the dam footprint is within serpentinite, despite serpentinite being recognized as an unsatisfactory and occasionally unacceptable foundation material. In fact, rock engineering literature warns the engineer: "*Dams should not be placed*

Zum besseren Verständnis der Festigkeiten von Melange Serpentinit und homogenem Serpentinit

Die vorliegende Arbeit umfasst zwei Projekte, in denen Serpentinit, jeweils geologisch unterschiedlich ausgebildet, erhebliche Probleme in der Planungsphase beziehungsweise in der Bauphase darstellte. Im Wasserkraftprojekt Kusan-3 besteht die Aufstandsfläche der geplanten 100 m hohen Schwergewichtsmauer zu 28 % aus Serpentinit. Serpentinit, der an der Sperrenstelle eine Bimrock-Struktur aufweist, stellt im Allgemeinen ein fragwürdiges Gründungsmaterial dar. Zur Bestimmung des felsmechanischen Datensatzes (Festigkeit) wurden Feld- und Laboruntersuchungen durchgeführt. Die Ableitung des Design-Parametersatzes basierte auf Ergebnissen der Labortests und erfolgte unter Einbezug des Maßstabseffekts und der Trennflächeneigenschaften. Die so ermittelten unerwartet hohen Materialfestigkeiten, die mit der Anwendung der GSI-Klassifikation bestätigt wurden, lassen sich nur mit lokal ausgeprägten mineralogischen und strukturellen Faktoren erklären, wobei insbesondere die Trennflächeneigenschaften innerhalb der Matrix eine wesentliche Rolle spielen.

Beim Bau des Zugangstunnels zur Zentrale der Berke-Wasserkraftanlage im Südosten der Türkei wurden Erfahrungen mit einem Serpentinit gemacht, der andere strukturelle und mechanische Eigenschaften aufweist. Im Gegensatz zum Kusan-3 Serpentinit erscheint das Material selbst im kleinen Maßstab homogen. Die Feldbeoachtungen und Berechnungen erbrachten Hinweise auf eine sehr geringe Gebirgsfestigkeit. Dies hatte wesentlichen Einfluss auf die Baumethode, die dann den vorherrschenden Gebirgsverhältnissen angepasst werden musste.

This paper describes two projects wherein serpentinite caused significant problems during design and construction, respectively. Serpentinite extends over 28 % of the dam footprint of the proposed 100 m high Kusan-3 gravity dam located in Indonesia and is well known to be a questionable foundation material. Both laboratory and in situ field tests were carried out on the serpentinite, which exhibits a bimrock structure. An estimate of the shear strength of the rock mass was conservatively developed from the laboratory data, taking scale effects and discontinuity characteristics into account. This resulted in a surprisingly high shear strength, which can only be explained with highly localized mineralogical and structural factors, particularly with the discontinuity characteristics in the matrix rock. However, applying the GSI-system to quantify the physical parameters of the serpentinite provided satisfactory confirmation of the selected values.

In the Berke HEPP in SE Turkey, a low-strength and homogeneous (even at small-scale) form of serpentinite was encountered during the construction of the powerhouse access tunnel. Field observation and results of numerical analyses indicated a very low strength rock, as one would expect for a serpentinite. The low strength resulted in considerable tunnel construction problems. On the basis of analysis the construction method was then tailored to the prevailing rock conditions.

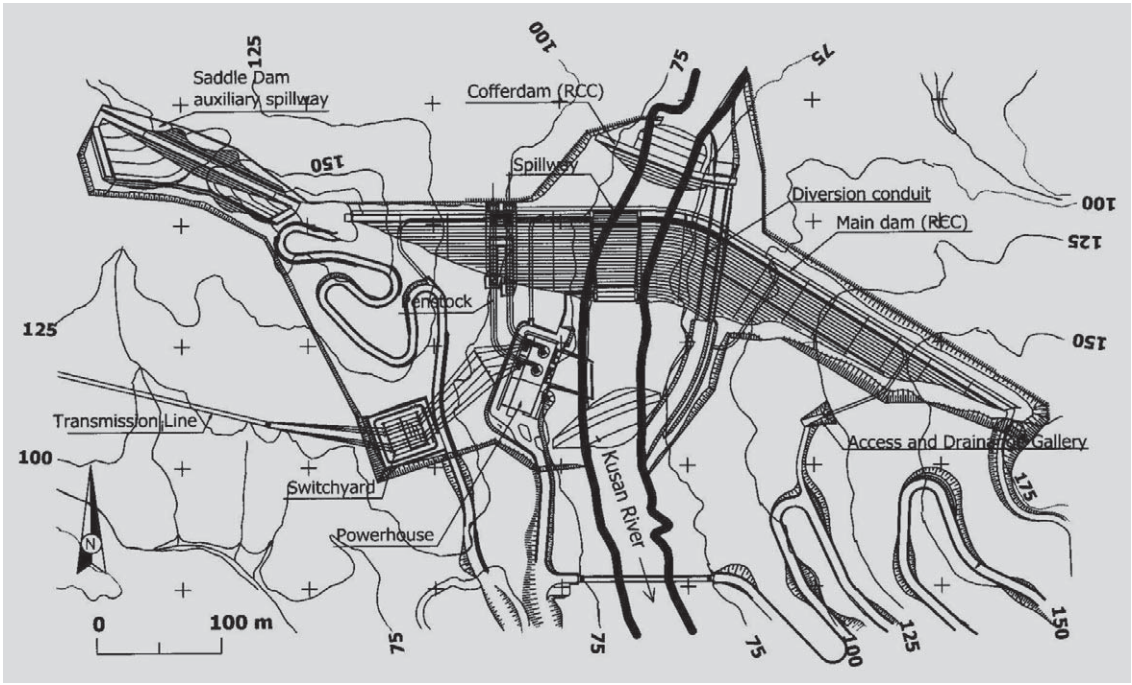

Fig. 1 General arrangement of the Kusan-3 HEPP.

Bild 1 *Auslegung der Wasserkraftanlage Kusan-3*

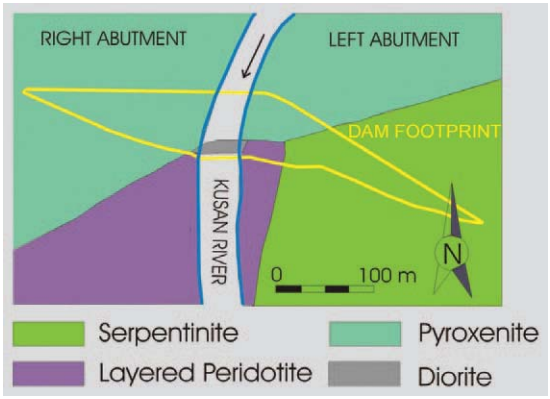

Fig. 2 Simplified geological map of the dam footprint area.

Bild 2 *Schematisierte geologische Karte des Bereichs der Sperrenaufstandsfläche.*

on serpentinite" and that the material is "*... unusable and unsuitable as the foundation for a dam*" (1, page 239). Taking into account these legitimate published cautions, geotechnical investigations were focused on quantifying the mechanical properties of the serpentinite rock mass.

Serpentinite: mineralogy, micro-structure and macro-structure

Serpentinite consists of three minerals, namely Chrysotile, Lizardite and Antigorite. X-ray diffraction analyses indicated only Chrysotile and Lizardite in the serpentinite (2) at the dam site. Thin section analyses revealed that the original rocks have undergone complete serpentinization and have fractured into blocks by cataclasites, making a form of "fault breccia". The blocks have been cemented by precipitated serpentinite minerals forming a block-in-matrix structure or bimrock (3) even at microscopic scale. The rocks can be designated as "cohesive cataclasites" with blocks ranging from a few mm in diameter to about 1 m^3 in volume.

Geological mapping revealed several slopes higher than 10 m and steeper than 45° within the serpentinite rock mass, with no visual signs of instability. On the left abutment, an adit (2 m x 2 m) was driven more than 20 m into a serpentinite rock mass by drilling and blasting: It required no rock reinforcement or support and showed no signs of instability even after being open for more than six months, and after the adit was widened at three locations to spans of more than 4 m. These extensions, made for the purpose of conducting in-situ direct shear tests, were excavated with great difficulty by pick and other hand tools.

The serpentinite rock mass in the adit appeared as a "mega-breccia", a mixture of strong, joint-bounded rock blocks embedded in weaker matrix rock, and as such conformed in appearance to other bimrocks (3). The rock mass structure within the adit is considered to be similar to that found in borehole cores drilled at several locations elsewhere in the serpentinite.

Matrix and blocks demonstrated a considerable difference in strength: Laboratory tests revealed the blocks to have average UCS of 66.5 MPa and the matrix rock to have an average UCS of 14.8 MPa. The ratio of block UCS to matrix UCS, being greater than 2, thus qualified the serpentinite to be considered a bimrock (3).

Serpentinite blocks, matrix and discontinuities

The volume of the individual blocks in outcrops ranges from 0.001 to approximately 1 m^3. In general, the edges of individual blocks are not longer than 0.4 m. Block shapes are random, although block edges typically are round and seldom angular. Blocks surfaces are generally undulated, some being concave, and with randomly oriented slickensides.

Site matrix rock is a "mini-breccia" or a fine-grained cataclasite, but it has the visual appearance of a homogeneous weak material. It was practically impossible to conventionally sample representative specimens for laboratory tests at outcrops or in the adit. Core recovery with conventional diamond drilling using triple-tube core barrels was very difficult. Intact core samples failed if bent with force by hand, or disintegrated into pieces at a light hammer blow. This fact is considered to reflect very low tensile strength of pre-existing discontinuities. The broken rock pieces exhibit slickensided and undulating fracture surfaces (Figure 3).

Despite the difficulties, the 60 mm drilled cores were further drilled along core axes to obtain eight 41 mm cores specimens of serpentinite matrix for laboratory testing. The success of this careful drilling, in the laboratory, to produce cores of the serpentinite matrix without "joints", clearly indicates that the serpentinite matrix lacked "joints", which are formally defined as "discontinuities without tensile strength". Consequently, the visible discontinuities in the serpentinite matrix are not considered as „joints", but as undulating or curvilinear surfaces of weakness. When tool-excavated or when exposed in laboratory testing, after failure, these undulating surfaces were observed to be randomly oriented, polished, glossy or slickensided. Some of the surfaces coincide with block surfaces or run through the serpentinite matrix.

Similar observations were made in-situ. Several thousands of discontinuity measurements were performed at outcrops and in the adit, which clearly showed that there are no dominant discontinuity orientations in the serpentinite at a scale larger than 0.2 m x 0.2 m. The surfaces of weakness are closed, tight and nearly entirely slickensided (88 %) and undulated (90 %). They exhibit a relatively small persistence, represented by trace lengths on exposures generally less than 1 m, with a maximum of 4 m.

Fig. 3 Drilled core specimen of the Kusan serpentinite.

Bild 3 *Bohrkernmaterial des Kusan Serpentinits.*

Determination of rock mass strength

Back-analyses of the relatively steep cliffs was considered as being inappropriate, because the actual failure mode and the theoretically analysed strengths might be different due to the existence of larger blocks in the serpentinite rock mass.

For the serpentinite rock mass at the dam site, the volumetric block portion in outcrops is estimated to be in the range of 10 to 15 %. This pro-

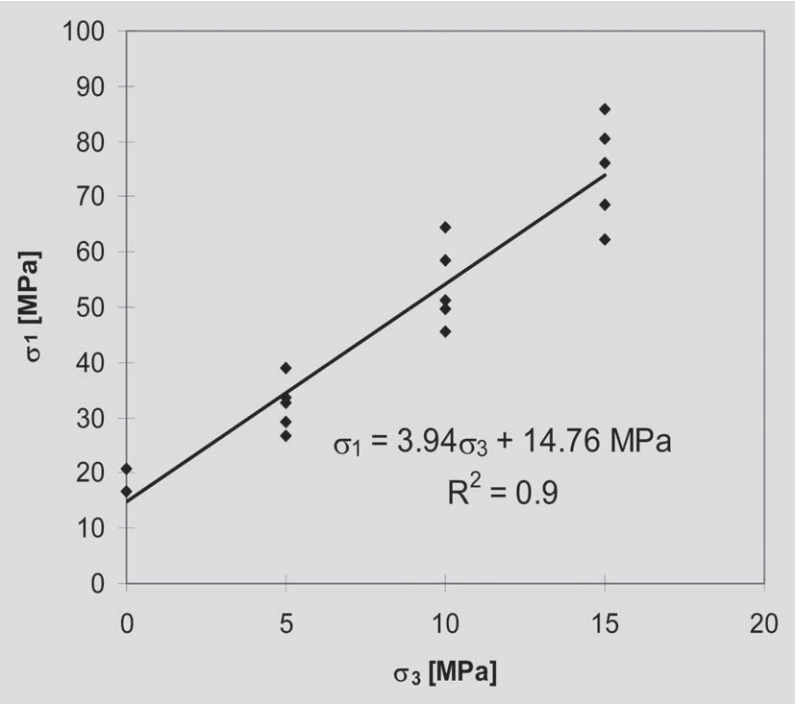

Fig. 4 Results of two uniaxial and five triaxial tests on the Kusan serpentinite.
Bild 4 *Resultate von zwei einachsialen und fünf triaxialen Druckversuchen des Kusan Serpentinits.*

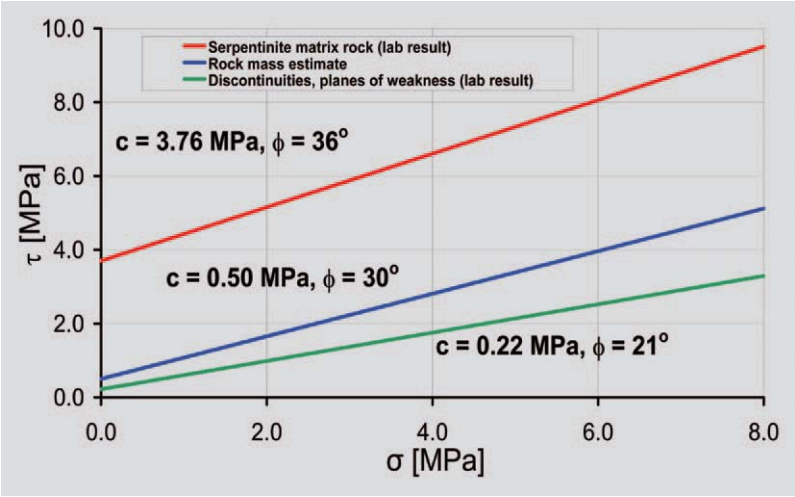

Fig. 5 Mohr-Coulomb strength envelops for the Kusan serpentinite.
Bild 5 *Mohr-Coulomb Bruchgeraden des Kusan Serpentinits.*

Table 1 Ranges of shear strength parameters surfaces of weakness in serpentinite.
Tabelle 1 *Scherfestigkeitsparameter der Trennflächen im Serpentinit.*

Peak cohesion [MPa]	Peak friction angle [°]	Residual cohesion [MPa]	Residual friction angle [°]
0.22 - 0.64	21.0 - 23.1	0.00 - 0.24	18.5 - 24.2

Table 2 Derivation of shear strength parameters for the serpentinite rock mass.
Tabelle 2 *Abgeleitete Scherfestigkeitsparameter des Serpentinit-Gebirges.*

	Laboratory results on intact matrix rock samples (0.041 m)	Extrapolating intact matrix strength to a large scale (80 m)	Final estimate considering intact matrix strength and discontinuities
Cohesion ... [MPa]	3.7	0.83	0.5
Friction angle .. [°]	36	36	30
Corresponding UCS ..... [MPa]	14.8	3.25	1.7

portion is also based on the evaluation of relative areas of exposed blocks and matrix rock in the left bank adit and is considered to be the upper bound for a relevant scale, such as the thickness of a potential failure zone beneath the dam.

Lindquist and Goodman (4) concluded that below 25 % block volumetric proportion the strength and deformation properties of the rock mass will be approximately that of the matrix rock. Accordingly, the serpentinite rock mass strength to be adopted for design purposes is the strength of the matrix.

Eight samples of the matrix rock were tested to determine the serpentinite matrix rock strength: Two in uniaxial compression and five in multistage triaxial compression (Figure 4). The strength parameters, derived by simple stress transformation, are 36° for the friction angle and 3.76 MPa for the cohesion (Figure 5).

In addition to the laboratory tests on intact rock, five direct shear tests on the surfaces of the undulating discontinuities in serpentinite were performed (2). The test areas ranged from approximately 0.02 to 0.06 m² .The tests were carried out with five incremental load stages at 1, 2, 4, 6 and 8 MPa normal stresses. The results are summarized in Table 1.

The tests were carried out on actual rock-block surfaces (block to block contacts in outcrop scale), which are considered to represent the weakest discontinuities in the serpentinite. These discontinuities exhibited geological appearances (surface condition) apparently similar to other surfaces of weakness in the serpentinite, such as those found in drill cores.

Sixty three point load tests were performed on the serpentinite rock cores. The mean Point Load Strength Index IS50 is 4.1 (standard deviation 1.9), which corresponds to a UCS of more than 50 MPa. During testing no distinction was made between matrix and blocks.

Plate loading tests and direct shear tests (0.8 m x 0.8 m) were performed in the adit. The results are discussed in (5). It was concluded from these results, however, that in both the in-situ direct shear tests and the plate loading tests there were possibilities for test specimen disturbance by routine handling during test preparation, leading to erroneous results. This is particularly true for tests in the serpentinite, which was considered to be highly sensitive to the vibrations from the blasting operations performed for the tunnelling of the adit. Therefore, for the derivation of the design parameters of the serpentinite, these results were not considered.

Derivation of Design Parameters

The compression tests carried out on 41 mm diameter cylinders of matrix rock resulted in selection of a design cohesion of 3.76 MPa and design friction angle of 36°. Research on the scale effect (6, 7, 8 and 9, all summarised in 10) suggested that for the extrapolation of laboratory

results from the UCS of small samples $\sigma_{c\ small}$ to the UCS on the larger scale $\sigma_{c\ large}$, a reduction factor, such as the following, should be used:

$$\sigma_{c\ large} = \sigma_{c\ small} \cdot (D_{small}/D_{large})^n$$

where D_{large} is the sample diameter considered in the large scale, D_{small} is the diameter of the laboratory sample and n ranges between 0.15 and 0.25. Assuming D_{small} = 41 mm, D_{large} = 80 m (which exceeds the maximum width of the dam footprint in serpentinite and a mean value of n = 0.2 yields a UCS $\sigma_{c\ large}$ = 3.25 MPa. This corresponds to the Mohr-Coulomb cohesion of 0.83 MPa, assuming that the friction angle remains constant at 36°. The laboratory direct shear tests on discontinuities in serpentinite indicated peak cohesion on the surfaces of weakness of 0.22 MPa and peak friction angle of 21° (lowest values, see Table 1). Taking into account the limited surface-area persistence of the discontinuities in the matrix and the fact that the laboratory tests were performed on test samples with a size similar to that of the discontinuity persistence, the scale effect of discontinuity strength becomes negligible. The discontinuities are randomly oriented and their persistence is small. Hence, it would be unduly conservative to consider discontinuity strength as being representative of the strength of the rock mass. The strength parameters of the rock mass should lie between those of the matrix rock and those of individual discontinuity surfaces. On a large scale of more than a few metres, as must be considered for the dam foundation, the values should be closer to those of the matrix rock.

In design, the uncertainties were accommodated by the application of reduction factors that were selected based on guidelines suggested by European standards. Hence factors of 0.6 for the cohesion, and 0.8 for the friction (tan ϕ) were adopted since the uncertainties were considered to be greater for cohesion than for the friction angle. Accordingly, the reduced cohesion was 0.5 MPa the reduced friction angle 30°. These values were used for the structural analyses of the dam section, assuming rigid-body sliding.

The derivation of the strength parameters are summarized in Table 2. The shear strength envelopes for the serpentinite are presented in Figure 5. These represent the peak shear strength of intact matrix rock and discontinuities, both as measured in the laboratory. The selected strength for the serpentinite rock mass for design purposes is also indicated.

Application of rock mass classifications

Joint data (e.g. RQD, joint spacing) represent the principal input data for the rock mass classification systems of Bieniawski (11) and Barton et al. (12). As discussed above, rock-matrix serpentinite discontinuities cannot be classified as "joints" as would be required for use of the available rock mass classifications schemes. Furthermore, due to the random orientation of the surfaces of weakness in the serpentinite, for this case, there is doubt about the use of an adjustment for the discontinuity orientation as required in Bieniawski's classification (which is applied after initial determination of the Rating).

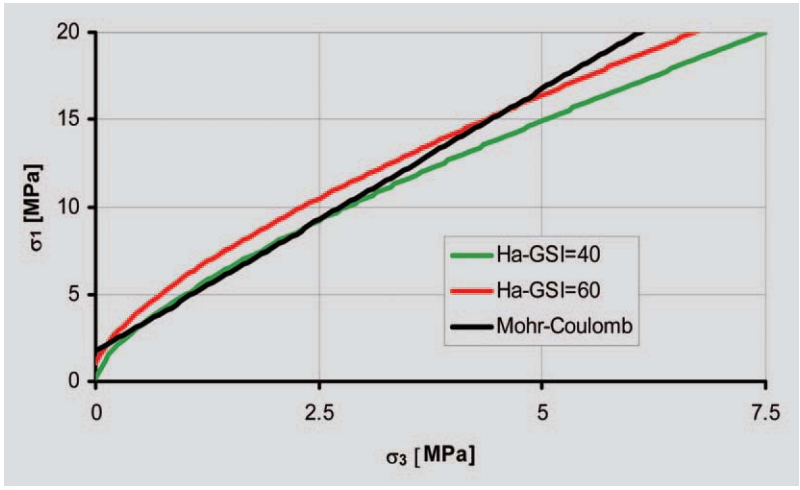

Fig. 6 Strength envelopes for the Kusan serpentinite rock mass for the criterion for GSI 40 and 60 (after 15). The Mohr-Coulomb envelope with the derived design parameters (c = 0.5 MPa, ϕ = 30°) is indicated for comparison.

Bild 6 *Hüllkurven für das Kusan Serpentinit Gebirge bei Anwendung des Bruchkriteriums von (15) für GSI 40 und 60. Die Mohr-Coulomb Bruchgerade mit den abgeleiteten Entwurfsparametern (c = 0,5 MPa, ϕ = 30°) ist zum Vergleich eingezeichnet.*

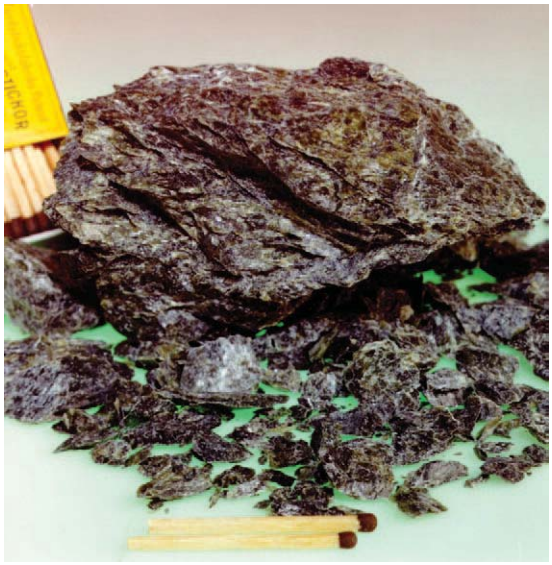

Fig. 7 Drilled core specimen of the Berke serpentinite.
Bild 7 *Handstück des Berke Serpentinits.*

Hoek's GSI classification method (13, 14) was extended by (15) to account particularly for tectonized cataclastic rocks. It is understood that Hoek's classification and Habimana's extension must be considered as "work in progress". Following (15) and classifying the serpentinite rock mass as "tectonized" leads to a GSI of 40 to 60. Note however: Rock mass structures that actually meet the serpentinite bimrock structural condition are not available from this classification. In Figure 6, the failure envelopes for the serpentinite are presented based on the extended Hoek/Brown failure criterion and the Mohr-Coulomb criterion selected for the dam design.

Other important parameters such as deformability, bearing capacity, interface strength rock/concrete, rock mass permeability/groutability, and rippability of the serpentinite are discussed by (5) in detail. These issues are beyond the scope of this paper.

Case history 2: Berke powerhouse access tunnel, Turkey

Location, geology and tunnel method

The project is located in the southeast of Turkey, close to the Syrian border, about 100 km northeast of Adana. It comprises a 202 m high concrete arch dam, a 4.5 km long pressure tunnel, an underground powerhouse and other relevant structures for such a large HEPP. The investigations were performed to quantify the geotechnical reasons contributing to large tunnel deformations, and to suggest an appropriate construction method and support for the powerhouse access tunnel.

The geology of this 411 m long tunnel consists primarily of laminated, sheared limestone of moderate to poor rock mass quality. From tunnel metre (Tm) 170 to the powerhouse (Tm 411) serpentinite was encountered during tunnelling, which was not predicted by the geological investigations. This refers to the tunnel sections Tm 170 to Tm 225 and Tm 266 to Tm 364. In addition from Tm 364 to Tm 400 brecciated and mylonized serpentinite is intercalated with highly fractured diabase and calcareous schist. This zone is water-bearing and it is considered as a large tectonic fault zone. For the rest of the tunnel, laminated limestone is dominant. In other words, along the tunnel there is a diverse geology of limestone, serpentinite, and diabase, and the rock mass could be considered a bimrock at a scale much larger than the 411 m long structure. However, the investigations were focused on a smaller scale of metres to 10s of metres. The overburden thickness for the relevant tunnel sections in the serpentinite ranges from approximately 150 to 200 m.

In general the serpentinite at this site is extremely closely fractured, with chlorite and talc infilling. The serpentinite exhibits a flaky and cataclastic rock texture (Figure 7) and is at some locations completely mylonized. The serpentinite rock mass could be easily excavated with a pick and the remaining small blocks of the serpentinite could be disintegrated by hand to sandy gravel size. The contact with the limestone sections was water-bearing and is also heavily tectonized.

The tunnel was excavated full-face by a backhoe with a U-shaped horseshoe profile, 8 m wide and 7.5 m high. In the serpentinite

sections, grouted rock bolts supported the tunnel, steel ribs (NPI 160) were placed at various spacings, and shotcrete and back-fill concrete was applied. As one would expect considering the geology, the selected profile and the support, the tunnel experienced large radial deformations of up to 1 m with unacceptable decrease in the free inner profile of this access tunnel, depending on the geological conditions encountered (Figure 8). As a result, re-design and reconstruction of the affected segments of the tunnel were required, which prompted the study summarized here.

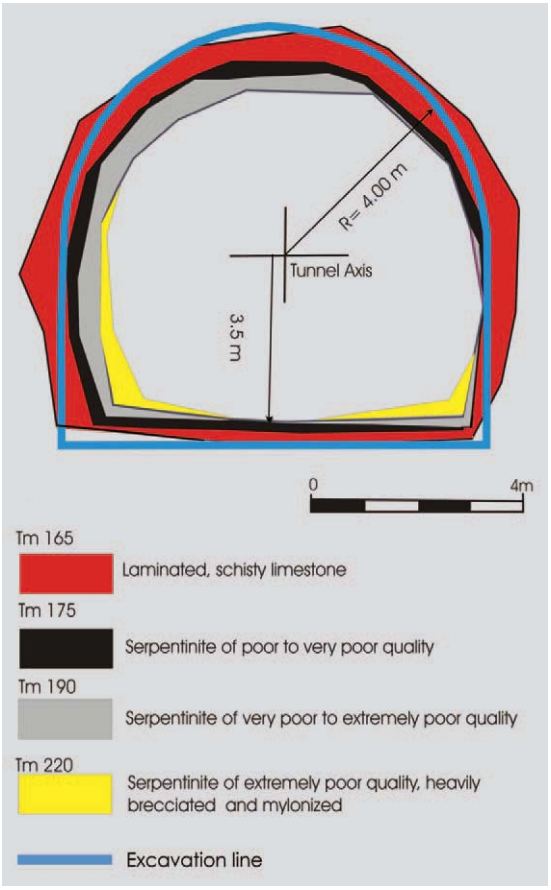

Fig. 8 Tunnel inner cross sections for the Berke powerhouse access tunnel for different tunnel chainages and different geology.

Bild 8 *Tunnelquerschnitte des Berke Zugangstunnels für verschiedene Tunnelbereiche und unterschiedliche Geologie.*

Mechanical properties of the Berke serpentinite

No laboratory or in situ test data were available for the serpentinite. This is understandable, since core sampling in the serpentinite was practically impossible. However, sufficient data from convergence and cross-sectional profile measurements throughout the tunnel was available to back-calculate appropriate mechanical properties for re-design of tunnel support.

For stability calculations an estimate of the Mohr-Coulomb strength parameters was required: the peak friction angle was estimated at 28° based on the field observation of serpentinite muck piles which showed slope angles steeper than 30° and the residual friction angle was estimated to be 25°. The cohesion was estimated to be similar to that of stiff clay, because of the relative stability of the face, which suffered only minor collapses. Accordingly, the peak cohesion was assumed to be 30 kPa and the residual cohesion to be 10 kPa. The assumed drop in cohesion from peak to residual strength was considered to be justified by the observation that the serpentinite disintegrated to a quasi-granular material, when excavating it with a pick.

Tunnel stability calculations

Using the finite difference code FLAC (17) rock pressures on the primary liner were determined following analysis of the monitored deformations in the tunnel. The acting rock pressure on the liner was so estimated to be approximately 0.4 MPa. Several runs were carried out with various serpentinite cohesive strengths, from which it appeared that incorporation of the higher possible strength of the serpentinite as in the range estimated above, resulted in less predicted deformation than actually measured in the tunnel; and the lower cohesion estimates resulted in predicted collapse of the structure. Accordingly, the estimated range (of c_p = 30 kPa, c_r = 10 kPa, ϕ_p = 28°, ϕ_r = 25°) were considered to be representative of serpentinite rock mass encountered in tunnelling. Based on these finding the tunnel was then re-designed. Reconstruction required a new profile and a curved excavation line to create stable conditions, while maintaining an acceptable amount of reinforcement in the concrete liner.

Conclusions

The serpentinite encountered in Berke tunnel was an extremely weak rock, which caused significant problems during tunnel construction, as one would expect when engineering in serpentinite. Hence, why did the serpentinite of the Kusan-3 dam site exhibit higher strength than reported elsewhere for serpentinite? On the basis of the case histories reported in this paper, varying high strength values for serpentinite may result from differences in localized lithologic factors, micro and macro structures, mineralogical compositions, and variations of interlocking of smaller grains, sheared and angular rock fragments, and re-cementation of matrix in serpentinite with bimrock fabric. A comparison of the serpentinites shown in the photographs of the serpentinites in Figures 2 and 7 indicate how differences in structure may impact rock mass strength.

The Kusan serpentinite is apparently a bimrock in which the low volumetric block portion of only 10 to 15 % indicates that the appropriate strength and deformability parameters of the rock mass are those of the matrix material.

The characteristics of discontinuities in the matrix are the key to the serpentinite being acceptable dam foundation rock. These characteristics include the relatively small degree of persistence and the random orientation of surfaces of weakness. These characteristics combined with the relatively high strength of the intact matrix material, result in unexpectedly higher shear strength design values for the rock mass.

References

1. Goodman, R.E.: Engineering Geology – *Rock in Engineering Construction*. Singapore: Wiley, 1993.
2. Hollmann, F.: *Felsmechanische und mikrostrukturelle Untersuchungen an Serpentinit-Proben aus SE-Kalimantan, Indonesien (in English: Rock Mechanics and Micro-structural investigations on serpentinite samples from SE-Kalimantan, Indonesia)*. MSc. thesis (2000); Institute of Geology, Department of Applied Geology, Ruhr-University Bochum, Germany.
3. Medley, E.W.: *Systematic Characterisation of Melange Bimrocks and Other Chaotic Soil/Rock Mixtures*. Felsbau 17 (1999), No. 3, pp. 152-162.
4. Lindquist, E.S. ; Goodman, R.E.: *The Strength and Deformation Properties of a Physical Model Melange*. In Nelson, P.P. ; Laubach, S.E. (eds.): Proc. 1st North American Rock Mechanics Conference (NARMS) Austin, Texas. Rotterdam: Balkema, 1994.
5. Glawe, U. ; Linard, J.: *High concrete dam on serpentinite*. Quarterly Journal of Engineering Geology and Hydrogeology, 36 (2003), pp. 273-285.
6. Bieniawski, Z.T. ; van Heerden, W.L.: *The significance of in situ tests of large rock specimens*. International Journal on Rock Mechanics and Mining Science 12 (1975), No. 4, pp. 101-113.
7. Einstein, H.H. ; Baecher, G.B. ; Hirschfeld, R.C.: *The effect of size on the strength of brittle rock*. Proceeding of the 2nd International Congress of the ISRM. Belgrade, Vol. 2, Paper 3-2, 1970.
8. Habib, P. ; Vouille, G.: *Sur la disparition de l'effet d'échelle aux hautes pressions*. Proc. of the Académie des Sciences, Paris, 1966.
9. Herget, G.: *Stresses in Rock*. Rotterdam: Balkema, 1988.
10. Cunha, A.P.: *Scale effects in rock mechanics*. Proceedings of the 1st International Workshop on Scale Effects in Rock Masses. Loen, Norway, pp. 3-27. Rotterdam, Balkema, 1990.
11. Bieniawski, Z.T.: *Engineering Rock Mass Classification*. New York: Wiley, 1989.
12. Barton, N.R. ; Lien, R. L; Lunde, J.: *Engineering Classification of Rock Masses for the Design of Tunnel Support*. Rock Mechanics 6 (1974), No. 4, pp. 189-239.
13. Hoek, E.: *Strength of Rock and Rock Masses*. ISRM News Journal 2 (1994), pp. 4-16.
14. Hoek, E. ; Marinos, P. ; Benissi, M.: *Applicability of the Geological Strength Index (GSI) Classification for Very Weak and Sheared Rock Masses. The Case of the Athens Schist Formation*. Bull. Eng. Geol. Env., 57 (1998), pp. 151-160.
15. Habimana, J. ; Labiouse, V. ; Descoeudres, F.: *Failure criterion for cataclastic rocks: Experience from the Cleuson-Dixence Project*. Proceedings of the 9th Int. Conf. on Rock Mech. (1999). Vol. 2, pp. 605-610.
16. Hoek, E. ; Brown, E.T.: *Practical Estimates of Rock Mass Strength*. Int. J. Rock Mech. Min. Sci. 34 (1998), pp. 1165-1186.
17. Itasca: *FLAC code*. Itasca Consulting Group, Inc., Minneapolis, USA.

Authors

Dr. Ulrich Glawe, Assoc. Professor, School of Civil Engineering, Asian Institute of Technology, PO Box 4, Khlong Luang, 12120 Pathumthani, Thailand, E-Mail glawe@ait.ac.th; Dr. Bishal N. Upreti, Professor, Department of Geology, Tribhuvan University, Tri-Chandra Campus, Ghantaghar, Kathmandu, Nepal, E-Mail bnupreti@wlink.com.np